Tagging RNA to probe for RNA subcellular localization

by

Hugo Cesar Medina-Muñoz

A dissertation submitted in partial fulfillment

of the requirements for the degree of

Doctor of Philosophy

(Biochemistry)

at

THE UNIVERSITY OF WISCONSIN-MADISON

2020

Date of oral examination: October 4, 2019

The dissertation is approved by the following members of the Final Oral Committee:

Marvin P. Wickens, Professor, Department of Biochemistry

Richard M. Amasino, Professor, Department of Biochemistry

Catherine A. Fox, Professor, Department of Biomolecular Chemistry

Judith E. Kimble, Professor, Department of Biochemistry

Michael D. Sheets, Professor, Department of Biochemistry

Tagging RNA to probe for RNA subcellular localization

Hugo Cesar Medina-Muñoz

Under the supervision of Professor Marvin P. Wickens

Thesis Summary

Records of RNA-site interactions within a cell's lifetime are needed to reveal new functions for RNA localization. Available methods can now track RNA movements or identify hundreds of localized RNAs within a brief period. However, strategies that detect RNA-site interactions in a comprehensive and genome-wide manner beyond a short period are needed. The Localized RNA tagging approach addresses this necessity. The method constitutively labels the 3' ends of localized RNAs with multiple uridine (U) tags, and are subsequently identified with high-throughput sequencing (HiTS). This thesis describes the development of the method, and its use to define records of ER- and mitochondria-localized RNAs in yeast. The method uncovered hundreds of localized mRNAs and non-mRNAs that interact with either the ER, the mitochondria, or both (dual-localized) in vivo. A subset of dual-localized RNAs in yeast have homologs that interact with both organelles in human cells, highlighting the conservation of the phenomenon. Among the dual-localized mRNAs are components of many multi-protein complexes in yeast, and the IRE1/ERN1 mRNA in yeast and human cells. These results indicate that the IRE1 mRNA dual-localization may be involved in the Ire1-dependent increase of mitochondrial respiration in response to ER stress. Further, the data produced facilitated the discovery of 3'UTR sequence motifs and RNA-binding

proteins that are potentially involved in the regulation of the localized RNAs. This work thus provides new insights into the functions and regulation of RNA localization and offers new capabilities to study RNA movements in vivo.

Acknowledgments

Completion of my Ph.D. is the culmination of a lot of personal effort and persistence, but finishing would've been difficult without support from my thesis advisor, Dr. Marvin P. Wickens. I thank the members of my thesis committee, Drs. Judith Kimble, Catherine A. Fox, Michael D. Sheets, and Richard M. Amasino for their helpful insights and support. I thank Drs. Alessandro Senes, and Sebastian Bednarek for allowing me to do rotation projects in their laboratories. I thank the Biochemistry Department at the UW-Madison, the Integrated Program in Biochemistry, and the UW-Madison community for being a nurturing environment for my development as a scientist.

I thank my colleagues, who were a source of support throughout my Ph.D. I thank members of the Wickens and Kimble laboratories for their helpful feedback and insights. Drs. Christopher P. Lapointe and Douglas F. Porter, thank you for your support and encouragement throughout my Ph.D. Drs. Shruti Sasaki, Scott Aoki, Kimberly Haupt, and Sarah Crittenden, thank you for your advice and insights. Natascha Buter, Carol C. Pfeffer, Peggy Kroll-Conner, Dr. Anne M Helsley-Marchbanks, Kate Ryan, and Elyse E. Meuer, thank you for your support. I want to thank Sarah Robinson for her friendship and for being a great bay mate. Brian Carrick and Drs. Amy Cooke, Daniel Wilinski, Carey Valley, Melanie A. Preston, and Zachary Campbell, thank you for being good coworkers.

I thank the many teachers who influenced me in my early education. I want to thank Dr. Johnie Scott (California State University Northridge) for his lessons and advice during Summer Bridge, 2003. I thank Dr. Maria Elena Zavala (California State University Northridge) for being a role model, advisor, and mentor. I thank my undergraduate thesis

advisor, Dr. Michael L. Summers (California State University Northridge), for giving me a solid foundation in science. I thank Dr. Marcelo Tolmasky (California State University Fullerton), and Drs. Angeles Zorreguieta and Rodrigo Sieira (Fundacion Instituto Leloir, Buenos Aires, Argentina) for their teachings and support in my scientific training.

I thank the funding programs that supported my education and scientific training. I thank the California State University Educational Opportunity Program (CSU EOP), the Federal Student Loan, Federal Pell Grant, and the National Science & Mathematics Access to Retain Talent (SMART) programs (United States Department of Education) for helping me pay for my undergraduate education. I thank the RISE pre-Doctoral and MHIRT International Research (National Institutes of Health) Fellowships for supporting my undergraduate research. I thank the Integrated Program in Biochemistry (IPiB), The National Institute on Minority Health and Health Disparities (NIMHD) Research Diversity Supplement awarded on my behalf to NIH grant (GM50942) to M.W. and the E.W. Hopkins fellowship for supporting my graduate research.

I thank my family, whom I love dearly, for their love, support, and their advice throughout my life and my Ph.D. I want to thank my wife, Karina A. Medina for her unwavering support and advice, and for sharing her life with me. I thank my daughter, Victoria K. Medina for loving me and for allowing me to see the world through the eyes of a child again. I want to thank my parents, Maria. C. Medina-Muñoz and Manuel Medina-Lizalde for the sacrifices they made to give my siblings and me opportunities that they never had, and for teaching me to be respectful of others, to work hard, and to sacrifice for my family. I thank my sister Maria D. Medina for her loving support and advice throughout my life and my Ph.D. I want to thank my brother Manuel D. Medina, my sisters

Christina and Ventura Medina, my godfather, Leonardo Viramontes, for their love and support. Thank you to my in-laws, Jesus and Maria-Elena Vasquez, for their generous and continuous support.

Table of Contents

Thesis Summary ..... i-ii

Acknowledgements ..... iii-v

Table of Contents ..... vi-viii

Chapter 1- An introduction to RNA localization 1-30

Cover page 1

Introduction 2-12

References 13-30

Chapter 2- Records of RNA localization through covalent tagging 31-178

Cover page 31

Abstract 32

Introduction 33-34

Results 35-46

Discussion 47-50

Materials and Methods 51-59

Acknowledgements 60

References 61-78

Main Figures 79-90

Supplementary Figures 91-108

Supplementary Tables 109-178

Supplementary Table I. ER-enriched RNAs: GO Terms 109-116

Supplementary Table II. Mitochondria-enriched RNAs: GO Terms 117-121

Supplementary Table III. 133 mRNAs common to Mitochondria tagging and Mitochondrial Profiling: GO Terms 122-125

Supplementary Table IV. Mitochondria tagging Unique vs Mitochondrial Profiling: GO Terms 126-130

Supplementary Table V. Mitochondrial Profiling Unique vs Mitochondria tagging: GO Terms 131-133

Supplementary Table VI. ER tagging Unique vs Mitochondria Tagging: GO Terms 134-139

Supplementary Table VII. Mitochondria Tagging Unique vs ER tagging: GO Terms 140-143

Supplementary Table VIII. Yeast Dual-tagged RNAs: GO Terms .. 144-150

Supplementary Table IX. 45 RNAs tagged about equally by both ER- and Mito-PUP 151-152

Supplementary Table X. Dual-localization conservation in yeast and HEK293T cells 153-156

Supplementary Table XI. Dual-, and ER- or Mito-PUP-tagged complex components 157-174

Supplementary Table XII. Tagged non-mRNAs 175-178

Chapter 3- Perspectives and future directions 179-193

Cover page 179

Perspectives 180-187

References 188-193

Chapter 1

Post-transcriptional Regulation by RNA localization: An introduction.

Overview of RNA localization

Eukaryotic gene expression is compartmentalized and involves cooperation among a staggering number of biomolecules. The process begins in the nucleus with the actions and control of RNA polymerase II (pol II) on DNA, in the form of chromatin. Pol II transcribes the DNA sequence into a single RNA strand. Upon emergence from Pol II, even *during* transcription, the RNA is immediately bound by RNA-binding proteins (RBPs) and non-coding RNAs (ncRNAs). The bound factors serve as scaffolds that link the pre-messenger RNA (pre-mRNA) to components that drive processing (i.e., splicing, 5' and 3' end maturation) into mature mRNA. The mRNA not only possesses instructions for the translation of a specific protein, but also contains non-coding regions (untranslated regions, or "UTRs") in the upstream (5' UTR) and downstream (3'UTR) that flank the coding sequences. These regions enable multiple forms of regulation.

The sequence and conformation of the 3' UTR often are critical for post-transcriptional regulation. RNA sequences and structures in the 3' UTR (*cis*-elements) often function as binding sites for RBPs and microRNAs (miRNAs) (*trans*-acting factors) that link the mRNA to effector proteins. Certain RNA-binding proteins associate with the 3'UTR in the nucleus (1-3) and create messenger ribonucleoprotein complexes ("mRNPs") (4). mRNPs protect the mRNA from the nuclear surveillance machinery and mark it for export from the nucleus into the cytoplasm. In the cytoplasm, the constellation of 3'-bound factors is remodeled, including the binding of specific RBPs and RNPs. These bound factors yield distinct effects on mRNA stability, translation, and localization.

The 3'UTR has classic roles in mRNA stability and translation. For example, the AAUAAA hexamer (and variants) located in the 3' UTR of pre-mRNAs promotes their

cleavage and polyadenylation (5). The poly(A) tail protects mRNAs from the surveillance machinery, while its interactions with the poly(A)-binding protein (PAB) promote translation (6, 7). mRNA decay after 3’ end maturation is controlled by additional factors, such as the Pumilio-Fem3 mRNA binding factor proteins (“PUF proteins”) (8). PUF proteins are conserved from yeast to humans, bind the 5'-UGUANAUA-3' motif, and recruit factors that promote mRNA turnover or translation (8-10). Many other 3’UTR-binding protein families, and small RNAs, are similarly implicated in controlling mRNA fate, underscoring the role of the 3’ UTR in mRNA metabolism (11).

Recent work has revealed that 3’UTRs have a more extensive regulatory repertoire than once appreciated. For example, in yeast and human cells, certain 3’ UTRs mediate interactions between the protein translated from the coding region and RBPs associated with the 3’ UTR (12). These UTR-mediated interactions have been proposed to concentrate components for faithful assembly of multi-subunit complexes, to influence the function of the encoded protein, and to drive protein localization independent of mRNA movement (12).

Superimposed on these mechanisms of control, the regulatory potential of 3’UTRs is diversified through RNA processing. Alternative polyadenylation sites located in the 3’ UTR of the same pre-mRNA species can yield mature mRNAs with distinct *cis*-element combinations, and therefore transcripts with different stability and translation rates can be produced from the same gene (13). Which factors bind and exert control depends on RNA structures that conceal or reveal *cis*-elements, levels of the RBPs and their interactors, and post-translational protein modifications (PTMs) (12). 3’ UTRs can also be transcribed independent of the coding sequence or generated via endonucleolytic cleavage to yield

3’ UTR fragments that regulate gene expression *à la* ncRNA (12). 3’ UTRs thus offer many ways to control gene expression.

Origins of the field of RNA localization

The ideas that led to the discovery of RNA localization rose from observations of development in early embryos. In the late nineteenth century, the German scientist, Wilhelm Roux, first postulated that early divisions (cleavage) of a fertilized oocyte are partially driven by localized “cytoplasmic determinants”. In the early twentieth century, an American embryologist, E. B. Wilson, proposed that localized “morphogenic potential” resident in specific regions drives early development (14). Forty-six years later, Eric H. Davidson and Roy J. Britten postulated that the localized morphogenic potential may include mRNAs since the potential could be inactivated by ultraviolet light and RNase treatments (15). The concept of RNA localization began to emerge, though no specific mRNAs with that property had been identified.

Several independent experiments provided the first direct evidence for RNA localization. In the early 1980s, Steward and Levy found polyribosomes associated with the base of neural dendrites in rats (16). The localized molecules appeared to undergo local regulation, as injury to the neuronal tissue activated the polyribosomes (17). After, Jefferey and colleagues observed that the actin mRNA was highly concentrated in the myoplasm of ascidian embryos, a striking result as only 5% of the total poly(A)$^+$ RNA was detected at that location (18).

A series of breakthroughs in mRNA localization emerged from studies of pattern formation during early development of *Drosophila melanogaster* (fruit fly) embryos (19-

24). In particular, the morphogen-encoding mRNA, *bicoid*, was localized to the anterior pole of oocytes in early development (19, 25). Local translation at the anterior pole generated a Bicoid protein gradient that helped pattern the anterior of the embryo (19, 26, 27). Similarly, pole plasm placement in the posterior of the fly embryo involves localization of *oskar* mRNA to that location, and mesoderm induction in the vertebrate *Xenopus* involves *Vg1* mRNA localization to the vegetal pole (21-23). Thus, RNA localization had gone from a theory to biological phenomenon, and the nascent field of RNA localization had emerged.

RNA localization today

mRNA localization is advantageous to the cell. A single localized mRNA molecule is translated many times, providing an energetic advantage over localization of protein molecules (28). Asymmetric translation – that is, preferential translation of an mRNA at a specific site– sequesters potentially toxic proteins and concentrates cell fate determinants and protein complex components where they are needed. The positive or negative effects on translation by pre-localized RBPs can also be linked to signaling pathways to help fine-tune protein synthesis in response to external stimuli (29-33).

mRNA localization occurs in a wide variety of cell types. In *Saccharomyces cerevisiae*, *ASH1* mRNA, which encodes a cell fate determinant, is moved from the mother to the daughter late in the mitotic cycle, such that its asymmetric translation only represses mating-type switching in the daughter cell (34). In chicken embryo fibroblasts, *β*-actin mRNA is moved to the leading edge of the cell so that its translation there supplies the actin demanded by cell motility (35). As with *bicoid*, *oskar* mRNA is localized to the posterior to mark the site of germ plasm placement, and its mis-localization to the anterior

misplaces the germ plasm there (22, 36). In *Aplysia californica* (giant sea hare), synapses between sensory neurons and motor neurons cause rapid recruitment of *sensorin* mRNA to the contact sites (37). In plants, *prolamine* and *glutelin* storage protein mRNAs in seeds are localized to cortical endoplasmic reticulum (cER) subdomains that facilitate endomembrane transport (38, 39), and in *Arabidopsis* flowering can be triggered via movement of FT mRNA from leaves to the shoot apex (40).

Many more RNAs than once appreciated are localized than once appreciated. Large-scale mRNA localization is vital in certain organelles. For example, hundreds of mRNAs are localized to the ER for co-translational translocation across the ER membrane for the secretory pathway (27, 33). Similarly, hundreds of nuclear-encoded mRNAs are localized to the mitochondria to supply the organelle with proteins required for its biosynthesis, and for metabolism (35, 41). Remarkably, a large-scale FISH study identified thousands of localized RNAs in early fly embryos (42). Thus, many RNAs are localized, and the phenomenon appears to be commonplace in eukaryotes.

RNA localization mechanisms

Several themes are conserved across all RNA localization mechanisms observed to date. For example, most include RNA-binding proteins (RBPs) that physically bind mRNAs to repress translation while the mRNA is in transit (30). “Zip-codes,” which are sequence motifs or secondary structures on the mRNA, serve as association sites for RBPs and are also common. While these are typically located in the mRNA 3’ untranslated regions (UTRs), they can also be in the coding sequences (CDS) or 5’ UTRs (43). Finally, most mechanisms use anchors that bind the localized RNAs to prevent de-localization via diffusion (30, 44).

mRNAs are localized by at least three distinct mechanisms: active transport, diffusion followed by local entrapment, and localized stability. We consider each in turn.

Active transport hinges on the association of mRNAs with motor proteins (myosins or kinesins) and allows for their directed movement along the cytoskeleton (actin or myosin) (30, 44). For example, *ASH1* mRNA is localized via its interaction with the myosin motor, Myo4p, in a complex that includes the RBP She2p associated with the *ASH1* 3'UTR, and the adapter She3p that links the mRNP to the motor (34, 45-47). Myo4p then treks along actin cables that traverse the mother-daughter axis to the bud-tip, where *ASH1* is locally anchored by Bni1p (34, 45, 48, 49).

Passive diffusion relies on cytoplasmic flows (rather than motors) to direct mRNAs, and on localized anchors that "catch" and tether the mRNA at its destination (30, 44). In fly development, cytoplasmic flows direct Nanos mRNA to the posterior oocyte pole of the embryo, where an anchor immobilizes it (50).

Selective stabilization works by protection of mRNAs that are anchored to the target site while mRNAs elsewhere are degraded (30, 44). For example, heat shock protein 83 (hsp 83) mRNA is found concentrated at the posterior pole of fruit fly embryos because the non-localized form is degraded while the localized form is not (51).

The same outcome – localization of mRNAs to specific sites in the cytoplasm – is the result of at least three distinct mechanisms. The mechanistic variety is likely the result of independent events in evolution, and it implies that mRNA localization increases cellular fitness. Indeed, despite the molecular difference between these mechanisms, they all ensure that protein is made at the right place and at the right time. The importance

of protein targeting by localization is also demonstrated by the devastating defects that are caused by mis-localization (52, 53). The variety of mechanisms and importance of localization hint that other ways to move RNAs await detection, and both existing and emerging techniques will assist in their discovery.

Imaging methods to study localization

Imaging techniques are commonly used to study mRNA localization. *in situ* hybridization (ISH), one of the earliest approaches uses anti-sense oligonucleotides ("probes") directed at the RNA of interest in a chemically fixed and permeabilized tissue and modified with molecules that emit a detectable signal (54-56).

The signals used in detection have greatly improved and are an active area of research. In early studies, radioactive isotopes (i.e., tritium, P32, etc.), antibodies, fluorophores, biotin, and enzymes were all found to be suitable labels (55-60). Fluorescently labeled probes (FISH) are also commonly used given their economy, their sensitivity for single mRNA quantitation, and the availability of spectrally distinct labels for simultaneous detection of multiple species (61, 62, 63).

Although spectral limitations initially limited FISH experiments, multiplexing strategies (Spectral barcoding, FISSEQ, and MERFISH) now permit the detection of thousands of mRNAs simultaneously (64-66). Strategies employed to increase signal where molecules are too short to accommodate FISH probes includes increasing the number of binding sites for fluorescent probes (RNAscope, Hybridization chain reaction, Direct *in situ* RT-PCR, and Padlock probes), and reducing non-specific probe binding (LNA-FISH (67-73). In addition, improvements to sample preparation and modulation of

probe concentration have cut the hybridization time to minutes (74, 75). A major drawback of ISH-based approaches, however, is that they require cell fixation, which can change RNA levels, alter cellular structures, and potentially cause de-localization (76-78).

Fluorescent RNA probes coupled with fluorescence microscopy have enabled a range of strategies to visualize RNA localization as it occurs *in vivo.* Localization of fluorescent micro-injected mRNAs can be observed in living cells (79). However, the reporters are transcribed *in vitro* so their movements may be artifactual, and excess reporter causes high background. Other techniques use fluorescent probes that bind endogenous RNAs, and signal to noise can be increased via self-binding probes (MTRIP), molecules that fluoresce only when bound the target RNA (Molecular beacons, ECHO, and FIT), or with probes that have inducible fluorescence (RNA aptamers) (80-85).

Engineered RNAs and proteins that tether a fluorescent moiety can also be used to track RNAs. A common strategy adds the binding site for the MS2 virus coat protein (MCP) to the 3' UTR of an mRNA, and the *trans*-gene is co-expressed with the coat protein fused to GFP (MCP) (34). The mRNA movement is seen as a fluorescent spot after the MCP-GFP binds its cognate site so that the distinct mRNA movements can be observed *in vivo* (34). An advantage of this approach is that distinct RNA-coat protein systems and proteins with distinct spectral profiles can be used to track several RNAs simultaneously *in vivo* (86, 87). However, this system can suffer from high background, and the MCP binding site can block 5' to 3' degradation (34, 88-90). Other systems circumvent these issues using fluorescent proteins (e.g., GFP) fused to factors that are required for localization (e.g., She2p-GFP); another that uses fluorescent proteins of engineered RNA-binding specificity; and another that uses nuclease defective Cas9-GFP

with RNA species-specific guide RNAs (91-94). These techniques are powerful, but they require species-specific probes and are thus impractical to screen many locations simultaneously for localized RNAs.

Transcriptome-wide approaches

Methods to identify all RNAs at a specific location, across the transcriptome, are needed to complement the many approaches that rely on imaging. Important early studies identified RNAs in specific, purified organelles, and later used cross-linking, immunoprecipitation, and microarrays (RIP-Chip) for similar purposes (95-97). These approaches yielded important findings, including the identification of hundreds of ribosome-bound mRNAs associated with cellular membrane systems, and identified others that co-localize with the well-studied *ASH1* mRNA (98-107). The advent of RNA-seq enabled new opportunities and more definitive answers (108-111). The RNA-seq technique touted greater specificity, sensitivity, and dynamic range than microarray (112-117). Indeed, RNA-seq can identify hundreds of membrane-associated mRNAs that were missed by microarray analysis (118, 119), and membranes could now be screened without gene-specific ISH or microarray chip probes.

Contemporary RNA-seq-based methods circumvent biochemical isolation of sites. “Proximity-specific ribosome profiling,” developed in the Weissman group, identifies mRNAs that are engaged by ribosomes near a membrane-anchored biotin ligase (41, 120). Avi-tagged ribosomes are biotinylated by the ligase, immunoprecipitated, and the associated mRNAs sequenced (41, 120). Using ribosome-protected footprints as a proxy, proximity profiling was used to deduce mRNA translation efficiencies near the ER and mitochondria, as well as a diversity of other applications unrelated to localization (41, 120,

121). While powerful, detection of RNAs by ribosome profiling requires that they are engaged in translation, and thus mRNAs that are not being translated – whether they are repressed mRNAs or ncRNAs – are missed.

To circumvent this issue, APEX-based methods, in which mRNAs proximal to a site-anchored peroxidase (APEX) are labeled, purified, and identified, were developed. In these approaches, the anchored APEX catalyzes the formation of biotin-phenoxyl radicals when biotin-phenol (BP) and hydrogen peroxide (H_2O_2) is added to cultured cells (122). In the first iteration, termed “APEX-Rip,” the radicals diffuse and covalently biotinylate nearby proteins, which are then cross-linked to RNA with formaldehyde, immunoprecipitated. The associated RNAs are then sequenced (122). APEX-Seq later circumvented the need for protein association by enabling biotinylation of any proximal RNA (123). These methods yield “snapshots” of RNA localization – the RNAs in the vicinity of the anchored peroxidase are labeled at the instant that the reactive agent is added to the cells. However, RNAs that contact a site outside of the selected time window are missed, and thus a method that enables genome-wide detection of localized RNAs at any point in the lifetime of cells was needed.

In this thesis, I report the development of a strategy to detect RNAs that contact any site in a general and genome-wide manner. An enzyme that adds uridines to the 3’ ends of RNAs is anchored to a specific location in the cell, such that only RNAs that encounter it *in vivo* are modified. The modified RNAs are then identified with high throughput sequencing (HiTS). I used the method to detect RNAs located at the endoplasmic reticulum (ER) and mitochondrial outer membrane (MOM) in *Saccharomyces cerevisiae*. Hundreds of RNAs were tagged by the organelle-anchored

PUPs, and a subpopulation of mRNAs that contact multiple organelles was identified. The approach, which I term “Localized RNA Tagging,” should be adaptable to other agents that result in covalent modification. The strategy provides a cumulative record of where individual RNAs have been within the cell.

REFERENCES

1. Xie X, Lu J, Kulbokas EJ, Golub TR, Mootha V, Lindblad-Toh K, et al. Systematic discovery of regulatory motifs in human promoters and 3′ UTRs by comparison of several mammals. Nature. 2005;434(7031):338-45.

2. Friedman RC, Farh KK, Burge CB, Bartel DP. Most mammalian mRNAs are conserved targets of microRNAs. Genome Res. 2009;19(1):92-105.

3. Kress TL, Yoon YJ, Mowry KL. Nuclear RNP complex assembly initiates cytoplasmic RNA localization. The Journal of Cell Biology. 2004;165(2):203.

4. Mitchell SF, Parker R. Principles and properties of eukaryotic mRNPs. Mol Cell. 2014;54(4):547-58.

5. Bienroth S, Keller W, Wahle E. Assembly of a processive messenger RNA polyadenylation complex. The EMBO journal. 1993;12(2):585-94.

6. Dreyfus M, Régnier P. The poly (A) tail of mRNAs: bodyguard in eukaryotes, scavenger in bacteria. Cell. 2002;111(5):611-3.

7. Gray NK, Coller JM, Dickson KS, Wickens M. Multiple portions of poly(A)-binding protein stimulate translation in vivo. The EMBO journal. 2000;19(17):4723-33.

8. Wickens M, Bernstein DS, Kimble J, Parker R. A PUF family portrait: 3'UTR regulation as a way of life. Trends Genet. 2002;18(3):150-7.

9. Goldstrohm AC, Seay DJ, Hook BA, Wickens M. PUF protein-mediated deadenylation is catalyzed by Ccr4p. J Biol Chem. 2007;282(1):109-14.

10. Lee C-D, Tu Benjamin P. Glucose-Regulated Phosphorylation of the PUF Protein Puf3 Regulates the Translational Fate of Its Bound mRNAs and Association with RNA Granules. Cell Reports. 2015;11(10):1638-50.

11. Wickens M, Takayama K. Deviants — or emissaries. Nature. 1994;367(6458):17-8.

12. Mayr C. Regulation by 3'-Untranslated Regions. Annu Rev Genet. 2017;51:171-94.

13. Lutz CS. Alternative polyadenylation: a twist on mRNA 3' end formation. ACS Chem Biol. 2008;3(10):609-17.

14. Wilson EB. The cell in development and heredity: Third edition, revised and enlarged. New York : Macmillan, 1925.; 1925.

15. Davidson EH, Britten RJ. Note on the control of gene expression during development. Journal of Theoretical Biology. 1971;32(1):123-30.

16. Steward O, Banker GA. Getting the message from the gene to the synapse: sorting and intracellular transport of RNA in neurons. Trends Neurosci. 1992;15(5):180-6.

17. Steward O, Fass B. Polyribosomes Associated with Dendritic Spines in the Denervated Dentate Gyrus: Evidence for Local Regulation of Protein Synthesis During Reinnervation. In: Changeux JP, Glowinski J, Imbert M, Bloom FE, editors. Progress in Brain Research. 58: Elsevier; 1983. p. 131-6.

18. Jeffery WR, Tomlinson CR, Brodeur RD. Localization of actin messenger RNA during early ascidian development. Developmental Biology. 1983;99(2):408-17.

19. Driever W, Nüsslein-Volhard C. The bicoid protein determines position in the Drosophila embryo in a concentration-dependent manner. Cell. 1988;54(1):95-104.

20. Berleth T, Burri M, Thoma G, Bopp D, Richstein S, Frigerio G, et al. The role of localization of bicoid RNA in organizing the anterior pattern of the Drosophila embryo. The EMBO Journal. 1988;7(6):1749-56.

21. Ephrussi A, Dickinson LK, Lehmann R. oskar organizes the germ plasm and directs localization of the posterior determinant nanos. Cell. 1991;66(1):37-50.

22. Kim-Ha J, Smith JL, Macdonald PM. oskar mRNA is localized to the posterior pole of the Drosophila oocyte. Cell. 1991;66(1):23-35.

23. Melton DA. Translocation of a localized maternal mRNA to the vegetal pole of Xenopus oocytes Nature. 1987;328:80-2.

24. Johnstone O, Lasko P. Translational regulation and RNA localization in Drosophila oocytes and embryos. Annu Rev Genet. 2001;35:365-406.

25. Frigerio G, Burri M, Bopp D, Baumgartner S, Noll M. Structure of the segmentation gene paired and the Drosophila PRD gene set as part of a gene network. Cell. 1986;47(5):735-46.

26. Schupbach T, Wieschaus E. Maternal-effect mutations altering the anterior-posterior pattern of the Drosophila embryo. Roux Arch Dev Biol. 1986;195(5):302-17.

27. Frohnhofer HG, Nussleinvolhard C. Maternal Genes Required for the Anterior Localization of Bicoid Activity in the Embryo of Drosophila. Genes & Development. 1987;1(8):880-90.

28. St Johnston D. The intracellular localization of messenger RNAs. Cell. 1995;81(2):161-70.

29. St Johnston D, Brown NH, Gall JG, Jantsch M. A conserved double-stranded RNA-binding domain. Proceedings of the National Academy of Sciences of the United States of America. 1992;89(22):10979-83.

30. Martin KC, Ephrussi A. mRNA localization: gene expression in the spatial dimension. Cell. 2009;136(4):719-30.

31. Cajigas IJ, Will T, Schuman EM. Protein homeostasis and synaptic plasticity. The EMBO journal. 2010;29(16):2746-52.

32. Doyle M, Kiebler MA. Mechanisms of dendritic mRNA transport and its role in synaptic tagging. The EMBO journal. 2011;30(17):3540-52.

33. Besse F, Ephrussi A. Translational control of localized mRNAs: restricting protein synthesis in space and time. Nat Rev Mol Cell Biol. 2008;9(12):971-80.

34. Bertrand E, Chartrand P, Schaefer M, Shenoy SM, Singer RH, Long RM. Localization of ASH1 mRNA Particles in Living Yeast. Molecular Cell. 1998;2(4):437-45.

35. Du TG, Schmid M, Jansen RP. Why cells move messages: the biological functions of mRNA localization. Semin Cell Dev Biol. 2007;18(2):171-7.

36. Ephrussi A, Lehmann R. Induction of germ cell formation by oskar. Nature. 1992;358(6385):387-92.

37. Lyles V, Zhao Y, Martin KC. Synapse formation and mRNA localization in cultured Aplysia neurons. Neuron. 2006;49(3):349-56.

38. Li X, Franceschi VR, Okita TW. Segregation of storage protein mRNAs on the rough endoplasmic reticulum membranes of rice endosperm cells. Cell. 1993;72(6):869-79.

39. Okita TW, Choi SB. mRNA localization in plants: targeting to the cell's cortical region and beyond. Curr Opin Plant Biol. 2002;5(6):553-9.

40. Huang T, Bohlenius H, Eriksson S, Parcy F, Nilsson O. The mRNA of the Arabidopsis gene FT moves from leaf to shoot apex and induces flowering. Science. 2005;309(5741):1694-6.

41. Williams CC, Jan CH, Weissman JS. Targeting and plasticity of mitochondrial proteins revealed by proximity-specific ribosome profiling. Science. 2014;346(6210):748-51.

42. Lecuyer E, Yoshida H, Parthasarathy N, Alm C, Babak T, Cerovina T, et al. Global analysis of mRNA localization reveals a prominent role in organizing cellular architecture and function. Cell. 2007;131(1):174-87.

43. Singer RH. RNA zipcodes for cytoplasmic addresses. Current Biology. 1993;3(10):719-21.

44. Jansen RP. mRNA localization: message on the move. Nat Rev Mol Cell Biol. 2001;2(4):247-56.

45. Takizawa PA, DeRisi JL, Wilhelm JE, Vale RD. Plasma membrane compartmentalization in yeast by messenger RNA transport and a septin diffusion barrier. Science. 2000;290(5490):341-4.

46. Böhl F, Kruse C, Frank A, Ferring D, Jansen RP. She2p, a novel RNA-binding protein tethers ASH1 mRNA to the Myo4p myosin motor via She3p. The EMBO journal. 2000;19(20):5514-24.

47. Long RM, Gu W, Lorimer E, Singer RH, Chartrand P. She2p is a novel RNA-binding protein that recruits the Myo4p-She3p complex to ASH1 mRNA. The EMBO journal. 2000;19(23):6592-601.

48. Long RM, Singer RH, Meng X, Gonzalez I, Nasmyth K, Jansen R-P. Mating Type Switching in Yeast Controlled by Asymmetric Localization of ASH1 mRNA. Science. 1997;277(5324):383.

49. Beach DL, Salmon ED, Bloom K. Localization and anchoring of mRNA in budding yeast. Current Biology. 1999;9(11):569-S1.

50. Forrest KM, Gavis ER. Live imaging of endogenous RNA reveals a diffusion and entrapment mechanism for nanos mRNA localization in Drosophila. Curr Biol. 2003;13(14):1159-68.

51. Bashirullah A, Cooperstock RL, Lipshitz HD. Spatial and temporal control of RNA stability. Proceedings of the National Academy of Sciences. 2001;98(13):7025.

52. Dictenberg JB, Swanger SA, Antar LN, Singer RH, Bassell GJ. A direct role for FMRP in activity-dependent dendritic mRNA transport links filopodial-spine morphogenesis to fragile X syndrome. Dev Cell. 2008;14(6):926-39.

53. Driever W, Siegel V, Nusslein-Volhard C. Autonomous determination of anterior structures in the early Drosophila embryo by the bicoid morphogen. Development. 1990;109(4):811-20.

54. Pardue ML, Gall JG. Molecular hybridization of radioactive DNA to the DNA of cytological preparations. Proceedings of the National Academy of Sciences of the United States of America. 1969;64(2):600-4.

55. John HA, Birnstiel ML, Jones KW. RNA-DNA Hybrids at the Cytological Level. Nature. 1969;223(5206):582-7.

56. Buongiorno-Nardelli M, Amaldi F. Autoradiographic detection of molecular hybrids between RNA and DNA in tissue sections. Nature. 1970;225(5236):946-8.

57. Rudkin GT, Stollar BD. High resolution detection of DNA–RNA hybrids in situ by indirect immunofluorescence. Nature. 1977;265(5593):472-3.

58. Bauman JGJ, Wiegant J, Borst P, van Duijn P. A new method for fluorescence microscopical localization of specific DNA sequences by in situ hybridization of fluorochrome-labelled RNA. Experimental Cell Research. 1980;128(2):485-90.

59. Langer-Safer PR, Levine M, Ward DC. Immunological method for mapping genes on Drosophila polytene chromosomes. Proceedings of the National Academy of Sciences. 1982;79(14):4381.

60. Guérin-Reverchon I, Chardonnet Y, Chignol MC, Thivolet J. A comparison of methods for the detection of human papillomavirus DNA by in situ hybridization with biotinylated probes on human carcinoma cell lines: Application to wart sections. Journal of Immunological Methods. 1989;123(2):167-76.

61. Femino AM, Fay FS, Fogarty K, Singer RH. Visualization of Single RNA Transcripts in Situ. Science. 1998;280(5363):585.

62. Raj A, van den Bogaard P, Rifkin SA, van Oudenaarden A, Tyagi S. Imaging individual mRNA molecules using multiple singly labeled probes. Nature Methods. 2008;5:877.

63. Hopman AH, Wiegant J, Raap AK, Landegent JE, van der Ploeg M, van Duijn P. Bi-color detection of two target DNAs by non-radioactive in situ hybridization. Histochemistry. 1986;85(1):1-4.

64. Lubeck E, Cai L. Single-cell systems biology by super-resolution imaging and combinatorial labeling. Nature Methods. 2012;9:743.

65. Lee JH, Daugharthy ER, Scheiman J, Kalhor R, Ferrante TC, Terry R, et al. Fluorescent in situ sequencing (FISSEQ) of RNA for gene expression profiling in intact cells and tissues. Nat Protoc. 2015;10(3):442-58.

66. Chen KH, Boettiger AN, Moffitt JR, Wang S, Zhuang X. Spatially resolved, highly multiplexed RNA profiling in single cells. Science. 2015;348(6233):aaa6090.

67. Wang F, Flanagan J, Su N, Wang LC, Bui S, Nielson A, et al. RNAscope: a novel in situ RNA analysis platform for formalin-fixed, paraffin-embedded tissues. J Mol Diagn. 2012;14(1):22-9.

68. Dirks RM, Pierce NA. Triggered amplification by hybridization chain reaction. Proc Natl Acad Sci U S A. 2004;101(43):15275-8.

69. Choi HM, Beck VA, Pierce NA. Next-generation in situ hybridization chain reaction: higher gain, lower cost, greater durability. ACS Nano. 2014;8(5):4284-94.

70. Lossi L, Gambino G, Salio C, Merighi A. Direct in situ rt-PCR. Methods Mol Biol. 2011;789:111-26.

71. Nilsson M, Malmgren H, Samiotaki M, Kwiatkowski M, Chowdhary BP, Landegren U. Padlock probes: circularizing oligonucleotides for localized DNA detection. Science. 1994;265(5181):2085.

72. Lu J, Tsourkas A. Imaging individual microRNAs in single mammalian cells in situ. Nucleic Acids Res. 2009;37(14):e100.

73. Lu J, Tsourkas A. Quantification of miRNA abundance in single cells using locked nucleic acid-FISH and enzyme-labeled fluorescence. Methods Mol Biol. 2011;680:77-88.

74. Shaffer SM, Wu M-T, Levesque MJ, Raj A. Turbo FISH: a method for rapid single molecule RNA FISH. PloS one. 2013;8(9):e75120-e.

75. Zhang Q-C, Liu Q, Kang Z-J, Yu R-C, Yan T, Zhou M-J. Development of a fluorescence in situ hybridization (FISH) method for rapid detection of Ulva prolifera. Estuarine, Coastal and Shelf Science. 2015;163:103-11.

76. Küpper H, Seib LO, Sivaguru M, Hoekenga OA, Kochian LV. A method for cellular localization of gene expression via quantitative in situ hybridization in plants. The Plant Journal. 2007;50(1):159-87.

77. Fox CH, Johnson FB, Whiting J, Roller PP. Formaldehyde fixation. J Histochem Cytochem. 1985;33(8):845-53.

78. Schnell U, Dijk F, Sjollema KA, Giepmans BN. Immunolabeling artifacts and the need for live-cell imaging. Nat Methods. 2012;9(2):152-8.

79. Amrute-Nayak M, Bullock SL. Single-molecule assays reveal that RNA localization signals regulate dynein–dynactin copy number on individual transcript cargoes. Nature Cell Biology. 2012;14(4):416-23.

80. Santangelo PJ, Lifland AW, Curt P, Sasaki Y, Bassell GJ, Lindquist ME, et al. Single molecule–sensitive probes for imaging RNA in live cells. Nature Methods. 2009;6:347.

81. Tyagi S, Kramer FR. Molecular Beacons: Probes that Fluoresce upon Hybridization. Nature Biotechnology. 1996;14(3):303-8.

82. Kubota T, Ikeda S, Yanagisawa H, Yuki M, Okamoto A. Hybridization-Sensitive Fluorescent Probe for Long-Term Monitoring of Intracellular RNA. Bioconjugate Chemistry. 2009;20(6):1256-61.

83. Okamoto A. ECHO probes: a concept of fluorescence control for practical nucleic acid sensing. Chemical Society Reviews. 2011;40(12):5815-28.

84. Hövelmann F, Gaspar I, Ephrussi A, Seitz O. Brightness Enhanced DNA FIT-Probes for Wash-Free RNA Imaging in Tissue. Journal of the American Chemical Society. 2013;135(50):19025-32.

85. Paige JS, Wu KY, Jaffrey SR. RNA mimics of green fluorescent protein. Science. 2011;333(6042):642-6.

86. Daigle N, Ellenberg J. LambdaN-GFP: an RNA reporter system for live-cell imaging. Nat Methods. 2007;4(8):633-6.

87. Larson DR, Zenklusen D, Wu B, Chao JA, Singer RH. Real-time observation of transcription initiation and elongation on an endogenous yeast gene. Science. 2011;332(6028):475-8.

88. Rackham O, Brown CM. Visualization of RNA–protein interactions in living cells: FMRP and IMP1 interact on mRNAs. The EMBO Journal. 2004;23(16):3346-55.

89. Wu B, Chen J, Singer RH. Background free imaging of single mRNAs in live cells using split fluorescent proteins. Scientific reports. 2014;4:3615.

90. Garcia JF, Parker R. MS2 coat proteins bound to yeast mRNAs block 5' to 3' degradation and trap mRNA decay products: implications for the localization of mRNAs by MS2-MCP system. RNA (New York, NY). 2015;21(8):1393-5.

91. Ozawa T, Natori Y, Sato M, Umezawa Y. Imaging dynamics of endogenous mitochondrial RNA in single living cells. Nature methods. 2007;4(5):413.

92. Yamada T, Yoshimura H, Inaguma A, Ozawa T. Visualization of nonengineered single mRNAs in living cells using genetically encoded fluorescent probes. Analytical chemistry. 2011;83(14):5708-14.

93. Wang Y, Cheong C-G, Tanaka Hall TM, Wang Z. Engineering splicing factors with designed specificities. Nature Methods. 2009;6:825.

94. Nelles DA, Fang MY, O'Connell MR, Xu JL, Markmiller SJ, Doudna JA, et al. Programmable RNA Tracking in Live Cells with CRISPR/Cas9. Cell. 2016;165(2):488-96.

95. Schena M, Shalon D, Davis RW, Brown PO. Quantitative monitoring of gene expression patterns with a complementary DNA microarray. Science. 1995;270(5235):467-70.

96. Eisen MB, Spellman PT, Brown PO, Botstein D. Cluster analysis and display of genome-wide expression patterns. Proceedings of the National Academy of Sciences. 1998;95(25):14863-8.

97. Shalon D, Smith SJ, Brown PO. A DNA microarray system for analyzing complex DNA samples using two-color fluorescent probe hybridization. Genome Res. 1996;6(7):639-45.

98. Morris AJ, Dickman SR. Biosynthesis of ribonuclease in mouse pancreas. J Biol Chem. 1960;235:1404-8.

99. Glaumann H. Studies on the synthesis and transport of albumin in microsomal subfractions from rat liver. Biochim Biophys Acta. 1970;224(1):206-18.

100. Diehn M, Eisen MB, Botstein D, Brown PO. Large-scale identification of secreted and membrane-associated gene products using DNA microarrays. Nat Genet. 2000;25(1):58-62.

101. Marc P, Margeot A, Devaux F, Blugeon C, Corral-Debrinski M, Jacq C. Genome-wide analysis of mRNAs targeted to yeast mitochondria. EMBO Rep. 2002;3(2):159-64.

102. Lerner RS, Seiser RM, Zheng T, Lager PJ, Reedy MC, Keene JD, et al. Partitioning and translation of mRNAs encoding soluble proteins on membrane-bound ribosomes. RNA. 2003;9(9):1123-37.

103. Diehn M, Bhattacharya R, Botstein D, Brown PO. Genome-scale identification of membrane-associated human mRNAs. PLoS Genet. 2006;2(1):e11.

104. Casolari JM, Thompson MA, Salzman J, Champion LM, Moerner WE, Brown PO. Widespread mRNA association with cytoskeletal motor proteins and identification and dynamics of myosin-associated mRNAs in S. cerevisiae. PLoS One. 2012;7(2):e31912.

105. Shepard KA, Gerber AP, Jambhekar A, Takizawa PA, Brown PO, Herschlag D, et al. Widespread cytoplasmic mRNA transport in yeast: identification of 22 bud-localized transcripts using DNA microarray analysis. Proc Natl Acad Sci U S A. 2003;100(20):11429-34.

106. Sylvestre J, Vialette S, Corral Debrinski M, Jacq C. Long mRNAs coding for yeast mitochondrial proteins of prokaryotic origin preferentially localize to the vicinity of mitochondria. Genome Biol. 2003;4(7):R44.

107. Pyhtila B, Zheng T, Lager PJ, Keene JD, Reedy MC, Nicchitta CV. Signal sequence- and translation-independent mRNA localization to the endoplasmic reticulum. RNA. 2008;14(3):445-53.

108. Bainbridge MN, Warren RL, Hirst M, Romanuik T, Zeng T, Go A, et al. Analysis of the prostate cancer cell line LNCaP transcriptome using a sequencing-by-synthesis approach. BMC Genomics. 2006;7:246.

109. Nagalakshmi U, Wang Z, Waern K, Shou C, Raha D, Gerstein M, et al. The transcriptional landscape of the yeast genome defined by RNA sequencing. Science. 2008;320(5881):1344-9.

110. Lister R, O'Malley RC, Tonti-Filippini J, Gregory BD, Berry CC, Millar AH, et al. Highly integrated single-base resolution maps of the epigenome in Arabidopsis. Cell. 2008;133(3):523-36.

111. Mortazavi A, Williams BA, McCue K, Schaeffer L, Wold B. Mapping and quantifying mammalian transcriptomes by RNA-Seq. Nat Methods. 2008;5(7):621-8.

112. Wang Z, Gerstein M, Snyder M. RNA-Seq: a revolutionary tool for transcriptomics. Nature Reviews Genetics. 2009;10:57.

113. Wilhelm BT, Landry JR. RNA-Seq-quantitative measurement of expression through massively parallel RNA-sequencing. Methods. 2009;48(3):249-57.

114. Zhao S, Fung-Leung WP, Bittner A, Ngo K, Liu X. Comparison of RNA-Seq and microarray in transcriptome profiling of activated T cells. PLoS One. 2014;9(1):e78644.

115. Wang C, Gong B, Bushel PR, Thierry-Mieg J, Thierry-Mieg D, Xu J, et al. The concordance between RNA-seq and microarray data depends on chemical treatment and transcript abundance. Nat Biotechnol. 2014;32(9):926-32.

116. Liu Y, Morley M, Brandimarto J, Hannenhalli S, Hu Y, Ashley EA, et al. RNA-Seq identifies novel myocardial gene expression signatures of heart failure. Genomics. 2015;105(2):83-9.

117. Li J, Hou R, Niu X, Liu R, Wang Q, Wang C, et al. Comparison of microarray and RNA-Seq analysis of mRNA expression in dermal mesenchymal stem cells. Biotechnol Lett. 2016;38(1):33-41.

118. Mercer Tim R, Neph S, Dinger Marcel E, Crawford J, Smith Martin A, Shearwood A-Marie J, et al. The Human Mitochondrial Transcriptome. Cell. 2011;146(4):645-58.

119. Reid DW, Nicchitta CV. Diversity and selectivity in mRNA translation on the endoplasmic reticulum. Nature Reviews Molecular Cell Biology. 2015;16:221.

120. Jan CH, Williams CC, Weissman JS. Principles of ER cotranslational translocation revealed by proximity-specific ribosome profiling. Science. 2014;346(6210):1257521.

121. Ingolia NT, Ghaemmaghami S, Newman JR, Weissman JS. Genome-wide analysis in vivo of translation with nucleotide resolution using ribosome profiling. Science. 2009;324(5924):218-23.

122. Kaewsapsak P, Shechner DM, Mallard W, Rinn JL, Ting AY. Live-cell mapping of organelle-associated RNAs via proximity biotinylation combined with protein-RNA crosslinking. eLife. 2017;6:e29224.

123. Fazal FM, Han S, Kaewsapsak P, Parker KR, Xu J, Boettiger AN, et al. Atlas of Subcellular RNA Localization Revealed by APEX-seq. bioRxiv. 2018:454470.

Chapter 2

Records of RNA localization through covalent tagging

This work is submitted and under review at a peer-reviewed journal: I developed the method, performed all the experiments and analyses, and I generated all the data shown. Authors of the paper will be Hugo C. Medina-Muñoz, Christopher P. Lapointe, Douglas F. Porter, and Marvin Wickens.

ABSTRACT

RNA movements and localization pervade biology, from embryonic development to disease. To identify RNAs at specific subcellular locations, we anchored a uridine-adding enzyme at those sites, which then marked RNAs in its vicinity with 3’ terminal uridines. RNAs were tagged independent of their translation status, and included not only mRNAs, but also ncRNAs and ncRNA processing intermediates. A battery of RNAs, including the stress sensor, *IRE1*, were tagged at both ER and mitochondria, and reveal RNAs whose dual localization is conserved from yeast to human cells.

INTRODUCTION

Localization of specific RNAs to discrete sub-cellular locations was first observed in striking examples during early development[1-6] and in yeast[7]. We now know RNA localization is widespread, and critical in secretion, patterning, cell fate determination, and neurobiology[8,9]. Many mRNAs in embryos and mammalian cells exhibit discrete patterns of localization, emphasizing its breadth. Localization hinges on interplay between sequences in the RNAs, RNA binding proteins, molecular motors, and subcellular structures, such as the ER or cytoskeleton[10-13]. Advancements in FISH[14-17], live imaging[18-20] and sequencing-based methods including proximity-specific ribosome profiling[21,22], APEX-RIP[23] and APEX-Seq[24,25] are very powerful, but typically provide snapshots of localized RNAs, since cells do not survive the required treatments. They also often require either custom oligonucleotide probes or sophisticated equipment. Approaches are needed to identify RNAs at any subcellular location across the entire transcriptome, and to do so in living cells.

We developed a strategy that registers RNAs as they interact with a cellular site *in vivo*. Our approach builds on RNA Tagging, used initially to identify RNAs that bind cognate proteins *in vivo*[26]. In those studies, the RBP to be tested was linked to an enzyme that adds uridine residues (termed a “PUP,” “TUTase”[27], or TENT[28]) to the RNA. When the chimeric protein bound an RNA molecule *in vivo*, the end was “tagged” with uridine residues. The number of uridines added to each mRNA molecule mirrored the affinity of its sites for the RBP, and likely the integrated dwell time of the RBP on that particular RNA molecule[26], as observed *in vitro*[29].

Here we describe Localized RNA Tagging, in which RNAs at specific sites are identified, focusing on the ER and mitochondria of the yeast, *S cerevisiae.* A U-adding enzyme is attached to an anchoring protein that resides at a specific location. The anchored enzyme tags RNA molecules it encounters *in vivo*, which are identified through deep sequencing. Since cells live during tagging, the number of U's added likely mirrors the cumulative time that an individual RNA molecule spends at that location.

RESULTS

Broad-specificity tagging

We first designed a protein construct intended to tag most or all cellular RNAs, and so provide a baseline for comparison. We selected *C. elegans* PUP-2[27] as the tagging agent. This enzyme adds uridines to RNA 3' ends, lacks RNA-binding domains, and has been used to identify RNAs bound to specific proteins in living cells[26,30,31] (Figure 1A). To facilitate tagging of most RNAs in the cytoplasm, we linked PUP-2 to the RNA-recognition motifs (RRMs) of yeast poly(A)-binding protein, generating a construct here termed “PUP alone (+PAB).” A control chimera, “PUP alone (-PAB),” was constructed that lacked the PAB RRMs (Figure 1A). Both proteins were expressed under control of the *SEC63* promoter[21] (used later to enable direct comparison to RNAs at the ER).

To identify tagged RNAs and the number of U’s they received, we prepared polyadenylated RNA via oligo(dT) selection and ribosomal RNA depletion[26] (see *Methods*). RNAs then were reverse-transcribed using a primer designed to enrich uridylated RNAs (Supp. Figure 1A). The resulting DNA libraries were analyzed on an Illumina sequencer using paired-end sequencing (Supplementary Fig. 1A). Sequencing data were processed using a computational pipeline[26] that identified all tagged RNAs, and for all tagged RNAs, the number of reads obtained and number of U's added (Supplementary Fig. 1B, C).

The two “PUP alone” proteins added U’s to cellular RNAs with very different efficiencies. PUP alone (+PAB) yielded 3-4 orders of magnitude more tagged reads per million (TRPMs) across all U-tag lengths (Supplementary Fig. 2A). PUP alone (+PAB)

was more reproducible (Figure 1B, C, Supplementary Fig. 2B, C), and yielded more U-tagged species (Figure 1D, Supplementary Fig. 2D). Tagging efficiency was correlated with RNA abundance with both proteins (Supplementary Fig. 2E). Tagged RNAs were ranked based on the number of U's added and number of reads obtained (Figure 1E), which revealed the dramatic differences with and without the PAB RRMs. We adopted the protein with RRMs for subsequent experiments due to its efficiency and ability to tag most cellular RNAs. We refer to it simply as "PUP alone" hereafter.

ER-localized RNA tagging

To detect RNAs that encounter the endoplasmic reticulum (ER), we fused the PUP alone chimera to the C-terminus of Sec63p, a protein embedded in the ER (Figure 2A), and expressed the chimeric protein from the endogenous *SEC63* locus. The Sec63p chimera, termed "ER-PUP", is predicted to be co-translationally embedded into the ER membrane by three trans-membrane segments of Sec63p, and place the C-terminal PUP-2 domain in the adjacent cytosol[32]. As predicted, GFP fluorescence from ER-PUP mirrored the pattern reported for Sec63p, and co-localized with signal from the Sec61p-mCherry ER-marker[33,34] (Figure 2B), indicating that ER-PUP was anchored to the ER membrane.

To identify RNAs tagged by ER-PUP, we compared RNAs tagged with and without the Sec63p anchor, using the analytical tool DESeq2[35], a method that identifies the statistical strengths of observed differences in RNA populations (Supplementary Fig. 3A, B, C, D). The data were highly reproducible (Figure 2C, Supplementary Fig. 3E). The ER-anchored PUP selectively tagged 1,148 RNAs, which we refer to as "ER-enriched," while the unanchored PUP preferentially tagged 1,167 ("ER-depleted"). Many mRNAs tagged

by ER-PUP encoded secreted proteins[36] ("secretome mRNAs", *p*-value = 2.1 e^{-352}) and had ER-related gene ontology (GO) associations[37,38], which were reduced or missing among RNAs tagged less efficiently at the ER (Figure 3D, E; Supplementary Fig. 3F; and Table 1). Thus, the Sec63p anchor directed tagging to RNAs that encounter the ER *in vivo*.

To aid in further analyses, we grouped RNAs tagged by ER-PUP and the control, PUP alone, into five tiers based on U-tag lengths. RNAs with the longest tags were grouped in Tier 1 and those with the shortest tags in Tier 5 (Figure 2F). Within a tier, each RNA was ranked by the fold-enrichments in that dataset relative to the other. With both ER-PUP and PUP alone, RNAs with the longest U-tags generally had the highest enrichment (Figure 2F). Among RNAs tagged by ER-PUP, the fraction of secretome mRNAs was highest in Tiers 1 and 2 (88% and 79%) and declined progressively to Tier 5 (25%) (Figure 2G). The control, PUP alone, yielded little enrichment or correlation with tiers (Figure 2F, G), demonstrating that ER-PUP preferentially tagged RNAs with ER-related functions.

To assess the relationship between ER-PUP enrichment and mRNA abundance, we binned all yeast RNAs into five tiers based on RNA seq[26] (FPKM), from most (Tier 1) to least abundant (Tier 5) (Supplementary Fig. 4A, B). The distribution of abundances of RNAs tagged by ER-PUP was much more similar across tiers as compared to mRNA abundances in the cell (Supplementary Fig. 4B). Indeed, highly abundant RNAs (Abundance Tiers 1&2) with secretome association were dramatically enriched by ER-PUP (4.6-fold enriched, *p*-value = 3.98e^{-233}) while ones that lack secretome association were depleted (2.9-fold depleted, *p*-value = 1.8e^{-74}, Supplementary Fig. 4C). Further, the

gamut of RNA abundances was represented across all ER-PUP tiers, while PUP alone tiers primarily contained the most abundant species (Supplementary Fig. 4D). Finally, the fraction of secretome mRNAs among ER-PUP tagged mRNAs dramatically exceeds that seen with PUP alone in tagging tiers 1, 2 and 3 (Supplementary Fig. 4E; see also Figure 2F, G), and is highest for the best-tagged RNAs in every abundance tier. Thus, the primary driver of ER-tagging is localization rather than abundance.

Many but not all ER-enriched RNAs are bound by ER-proximal ribosomes

mRNAs tagged by ER-PUP are predicted to include ones translated at or near the ER. We compared mRNAs identified in ER-tagging with those detected in proximity-specific ribosome profiling experiments that had used the same Sec63p anchor[21] (termed "ER profiling"). ER-profiling identifies ribosome-bound mRNAs near an ER-anchored biotin ligase that biotinylates Avi-tagged ribosomes[21]. 79% of mRNAs associated with Sec63-proximal ribosomes were also preferentially tagged by ER-PUP (4.7-fold enriched, *p*-value = 5.6 e^{-415}), and only 0.2% were tagged better by PUP alone than ER-PUP (70-fold depleted, *p*-value = 7.9 e^{-69}, Figure 3A). However, a sizable fraction (43%) of ER-PUP-enriched mRNAs were not identified via ER ribosome profiling (Figure 3A). By contrast, ER-PUP enriched mRNAs were depleted in mRNAs identified by mitochondria-specific ribosome profiling[22] (1.7-fold depleted, *p*-value = 7.3 e^{-6}, Supplementary Fig. 5A). Tagging also uniquely identified 453 mRNAs and 50 non-coding (nc) at the ER, while profiling detected 169 mRNAs not detected by tagging (Figure 3A, left panel, and Supplementary Fig. 5B). Thus, many but not all tagged RNAs were detected as translated at the ER under normal conditions.

ER-tagging detects RNAs seen in profiling only when ribosomes are arrested. Cycloheximide blocks translation elongation and so likely increases the time that ribosome-nascent chain complexes are near the ER-anchored biotin ligase in profiling [21,39]. mRNAs enriched by ER-tagging include those that are enriched by profiling only when ribosomes are trapped by cycloheximide treatment (Figure 3B). We suspect that tagging detects ribosome-bound mRNAs that have only brief interactions with the ER, and so can be detected independent of elongation arrest (Figure 3B). In that sense, tagging is more sensitive, detecting transient proximity to the ER.

We next analyzed the relationship between U-tag length and ribosome profiling. mRNAs detected by Sec63p-mediated profiling[21] were grouped into five tiers using k-means clustering, from highest ribosome association (Tier 1) to least (Tier 5, Supplementary Fig. 5C). mRNAs with the longest U-tags were more likely to associate with ER-proximal ribosomes (Tiers 1-3, *p*-value = $1.2e^{-40}$), and mRNAs were tagged regardless of their rank in profiling (Figure 3C). The most robustly ER-tagged mRNAs (Tiers 1 and 2) were more engaged with ribosomes, as inferred from profiling; poorly tagged RNAs progressively decreased in their associations with ribosomes[21] (Figure 3D). As expected, ER-tagged RNAs did not exhibit this correlation with RNAs translated by mitochondria-proximal ribosomes, as inferred from Om45p-mediated profiling[22] (Figure 3E).

Taken together, these findings indicate that tagging identified RNAs with ER-ribosome association, as well as RNAs that do not. Thus, tagging and profiling yield overlapping but non-identical sets of RNAs, and together provide a more complete view of RNAs that encounter the ER than does either approach alone.

Mitochondria-localized RNA tagging

To detect RNAs near the mitochondrial outer membrane, we inserted PUP downstream of the *OM45* gene, resulting in an Om45p-PUP-2 chimera, which we refer to as "Mito-PUP" hereafter. Om45p is predicted to be co-translationally inserted into the mitochondrial membrane with its C-terminal PUP-2 domain in the cytosol[40-45] (Figure 4A). GFP from Mito-PUP co-localized with the Tom70p-mCherry mitochondrial marker in yeast, and both proteins yielded fluorescence patterns comparable to those of the endogenous proteins fused to GFP[34] (Figure 4B).

Mito-PUP preferentially tagged mRNAs that encode proteins physically associated with mitochondria and mitochondrial functions. Compared to PUP alone, Mito-PUP tagged 598 RNAs at least two-fold more efficiently (mitochondria-enriched), and 465 RNAs less efficiently (mitochondria-depleted, Figure 4C, and Supplementary Fig. 6). The entire set of RNAs that were preferentially tagged by Mito-PUP had statistically significant association with mitochondria-related GO terms[37,38], and for mRNAs that encode mitochondria-associated proteins[46,47] (2-fold enriched, $p = 1.7e^{-30}$, Figure 4C, D, Table 2). mRNAs depleted from mitochondria by our DESeq2 analyses did not have these associations (Figure 4C, D). RNAs in the highest tagging tiers were more likely to encode mitochondrial proteins than those in lower tiers (Figure 4E, and Supplementary Fig. 7A). The efficiency of tagging at mitochondria also correlated with mitochondrial translation at that location, as judged by ribosome profiling[22] (3-fold enriched, *p*-value = $1.8\ e^{-34}$, Figure 4F, and Supplementary Fig. 7B). Together, these analyses strongly suggest that Mito-PUP preferentially tags mRNAs near mitochondria.

Despite the overlap between tagging and profiling, each method identified a unique set of mRNAs. Tagging and profiling detected 133 mRNAs in common, and these were enriched for mitochondrial functions by GO analysis (Table 3). The rank of commonly detected RNAs greatly differed between methods; for example, they trended toward longer uridine tags (Tiers 1-3) but tagging rank was reduced among RNAs detected most efficiently in ribosome profiling (Tier 1, Supplementary Fig. 7C, D). Instead, the common RNAs were distributed nearly evenly across the mid-range ribosome profiling tiers (Tiers 2-4), which likely indicates that differences in detection requirements influence the rank for each method (Supplementary Fig. 7C, D).

Mito-PUP tagged hundreds of RNAs that were not identified by ribosome profiling. Of these, 457 were mRNAs, and eight were ncRNAs (Supplementary Fig. 7E). Conversely, profiling identified 325 mRNAs that were not detected by tagging, but these were mostly lower abundance RNAs (Supplementary Fig. 7E, F). Of the RNAs uniquely identified by each method, those unique to tagging were associated with ion transport processes, and those unique to profiling were associated with tRNAs and respiration (Tables 4 & 5). Thus, tagging and profiling yield unique, but complementary results.

mRNAs localized to the outer periphery of mitochondria fall into two classes: Class 1, which require Puf3p for localization, and Class II, whose localization is independent of Puf3p.[48] A third group of mRNAs, termed Class 3, are translated in the cytoplasm, not near mitochondria.[48] Mito-PUP tags mRNAs localized near mitochondria, whether they require Puf3p for localization (Class 1, 3.4-fold enriched, $p = 6.0e^{-24}$) or not (Class 2, 3.5-fold enriched, $p = 3.1e^{-22}$). In contrast, Mito-PUP tags Class 3 mRNAs poorly, indicating those mRNAs are too far from the Om45p anchor to be tagged. Thus, localized tagging

specifically discriminates localization among classes of RNAs whose proteins are destined for the same organelle.

RNAs at both ER and mitochondria in yeast and human cells

Most RNAs were tagged by either ER-PUP or by Mito-PUP (Figure 5A), and so yielded GO enrichments anticipated for that organelle (Tables 6 & 7). For example, several components of the TOM (Tom70p, Tom40p. and Tom71p) and TIM (Tim18p, Tim50p, Tim22p, Tim44p, and Tim54p) protein import complexes exhibit high tagging only by Mito-PUP, while those that encode certain secreted proteins (e.g., Ecm14p and Pff1p), ER-resident chaperones and translocon components (e.g., Kar2p, Ssh1p, and Sec63p), and the ncRNA of the SRP particle, *SCR1*[49], were tagged only at the ER (Figure 5B).

Strikingly, however, a substantial fraction (ER: 23%, Mito: 44%) of all tagged mRNAs were detected by both ER-PUP and Mito-PUP (p-value = 4.7 e^{-63}; Figure 5A). Tagging of these mRNAs with both Om45p and Sec63p anchors suggests these mRNAs come near both the ER and mitochondrial outer membrane. As a whole, the dual-tagged mRNAs encoded primarily secreted proteins (4.9-fold enriched, p-value = 5.1e^{-115}, Figure 5C, Table 8), were translated (Figure 5D) and received longer tails at the ER (Figure 5E), suggesting a longer cumulative time at that location.

A second group of 45 shared RNAs were tagged roughly equally by ER- and mitochondria-anchored proteins (normalized to PUP alone in each location; Figure 5B, and Table 9). High-ranking, shared mRNAs of this type include ones associated with lipid biosynthesis (*ISC1*, *IPT1*, *YFT2*, and *TAZ1*), ion transport (*MDL1*, *MCH5*, and *CCC2*), RNA polymerase II transcription (*SNF11* and *BUR2*), a plasma membrane-associated

proteolipid (*PMP2*), and a GPI-anchored cell wall endonuclease (*EGT2*) (Figure 5B, and Table 9). These commonly-enriched mRNAs may reside where the two organelles are in close proximity[50,51] or move from one location to the other (see Discussion).

Localization of specific RNAs to the proximity of both ER and the outer mitochondrial membrane is conserved. We compared our tagging results to data recently reported from human embryonic kidney (HEK293T) cells using APEX-Seq[25]. The high fraction of RNAs tagged at both locations in yeast (ER: 268 of 1,148; Mitochondria: 268 of 598, Figure 5A, B) was mirrored in HEK293T cells[25], as was the identity of many of the RNAs (ERM: 50%; OMM: 67%, Supplementary Fig. 8A, B, C). Among the dual-tagged RNAs detected in both yeast (Figure 5B) and human cells (Supplementary Fig. 8C) were ones that encode functions linked to ERMES[51] (ER-mitochondria encounter structure), formed where ER and mitochondria are in close proximity. These included mRNAs that encode proteins and functions that are associated with MAMs[50,52] (ER-mitochondrial associated membranes) including transmembrane transporters (Figure 5B and Supplementary Fig. 8C, and Table 10), and proteins involved in lipid (*CAX4*, *LAC1*, *TGL1*, and *ALE1*) or glycoprotein (*ROT2*, *CAX4*, *OST6*) metabolism. Strikingly, the ER stress sensor, *IRE1/ERN1*[53-59] was detected at both organelles, consistent with the presence of Ire1p protein at both organelles[52], and the requirement for Ire1p for the increase of mitochondrial respiration during the UPR[60] (Figure 5B and Supplementary Fig. 8C, and Table 10).Conservation of many shared targets suggests the importance of their presence at both locales, particularly given the substantial differences between the two techniques.

mRNAs that encode components of multi-protein complexes (identified through GO annotations[37,38]) comprise three classes based on the range of locations between ER and mitochondria (Figure 5F, Table 11). Thirty-one complexes fell into Class A, and included dual tagged mRNAs (Figure 5F, Table 11; e.g., HRD1 ubiquitin ligase complex). Most strikingly, thirteen complexes fell into Class B, with mixtures of mRNAs tagged at one or the other location (Figure 5F; e.g., Prp19 complex). Ninety-three complexes were uniquely enriched by ER-PUP (e.g., the signal peptidase) and seventy-four by Mito-PUP (Class C; Figure 5F, Table 11, e.g., the 54S mitochondria ribosomal subunit). The presence of mRNAs for subunits in different locales suggests coordination to assemble the complexes, or that certain of the proteins have other roles.

Regulatory sites and RNA-binding proteins

RNA localization often is controlled by RNA-binding proteins (RBPs). We therefore identified sequence motifs in the 3'UTRs of RNAs identified by localized tagging using MEME[61], and compared those motifs to known RNA-binding specificities[26,62].

The top motif among RNAs tagged by Mito-PUP was a degenerate form of the Puf3p binding site (Supplementary Fig. 9A). Puf3p binds and controls nuclear-encoded mRNAs with mitochondrial functions, and participates in their localization near mitochondria[26,30,48,63-66]. The proportion of mito-tagged RNAs with such elements was similar across all tagging tiers (Supplementary Fig. 9B, dark blue line). This prompted re-analysis of Om45p-mediated profiling data[22]), which revealed the same phenomenon (Fig 9A, B, light blue line). Our findings suggest that Puf3p promotes mitochondrial localization of only certain mRNAs, and that others arrive there through other mechanisms[48].

ER-tagged RNAs were enriched for Bfr1p targets (*p*-value = 1.9 e^{-280}), consistent with the role of Bfr1p in the secretory pathway and RNA metabolism[26,67-71]; similarly, mitochondria-tagged RNAs were enriched for Puf3p targets (*p*-value = 1.2 e^{-26}) (Supplementary Fig. 9C). ER-tagged RNAs were moderately enriched among RNAs that bind Pub1p (*p*-value = 2.8e^{-36}), Mrn1p (*p*-value = 4.5e^{-16}), and Scp160p (*p*-value = 4.6e^{-11}); of these, only Scp160p is known to localize to the ER[72,73] (Supplementary Fig. 9D). Sec63-tagged mRNAs revealed AU- or U-rich motifs (Supplementary Fig. 9E). These analyses point to proteins likely involved in control of these mRNAs.

Non-coding RNAs and RNA metabolism

Analysis of tagged RNAs revealed connections between RNA metabolism and cell biology. ncRNAs from 53 genes were significantly enriched at mitochondria or the ER relative to the PUP alone control (Figure 6; three representative paired reads are shown for each type of RNA, and Table 12). *SCR1*, the RNA component of the Signal Recognition Particle[49], was the ncRNA tagged best by ER-PUP (Figure 5B, and Figure 6A); *HAC1* mRNA, which is critical in the UPR[53-59], also was detected (Figure 6A; see also Figure 5B).

21 tRNA-related transcripts were tagged at the ER. These lacked CCA, contained 3' extensions beyond the 3' end of the mature tRNA, and possessed poly(A) tails upstream of the uridines added in tagging (Figure 6B). Poly(A) is added to some ncRNAs as part of nuclear RNA surveillance, mediated by the TRAMP complex and exosome[74-77]. We obtained no reads upstream of anticodons, which may be due to the presence of modified bases that arrest reverse transcriptase[78-80] or RNA cleavage events that may leave tRNA halves[78,81]. Among proteins that participate in tRNA splicing[82], mRNAs

encoding Sen2p*,* a subunit of the endonuclease, were detected at the ER; while those encoding Tom70p, an enhancer of tRNA splicing *in vivo,*[83] was detected at mitochondria, where it also is part of a translocase (Figure 5B).

25 snRNA- and snoRNA-related RNAs were tagged by either ER- or Mito-PUPs. These included snRN7-L, which was tagged at both organelles (ER: Tier 3, Mito: Tier 4), and snR7-S and snR6, which were only tagged at the ER (Figure 6C). Yeast snRNAs can shuttle to the cytoplasm as part of their maturation, perhaps to help prevent inclusion of misprocessed snRNAs in the spliceosome[84]. Some snoRNAs were also tagged at one or both sites, including *NME1,* the RNA component of MRP that catalyzes RNA cleavage events[85] (Figure 6D; see also Figure 5B). While snoRNAs are thought to be restricted to the nucleus, failure to properly process their guanosine cap can cause their accumulation in the cytoplasm[86]. Together, the data on ncRNAs suggest tagging captures mature ncRNAs as well as ones undergoing maturation and surveillance.

DISCUSSION

Localized RNA Tagging identifies RNAs located to specific sites transcriptome-wide and is independent of hybridization, affinity purification, fractionation, cross-linking, or chemical treatments. RNAs tagged using Sec63p or Om45p displayed distinct properties consistent with each anchor. The number of uridines added to an individual RNA molecule likely reflects the integrated time it was at that location. mRNAs with longer U-tags were more likely to have predicted biological functions consistent with their location and to associate with local ribosomes. These findings mirror analyses of RNA-protein interactions using tagging, in which the number of uridines added to an individual RNA molecule correlated well with its binding affinity for the protein, as determined *in vitro*.[26,29] Other variables, such as the structure of specific RNAs, may also effect tagging efficiency.

Tagging provides a cumulative "record" of an RNA's movements, while the recently described APEX-Seq[25] approach yields a snapshot – a "registry" of RNA locations at a specific time. The two approaches are complementary and provide a fuller view of RNA movements than either alone. Similarly, localized tagging and global studies of RBPs are synergistic (e.g., Supp. Figure 9). For example, Puf3p binds to and controls expression and localization of nuclear-encoded mitochondrial mRNAs.[26,30,48,63-66] Mito-tagged RNAs often contained suboptimal binding sites for Puf3p, consistent with the existence Puf3p-independent mechanisms for mitochondrial localization. Comparison with profiling suggests other roles for optimal binding, perhaps including its ability to enhance rather than repress translation[87] (Supp. Figure 9B, C). ER-tagged RNAs contained novel motifs, some of which may be involved in the SRP-independent localization of mRNAs to the

ER[88] or may bind RBPs, such as Bfr1p. [26,71] Indeed, Bfr1p is implicated in the secretory pathway, co-purifies with secretory mRNPs and mRNAs, and localizes to the ER in a manner that requires its RNA binding activity.[26,67-71]

A specific and large subset of RNAs were tagged using both ER (Sec63p) and mitochondrial (Om45p) anchors. These “dual-tagged” RNAs might arise in three ways. First, they may be located where the two organelles are very close, perhaps as promoted by ERMES[51,89] (ER-mitochondria encounter structure). Second, a single RNA molecule may move between organelles. Certain dual-tagged RNAs are tagged poorly at one or both locations, suggesting transient interactions, much as RNAs tagged poorly by an RBP possess poor (if any) cognate binding sites[26]. Third, individual RNA molecules may go from the nucleus to either one or the other location, rather than between the two organelles. The mechanism of dual localization we detect is potentially independent of translation, since dual localization is very rare among mRNAs detected by yeast ribosome profiling at these two organelles[21,22], but a technical limitation may be at play: mRNAs might be translated near the ER or mitochondria, but not in a manner that enables detection by proximity profiling, which requires ribosomes with their exit tunnel near the membrane[21,22]. Underlying mechanisms may be identified through use of multiple tagging devices in the same cell, live imaging, [8,18-20,90] or strategies that track localization and translation simultaneously[91,92].

Dual localization of specific mRNAs is conserved between yeast and human cells, and may reflect proximity to MAMs. Dual localization may help integrate events between ER and mitochondria. IRE1 mRNA is exemplary, and is dual-localized in both yeast and human cells. Its dual localization may integrate inputs from both organelles and facilitate

coordinated responses, such as the Ire1p-dependent rise in respiration after ER stress in yeast[60] or sustained UPR-induced apoptosis in mammalian cells[93].

Non-coding RNAs were readily detected in tagging, and include *SCR1 and NME1*, the RNA components of SRP[49] and MRP[85]. Indeed, SCR1 was the most strongly tagged ncRNA at the ER. Tagged RNAs related to tRNAs, snRNAs and snoRNAs appear to have been caught during their maturation or surveillance. Tagged tRNAs were 3'-extended and polyadenylated upstream of the U-tag. Their polyadenylation suggests action of the nuclear TRAMP complex prior to their encounter with the tagging enzyme. 3'-extended tRNAs may subsequently be processed by the endonuclease Trz1p[94], which is both nuclear and mitochondrial[34,94,95]. The presence of tagged snRNAs supports the recent finding that yeast snRNAs are shuttled to the cytoplasm as part of their maturation to prevent inclusion of misprocessed snRNAs in the spliceosome[84]. Tagged snoRNAs may arise through a different form of surveillance, as failure to properly process the guanosine cap of snoRNAs can lead to their accumulation into the cytoplasm[86].

Tagging can be performed in living organisms, as is true of "TRIBE," in which ADAR-catalyzed deaminations mark the binding of specific proteins[96,97]. APEX-seq, as currently configured, is not suitable in intact organisms. Conversely, in cells with endogenous uridylation activities, application of tagging would be simplified through enzymes with different nucleotide specificities[98] or by reduction of endogenous uridylation activities.

The use of localized devices to covalently mark RNAs provides an entrée to creating histories of individual RNA molecules. Combinations of Localized RNA Tagging, APEX-Seq, or TRIBE, performed in the same cell, will yield biographies of individual

RNAs, in which their movements and protein encounters are written in unique combinations of modifications and tail sequences.

MATERIAL AND METHODS

RNA extraction and library preparation

Total RNAs and libraries were prepared in accordance with previous reports[26]. Sequencing libraries were submitted to the UW-Madison biotechnology center for paired-end sequencing (2X50 bp) on the HiSeq2500 platform. Libraries were loaded at equal concentrations with PhiX loaded at 30% of the total concentration.

Mapping reads to the genome

FastQ files were processed with a custom sequencing pipeline[26]. Reads from libraries that were sequenced on multiple lanes were pooled and processed together.

Processing read counts

Read counts were processed differently to determine either (A) absolute RNA tagging values or (B) tagging enrichment at a given site.

A) Calculation of tagged reads per million across ten minimum U-tag lengths.

RNAs species that were tagged reproducibly across three replicates were identified with BioVenn[99] (http://www.biovenn.nl/). The Read counts in each replicate were then normalized to the total number of reads (in millions) for that replicate, yielding the tagged reads per million (TRPM) across ten minimum U-tag lengths (1U to 10U) for each tagged RNA species. The TRPM values for each RNA species in each replicate were then averaged to yield the average TRPM (TRPM Avg.) for each RNA species at each of the U-tag length levels. RNAs species were then ranked by U-tag length and reads, and

RNAs with the longest U-tag length reads, but less total reads having priority over those with more reads but shorter U-tag length.

B) Deseq2 analyses to determine enrichment at the ER and Mitochondria.

Raw read counts for RNAs detected in each experimental replicate were analyzed with Deseq2[35]. For each individual analysis (ER- or Mitochondria-localized RNA tagging data), the PUP alone (+PAB) read counts were used as a control. In all our analyses, a $\log_2$ fold change of two-fold or greater ($\log_2(FC \geq 2)$) and an adjusted p-value (*p*-adj) cutoff of < 0.05 was applied. RNAs that met these criteria were considered "enriched (i.e., “ER-enriched”) or depleted (i.e., “ER-depleted” or PUP “alone-enriched”).

K-means clustering to generate tiers and heatmaps

Clustering was done using Cluster 3.0[100] (C clustering Library 1.52) using the K-means option as previously reported[26]. Five groups (Tiers) were arbitrarily selected, and $\log_2$-transformed data were clustered based on detection efficiency (i.e., L_2FC). Tiers were ranked based on highest to lowest efficiency of detection (i.e., most enriched to least enriched), with priority given to enrichment at the highest U-tag lengths. Heat maps were generated with MatLab.

Data Mining

Proximity-specific ribosome profiling.

Proximity-specific ribosome profiling data were mined published experiments. [21,22] mRNAs with greater than or equal to two-fold or higher ribosome-protected fragment reads relative to the input were determined to be “enriched”. Since we omitted did not use

cycloheximide in our experiments, we selected Sec63p[21] (1 min biotin pulse) and Om45p[22] (2 min biotin pulse) mediated profiling data that omitted the translation inhibitor.

Mitochondrial proteome mRNAs. Mitochondria-copurified proteins from two experiments[46,47] were consolidated into a single list termed, “mitochondrial proteins”.

RBP targets. RNA that interact with RNA-binding proteins were mined from published RNA tagging[26] and RIP-Chip[62] data. RNA tagging data were reprocessed using the DESeq2[35] approach described here for ER-Pup and Mito-PUP, also using PUP alone (+PAB) as a control set. RNAs that were tagged $\log_2(\Delta \text{ Tagged Reads}) \geq 1)$ and significance (p-adj) < 0.05 relative to PUP alone (+PAB) were considered enriched. These analyses were done across ten minimum U-tag lengths, and the RNA were ranked by highest to lowest U-tag length enrichment. For RIP-Chip, RNAs that had a Significance Analysis of Microarrays (SAM) q-value < 10% were considered targets. The classes of Puf3p mRNA targets were retrieved from published biochemical experiments[48].

APEX-Seq. APEX-Seq data[25] as used for these analyses. Similar cutoffs applied to our data ($\log_2(\text{Fold Change}) \geq 1$, p-adj < 0.05) were applied to ER (ERM) and mitochondrial (OMM) APEX-Seq data to facilitate comparison.

Dual-tagged RNA conservation. Human homologs of dual-tagged yeast genes were retrieved using YeastMine[37,38] (https://yeastmine.yeastgenome.org/yeastmine/begin.do).

3’ UTR motif enrichment analyses

Command line MEME[61] Version 5.0.4 was used for all analyses. The order (Rank) of all yeast 3’ UTRs from[26] was randomized using the excel rand (=RAND()) function, and

the resulting list was used as background (-neg) for all MEME analyses. Motifs that were enriched in the 3 UTRs of tagged RNAs (ranked by longest U-tag length) were done using the differential enrichment (-objfun de) function, and MEME was prometed to return the top ten motifs (-nmotifs 10) that range from 8-10 nts in length (-minw 8 -maxw 12) with all lengths between those limits included in the scan (-allw). The rank of the 3' UTR within the list of tagged RNAs or the list of 3' UTRs with randomized rank was taken into account (-norand) in the analyses.

Puf3p binding element incidence in the 3' UTRs of RNAs was determined using a custom perl script[31].

Tools used

Gene ontology (GO). All GO analyses were done using yeast mine lists[37,38] (https://yeastmine.yeastgenome.org/yeastmine/bag.do). The analyses used the default background, and considered enrichments with a maximum p-value of 0.05 after Holm-Bonferroni correction.

Venn Diagrams. Venn diagrams were generated using BioVenn[99] (http://www.biovenn.nl).

Hypergeometric Distribution Analyses. Hypergeometric distribution calculations were done with the online calculator available from the Graeber Lab (https://systems.crump.ucla.edu/hypergeometric/). The total number of yeast transcripts used was 6,712 RNAs, as defined by RNA-seq[26].

Cumulative Fraction Plots. Cumulative fraction plots were done in either RStudio (Figures 3D, E, 4F) (as previously reported[26]) or Excel (this report, Figure 5D).

Tab file conversion to Fasta. Tab files that contained 3' UTR sequences were converted to Fasta format using the HIV sequence database Format Converter (https://www.hiv.lanl.gov/content/sequence/FORMAT_CONVERSION/form.html)

Confocal Microscopy Strains were grown to mid-log (OD_{660} 0.5-0.8) phase in 25 mL cultures at 30 °C in a horizontal shaker at 180 RPM. Cells were grown in synthetic complete[101] (SC) Low fluorescence[102] (LOFLO) media

Yeast cells were immobilized on Concanavalin A (ConA Sigma: 11028-71-0) coated coverslips for imaging with a modified version of a published imaging protocol[103].

Coverslip Preparation

Coverslips were first incubated in a methanol/hydrochloric acid (1:1) solution in 50 mL conical tube in a fume hood overnight. The next day, coverslips were rinsed 3Xs with deionized water, and then placed on one edge inside 65 °C oven until fully dry (~ 30 mins). The dry coverslips were then cooled to RT, and 400 uL of 2 mg/mL concanavalin A (ConA) was spread evenly in the center. After drying for 60 mins at RT, the coverslips were then tilted on their side to remove excess ConA. The coverslips were then covered and dried at RT overnight.

Fixation

Mid-log phase cultures were spun down, and resuspended in 500 uL of fresh SC LOFLO media. 100 uL of cells were then placed evenly on the center of the ConA-coated coverslip and allowed to bind for 30 mins in a 30 °C incubator without shaking. Once immobilized on the coverslip, the cells were fixed by submerging the coverslip in SC LOFLO (5% Formaldehyde, Fisher: BP531-500) for 20 minutes. After, the coverslip was

washed with 3Xs with fresh SC LOFLO media, and the coverslip was then placed on a slide containing SC LOFLO.

Confocal settings

Cells were imaged on a Leica TCS SP8 confocal microscope using LAS X 3.1.1.15751. The microscope is equipped with a Photomultiplier (PMT) and Hybrid detectors (HyD). A 63x 1.4NA HC Plan Apochromat oil immersion objective was used with 3.01 zoom and standard scanner with 400Hz scanning speed. Z-stacks with a 0.3 uM step size were collected, and yeGFP (495nm - 530nm) and mCherry (600nm - 650nm) were sequentially imaged.

Fluorescence quantitation

Images were processed using FIJI[104]/ImageJ[105] Version: 2.0.0-rc-69/1.52i. Noise reduction was done on the images using the “Despeckle” function. Fluorescence intensities (gray values) quantified using the measure (Ctrl+M) function along a straight line that was drawn across individual cells. The measurements were then normalized for each individual sample to get the Normalized Gray Value at each individual measurement. This was done with the following equation, Normalized Gray Value at a specific point on the line = (Raw intensity value at a specific point on the line – Minimum of all intensities on the line)/(Maximum of all intensities on the line – Minimum of all intensities on the line). The normalized Gray values for each sample were plotted on a line graph using Microsoft Excel.

Yeast Strains (BY4742 background)

Strain	Description	Construct	Auxotrophic Marker
yHCMM1	Wildtype	BY4742	-U
yHCMM2	PUP (+PAB)	PSEC63_yeGFP_ScPAB14RRMs_CePUP-2_URA3_TADH1 inserted into URA3 locus	-U
yHCMM3	PUP (-PAB)	PSEC63_yeGFP_CePUP-2_URA3_TADH1 inserted into URA3 locus	-U
yHCMM4	ER-PUP	yeGFP_ScPAB14RRMs_CePUP-2_URA3 inserted downstream of SEC63 CDS	-U
yHCMM5	Mito-PUP	yeGFP_ScPAB14RRMs_CePUP-2_URA3 inserted downstream of OM45 CDS	-U
yHCMM6	ER-PUP & ER marker	mCherry_LEU2 inserted downstream of SEC61 CDS in ER-PUP strain	-UL
yHCMM7	Mito-PUP & Mito marker	mCherry_LEU2 inserted downstream of TOM70 CDS in Mito-PUP strain	-UL

Plasmids

Plasmid	Construct	Auxotrophic Marker
pHCMM1	PTEF1_yeGFP_*Sc*PAB14RRMs_*Ce*PUP-2_URA3_TADH1	-UL
pHCMM2	PSEC63_yeGFP_*Sc*PAB14RRMs_*Ce*PUP-2_URA3_TADH1	-UL
pHCMM3	PSEC63_yeGFP_CePUP-2_URA3_TADH1	-UL
pHCMM4	PCYC1_SEC61_mCherry_LEU2_TCYC1	-L

Primers

Makes	Input	Primers	Primer Sequence
yHCMM2	pHCMM2	primHCMM1	ATTTATGGTGAAGGATAAGTTTTGACCATCAAA GAAGGTTAATGTGGCTGTGGTTTCAGGGTCCAT AAAGCTGGTGCTCTCATGCTTCTT
		primHCMM2	GGCCATGAAGCTTTTTCTTTCCAATTTTTTTTTTT TCGTCATTATAGAAATCATTACGACCGAGATTC CCGGGCGGTAGAGGTGTGGTCA
yHCMM3	pHCMM3	primHCMM1	ATTTATGGTGAAGGATAAGTTTTGACCATCAAA GAAGGTTAATGTGGCTGTGGTTTCAGGGTCCAT AAAGCTGGTGCTCTCATGCTTCTT
		primHCMM2	GGCCATGAAGCTTTTTCTTTCCAATTTTTTTTTTT TCGTCATTATAGAAATCATTACGACCGAGATTC CCGGGCGGTAGAGGTGTGGTCA
yHCMM4	pHCMM1	primHCMM3	AGTGATGCTAGCGATTATACTGATATCGATACG GATACAGAAGCTGAAGATGATGAATCACCAGAA ATGTCTAAAGGTGAAGAATTATTC
		primHCMM4	TTTTTATAAAGATGAAATATATACGTCTAAGAGC TAAAATGAAAAACTATACTAATCACTTATATCTA CGGTTTCTTTGAAATTTTTTTG
yHCMM5	pHCMM1	primHCMM5	GCCAAGAACAAATTCAAAGAATGGAATGATAAG GGTGATGGTAAATTCTGGAGCTCGAAAAAGGAC ATGTCTAAAGGTGAAGAATTATTC
		primHCMM6	ATGAGAAACATGTGAATATGTATATATGTTATGC GGGAACCAACCCTTTACAATTAGCTATCTAACT ACGGTTTCTTTGAAATTTTTTTG
yHCMM6	pHCMM4	primHCMM7	ATGTCCTCCAACCGTGTTC
		primHCMM8	AAAAATAGAGGGAGGGGTGTGGCTAAATGCGA TTTTTTTTTTCTTTGGATATTATTTTCATTTTATAT AACTGTGGGAATACTCAGGTAT
yHCMM7	pHCMM4	primHCMM9	ACTTTAGCTAAATTACGCGAACAGGGTTTAATG GGATCCCCCGGGATGGTGAGCAAGGGC
		primHCMM10	TGTCTTCTCCTAAAAGTTTTTAAGTTTATGTTTAC TGTAACTGTGGGAATACTCAGGTAT

ACKNOWLEDGMENTS

We thank the Wickens and Kimble laboratories, and members of the UW-Madison community, particularly Judith Kimble and Dave Brow, for helpful advice and discussions. We thank Eric Phizicky and Elizabeth Grayhack (University of Rochester), and Scott Aoki (Indiana University) for their insights. We thank Sarah Crittenden for help with confocal microscopy, Kim Haupt and Elle Kielar Grevstad (UW-Madison Optical Core) for assistance with image analyses, and Aaron Hoskins, Tucker Carrocci, and Ian Norden for help with fluorescent proteins. We are grateful to Joshua R. Hyman, Molly Zeller, Amanda Maegli and Mike Sussman (UW-Madison Biotechnology Center) for help with sequencing, and to Laura Vanderploeg and the Biochemistry Media Lab for help preparing figures. This work was supported by an NIH grant to M.W. (GM50942) and an E.W. Hopkins Fellowship to H.C.M.M. While in UW-Madison, C.P.L. was supported by Wharton and Biochemistry Scholar Fellowships, and D.F.P. was supported by T32 GM008349 (NIH) and a WARF scholarship.

AUTHOR CONTRIBUTIONS

H.C.M-M. and M.W. conceived the method. H.C.M-M. developed the method and designed experiments; H.C.M-M. performed all experiments, analyzed the data, and interpreted the results. H.C.M-M. and M.W. wrote the paper and figures; C.P.L. provided advice on tagging and helped with revisions, and D.F.P. provided advice on protein design.

COMPETING INTERESTS

The authors declare no competing interest.

REFERENCES

1 Driever, W. & Nusslein-Volhard, C. The bicoid protein determines position in the Drosophila embryo in a concentration-dependent manner. *Cell* **54**, 95-104, doi:10.1016/0092-8674(88)90183-3 (1988).

2 Berleth, T. *et al.* The role of localization of bicoid RNA in organizing the anterior pattern of the Drosophila embryo. *The EMBO Journal* **7**, 1749-1756, doi:10.1002/j.1460-2075.1988.tb03004.x (1988).

3 Ephrussi, A., Dickinson, L. K. & Lehmann, R. Oskar organizes the germ plasm and directs localization of the posterior determinant nanos. *Cell* **66**, 37-50, doi:10.1016/0092-8674(91)90137-n (1991).

4 Kim-Ha, J., Smith, J. L. & Macdonald, P. M. oskar mRNA is localized to the posterior pole of the Drosophila oocyte. *Cell* **66**, 23-35, doi:10.1016/0092-8674(91)90136-m (1991).

5 Melton, D. A. Translocation of a localized maternal mRNA to the vegetal pole of Xenopus oocytes *Nature* **328**, 80-82 (1987).

6 Johnstone, O. & Lasko, P. Translational regulation and RNA localization in Drosophila oocytes and embryos. *Annu Rev Genet* **35**, 365-406, doi:10.1146/annurev.genet.35.102401.090756 (2001).

7 Long, R. M. *et al.* Mating Type Switching in Yeast Controlled by Asymmetric Localization of ASH1 mRNA. *Science* **277**, 383, doi:10.1126/science.277.5324.383 (1997).

8 Tutucci, E., Livingston, N. M., Singer, R. H. & Wu, B. Imaging mRNA In Vivo, from Birth to Death. *Annu Rev Biophys* **47**, 85-106, doi:10.1146/annurev-biophys-070317-033037 (2018).

9 Das, S., Singer, R. H. & Yoon, Y. J. The travels of mRNAs in neurons: do they know where they are going? *Curr Opin Neurobiol* **57**, 110-116, doi:10.1016/j.conb.2019.01.016 (2019).

10 Chin, A. & Lecuyer, E. RNA localization: Making its way to the center stage. *Biochim Biophys Acta Gen Subj* **1861**, 2956-2970, doi:10.1016/j.bbagen.2017.06.011 (2017).

11 Martin, K. C. & Ephrussi, A. mRNA localization: gene expression in the spatial dimension. *Cell* **136**, 719-730, doi:10.1016/j.cell.2009.01.044 (2009).

12 Lipshitz, H. D. & Smibert, C. A. Mechanisms of RNA localization and translational regulation. *Curr Opin Genet Dev* **10**, 476-488 (2000).

13 Besse, F. & Ephrussi, A. Translational control of localized mRNAs: restricting protein synthesis in space and time. *Nat Rev Mol Cell Biol* **9**, 971-980, doi:10.1038/nrm2548 (2008).

14 Chen, K. H., Boettiger, A. N., Moffitt, J. R., Wang, S. & Zhuang, X. Spatially resolved, highly multiplexed RNA profiling in single cells. *Science* **348**, aaa6090, doi:10.1126/science.aaa6090 (2015).

15 Lee, J. H. *et al.* Fluorescent in situ sequencing (FISSEQ) of RNA for gene expression profiling in intact cells and tissues. *Nat Protoc* **10**, 442-458, doi:10.1038/nprot.2014.191 (2015).

16 Raj, A., van den Bogaard, P., Rifkin, S. A., van Oudenaarden, A. & Tyagi, S. Imaging individual mRNA molecules using multiple singly labeled probes. *Nat Methods* **5**, 877-879, doi:10.1038/nmeth.1253 (2008).

17 Femino, A. M., Fay, F. S., Fogarty, K. & Singer, R. H. Visualization of Single RNA Transcripts in Situ. *Science* **280**, 585, doi:10.1126/science.280.5363.585 (1998).

18 Bertrand, E. *et al.* Localization of ASH1 mRNA particles in living yeast. *Mol Cell* **2**, 437-445, doi:10.1016/s1097-2765(00)80143-4 (1998).

19 Tutucci, E., Livingston, N. M., Singer, R. H. & Wu, B. Imaging mRNA In Vivo, from Birth to Death. *Annual Review of Biophysics* **47**, 85-106, doi:10.1146/annurev-biophys-070317-033037 (2018).

20 Tutucci, E. *et al.* An improved MS2 system for accurate reporting of the mRNA life cycle. *Nature methods* **15**, 81-89, doi:10.1038/nmeth.4502 (2018).

21 Jan, C. H., Williams, C. C. & Weissman, J. S. Principles of ER cotranslational translocation revealed by proximity-specific ribosome profiling. *Science* **346**, 1257521, doi:10.1126/science.1257521 (2014).

22 Williams, C. C., Jan, C. H. & Weissman, J. S. Targeting and plasticity of mitochondrial proteins revealed by proximity-specific ribosome profiling. *Science* **346**, 748-751, doi:10.1126/science.1257522 (2014).

23 Kaewsapsak, P., Shechner, D. M., Mallard, W., Rinn, J. L. & Ting, A. Y. Live-cell mapping of organelle-associated RNAs via proximity biotinylation combined with protein-RNA crosslinking. *eLife* **6**, e29224, doi:10.7554/eLife.29224 (2017).

24 Padròn, A., Iwasaki, S. & Ingolia, N. T. Proximity RNA labeling by APEX-Seq Reveals the Organization of Translation Initiation Complexes and Repressive RNA Granules. *bioRxiv*, 454066, doi:10.1101/454066 (2018).

25 Fazal, F. M. *et al.* Atlas of Subcellular RNA Localization Revealed by APEX-seq. *bioRxiv*, 454470, doi:10.1101/454470 (2018).

26 Lapointe, C. P., Wilinski, D., Saunders, H. A. & Wickens, M. Protein-RNA networks revealed through covalent RNA marks. *Nat Methods* **12**, 1163-1170, doi:10.1038/nmeth.3651 (2015).

27 Kwak, J. E. & Wickens, M. A family of poly(U) polymerases. *RNA* **13**, 860-867, doi:10.1261/rna.514007 (2007).

28 Warkocki, Z., Liudkovska, V., Gewartowska, O., Mroczek, S. & Dziembowski, A. Terminal nucleotidyl transferases (TENTs) in mammalian RNA metabolism. *Philosophical transactions of the Royal Society of London. Series B, Biological sciences* **373**, 20180162, doi:10.1098/rstb.2018.0162 (2018).

29 Webster, M. W., Stowell, J. A. & Passmore, L. A. RNA-binding proteins distinguish between similar sequence motifs to promote targeted deadenylation by Ccr4-Not. *Elife* **8**, doi:10.7554/eLife.40670 (2019).

30 Lapointe, C. P. *et al.* Multi-omics Reveal Specific Targets of the RNA-Binding Protein Puf3p and Its Orchestration of Mitochondrial Biogenesis. *Cell Syst* **6**, 125-135 e126, doi:10.1016/j.cels.2017.11.012 (2018).

31 Lapointe, C. P. *et al.* Architecture and dynamics of overlapped RNA regulatory networks. *RNA (New York, N.Y.)* **23**, 1636-1647, doi:10.1261/rna.062687.117 (2017).

32 Feldheim, D., Rothblatt, J. & Schekman, R. Topology and functional domains of Sec63p, an endoplasmic reticulum membrane protein required for secretory protein translocation. *Molecular and cellular biology* **12**, 3288-3296, doi:10.1128/mcb.12.7.3288 (1992).

33 Finke, K. *et al.* A second trimeric complex containing homologs of the Sec61p complex functions in protein transport across the ER membrane of S. cerevisiae. *The EMBO journal* **15**, 1482-1494 (1996).

34 Huh, W. K. *et al.* Global analysis of protein localization in budding yeast. *Nature* **425**, 686-691, doi:10.1038/nature02026 (2003).

35 Love, M. I., Huber, W. & Anders, S. Moderated estimation of fold change and dispersion for RNA-seq data with DESeq2. *Genome Biol* **15**, 550, doi:10.1186/s13059-014-0550-8 (2014).

36 Ast, T., Cohen, G. & Schuldiner, M. A network of cytosolic factors targets SRP-independent proteins to the endoplasmic reticulum. *Cell* **152**, 1134-1145, doi:10.1016/j.cell.2013.02.003 (2013).

37 Balakrishnan, R. *et al.* YeastMine--an integrated data warehouse for Saccharomyces cerevisiae data as a multipurpose tool-kit. *Database (Oxford)* **2012**, bar062-bar062, doi:10.1093/database/bar062 (2012).

38 Hong, E. L. *et al.* Gene Ontology annotations at SGD: new data sources and annotation methods. *Nucleic acids research* **36**, D577-D581, doi:10.1093/nar/gkm909 (2008).

39 Ogg, S. C. & Walter, P. SRP samples nascent chains for the presence of signal sequences by interacting with ribosomes at a discrete step during translation elongation. *Cell* **81**, 1075-1084, doi:10.1016/s0092-8674(05)80012-1 (1995).

40 Yaffe, M. P., Jensen, R. E. & Guido, E. C. The major 45-kDa protein of the yeast mitochondrial outer membrane is not essential for cell growth or mitochondrial function. *J Biol Chem* **264**, 21091-21096 (1989).

41 Sesaki, H. & Jensen, R. E. UGO1 encodes an outer membrane protein required for mitochondrial fusion. *J Cell Biol* **152**, 1123-1134, doi:10.1083/jcb.152.6.1123 (2001).

42 Dukanovic, J. & Rapaport, D. Multiple pathways in the integration of proteins into the mitochondrial outer membrane. *Biochim Biophys Acta* **1808**, 971-980, doi:10.1016/j.bbamem.2010.06.021 (2011).

43 Riezman, H. *et al.* The outer membrane of yeast mitochondria: isolation of outside-out sealed vesicles. *The EMBO Journal* **2**, 1105-1111, doi:10.1002/j.1460-2075.1983.tb01553.x (1983).

44 Rapaport, D. The mitochondrial protein OM45 is exposed to the cytosol. *The Journal of biological chemistry* **287**, 27415-27416, doi:10.1074/jbc.L112.392969 (2012).

45 Lauffer, S., Rödel, G. & Krause-Buchholz, U. Reply to Rapaport: The Mitochondrial Protein OM45 Is Exposed to the Cytosol. *Journal of Biological Chemistry* **287**, 27416-27416 (2012).

46 Reinders, J., Zahedi, R. P., Pfanner, N., Meisinger, C. & Sickmann, A. Toward the complete yeast mitochondrial proteome: multidimensional separation techniques for mitochondrial proteomics. *J Proteome Res* **5**, 1543-1554, doi:10.1021/pr050477f (2006).

47 Morgenstern, M. *et al.* Definition of a High-Confidence Mitochondrial Proteome at Quantitative Scale. *Cell Rep* **19**, 2836-2852, doi:10.1016/j.celrep.2017.06.014 (2017).

48 Saint-Georges, Y. *et al.* Yeast mitochondrial biogenesis: a role for the PUF RNA-binding protein Puf3p in mRNA localization. *PLoS One* **3**, e2293, doi:10.1371/journal.pone.0002293 (2008).

49 Hann, B. C. & Walter, P. The signal recognition particle in S. cerevisiae. *Cell* **67**, 131-144, doi:10.1016/0092-8674(91)90577-l (1991).

50 Vance, J. E. Phospholipid synthesis in a membrane fraction associated with mitochondria. *J Biol Chem* **265**, 7248-7256 (1990).

51 Kornmann, B. *et al.* An ER-mitochondria tethering complex revealed by a synthetic biology screen. *Science* **325**, 477-481, doi:10.1126/science.1175088 (2009).

52 Mori, T., Hayashi, T., Hayashi, E. & Su, T.-P. Sigma-1 Receptor Chaperone at the ER-Mitochondrion Interface Mediates the Mitochondrion-ER-Nucleus Signaling for Cellular Survival. *PLOS ONE* **8**, e76941, doi:10.1371/journal.pone.0076941 (2013).

53 Mori, K., Kawahara, T., Yoshida, H., Yanagi, H. & Yura, T. Signalling from endoplasmic reticulum to nucleus: transcription factor with a basic-leucine zipper motif is required for the unfolded protein-response pathway. *Genes Cells* **1**, 803-817 (1996).

54 Cox, J. S., Shamu, C. E. & Walter, P. Transcriptional induction of genes encoding endoplasmic reticulum resident proteins requires a transmembrane protein kinase. *Cell* **73**, 1197-1206, doi:10.1016/0092-8674(93)90648-a (1993).

55 Cox, J. S. & Walter, P. A novel mechanism for regulating activity of a transcription factor that controls the unfolded protein response. *Cell* **87**, 391-404, doi:10.1016/s0092-8674(00)81360-4 (1996).

56 Mori, K., Ma, W., Gething, M. J. & Sambrook, J. A transmembrane protein with a cdc2+/CDC28-related kinase activity is required for signaling from the ER to the nucleus. *Cell* **74**, 743-756, doi:10.1016/0092-8674(93)90521-q (1993).

57 Nikawa, J., Akiyoshi, M., Hirata, S. & Fukuda, T. Saccharomyces cerevisiae IRE2/HAC1 is involved in IRE1-mediated KAR2 expression. *Nucleic Acids Res* **24**, 4222-4226, doi:10.1093/nar/24.21.4222 (1996).

58 Sidrauski, C., Cox, J. S. & Walter, P. tRNA ligase is required for regulated mRNA splicing in the unfolded protein response. *Cell* **87**, 405-413, doi:10.1016/s0092-8674(00)81361-6 (1996).

59 Sidrauski, C. & Walter, P. The transmembrane kinase Ire1p is a site-specific endonuclease that initiates mRNA splicing in the unfolded protein response. *Cell* **90**, 1031-1039, doi:10.1016/s0092-8674(00)80369-4 (1997).

60 Knupp, J., Arvan, P. & Chang, A. Increased mitochondrial respiration promotes survival from endoplasmic reticulum stress. *Cell Death & Differentiation* **26**, 487-501, doi:10.1038/s41418-018-0133-4 (2019).

61 Bailey, T. L. & Elkan, C. Fitting a mixture model by expectation maximization to discover motifs in biopolymers. *Proc Int Conf Intell Syst Mol Biol* **2**, 28-36 (1994).

62 Hogan, D. J., Riordan, D. P., Gerber, A. P., Herschlag, D. & Brown, P. O. Diverse RNA-binding proteins interact with functionally related sets of RNAs, suggesting an extensive regulatory system. *PLoS Biol* **6**, e255, doi:10.1371/journal.pbio.0060255 (2008).

63 Jackson, J. S., Jr., Houshmandi, S. S., Lopez Leban, F. & Olivas, W. M. Recruitment of the Puf3 protein to its mRNA target for regulation of mRNA decay in yeast. *RNA* **10**, 1625-1636, doi:10.1261/rna.7270204 (2004).

64 Gerber, A. P., Herschlag, D. & Brown, P. O. Extensive association of functionally and cytotopically related mRNAs with Puf family RNA-binding proteins in yeast. *PLoS Biol* **2**, E79, doi:10.1371/journal.pbio.0020079 (2004).

65 Gadir, N., Haim-Vilmovsky, L., Kraut-Cohen, J. & Gerst, J. E. Localization of mRNAs coding for mitochondrial proteins in the yeast Saccharomyces cerevisiae. *RNA* **17**, 1551-1565, doi:10.1261/rna.2621111 (2011).

66 Zhu, D., Stumpf, C. R., Krahn, J. M., Wickens, M. & Hall, T. M. A 5' cytosine binding pocket in Puf3p specifies regulation of mitochondrial mRNAs. *Proc Natl Acad Sci U S A* **106**, 20192-20197, doi:10.1073/pnas.0812079106 (2009).

67 Jackson, C. L. & Kepes, F. BFR1, a multicopy suppressor of brefeldin A-induced lethality, is implicated in secretion and nuclear segregation in Saccharomyces cerevisiae. *Genetics* **137**, 423-437 (1994).

68 Trautwein, M., Dengjel, J., Schirle, M. & Spang, A. Arf1p provides an unexpected link between COPI vesicles and mRNA in Saccharomyces cerevisiae. *Mol Biol Cell* **15**, 5021-5037, doi:10.1091/mbc.e04-05-0411 (2004).

69 Lang, B. D., Li, A., Black-Brewster, H. D. & Fridovich-Keil, J. L. The brefeldin A resistance protein Bfr1p is a component of polyribosome-associated mRNP complexes in yeast. *Nucleic Acids Res* **29**, 2567-2574, doi:10.1093/nar/29.12.2567 (2001).

70 Weidner, J., Wang, C., Prescianotto-Baschong, C., Estrada, A. F. & Spang, A. The polysome-associated proteins Scp160 and Bfr1 prevent P body formation under normal growth conditions. *J Cell Sci* **127**, 1992-2004, doi:10.1242/jcs.142083 (2014).

71 Manchalu, S., Mittal, N., Spang, A. & Jansen, R.-P. Local translation of yeast ERG4 mRNA at the endoplasmic reticulum requires the brefeldin A resistance protein Bfr1. *bioRxiv*, 656405, doi:10.1101/656405 (2019).

72 Wintersberger, U., Kuhne, C. & Karwan, A. Scp160p, a new yeast protein associated with the nuclear membrane and the endoplasmic reticulum, is necessary for

maintenance of exact ploidy. *Yeast* **11**, 929-944, doi:10.1002/yea.320111004 (1995).

73 Frey, S., Pool, M. & Seedorf, M. Scp160p, an RNA-binding, polysome-associated protein, localizes to the endoplasmic reticulum of Saccharomyces cerevisiae in a microtubule-dependent manner. *J Biol Chem* **276**, 15905-15912, doi:10.1074/jbc.M009430200 (2001).

74 LaCava, J. *et al.* RNA degradation by the exosome is promoted by a nuclear polyadenylation complex. *Cell* **121**, 713-724, doi:10.1016/j.cell.2005.04.029 (2005).

75 Wyers, F. *et al.* Cryptic pol II transcripts are degraded by a nuclear quality control pathway involving a new poly(A) polymerase. *Cell* **121**, 725-737, doi:10.1016/j.cell.2005.04.030 (2005).

76 Vanacova, S. *et al.* A new yeast poly(A) polymerase complex involved in RNA quality control. *PLoS Biol* **3**, e189, doi:10.1371/journal.pbio.0030189 (2005).

77 Houseley, J., LaCava, J. & Tollervey, D. RNA-quality control by the exosome. *Nat Rev Mol Cell Biol* **7**, 529-539, doi:10.1038/nrm1964 (2006).

78 Motorin, Y., Muller, S., Behm-Ansmant, I. & Branlant, C. Identification of modified residues in RNAs by reverse transcription-based methods. *Methods Enzymol* **425**, 21-53, doi:10.1016/s0076-6879(07)25002-5 (2007).

79 Machnicka, M. A. *et al.* MODOMICS: a database of RNA modification pathways--2013 update. *Nucleic acids research* **41**, D262-D267, doi:10.1093/nar/gks1007 (2013).

80 Hrabeta-Robinson, E., Marcus, E., Cozen, A. E., Phizicky, E. M. & Lowe, T. M. High-Throughput Small RNA Sequencing Enhanced by AlkB-Facilitated RNA de-Methylation (ARM-Seq). *Methods in molecular biology (Clifton, N.J.)* **1562**, 231-243, doi:10.1007/978-1-4939-6807-7_15 (2017).

81 Thompson, D. M. & Parker, R. The RNase Rny1p cleaves tRNAs and promotes cell death during oxidative stress in Saccharomyces cerevisiae. *The Journal of cell biology* **185**, 43-50, doi:10.1083/jcb.200811119 (2009).

82 Trotta, C. R. *et al.* The yeast tRNA splicing endonuclease: a tetrameric enzyme with two active site subunits homologous to the archaeal tRNA endonucleases. *Cell* **89**, 849-858, doi:10.1016/s0092-8674(00)80270-6 (1997).

83 Wan, Y. & Hopper, A. K. From powerhouse to processing plant: conserved roles of mitochondrial outer membrane proteins in tRNA splicing. *Genes Dev* **32**, 1309-1314, doi:10.1101/gad.316257.118 (2018).

84 Becker, D. *et al.* Nuclear Pre-snRNA Export Is an Essential Quality Assurance Mechanism for Functional Spliceosomes. *Cell Rep* **27**, 3199-3214 e3193, doi:10.1016/j.celrep.2019.05.031 (2019).

85 Schmitt, M. E. & Clayton, D. A. Yeast site-specific ribonucleoprotein endoribonuclease MRP contains an RNA component homologous to mammalian RNase MRP RNA and essential for cell viability. *Genes Dev* **6**, 1975-1985, doi:10.1101/gad.6.10.1975 (1992).

86 Grzechnik, P. *et al.* Nuclear fate of yeast snoRNA is determined by co-transcriptional Rnt1 cleavage. *Nat Commun* **9**, 1783, doi:10.1038/s41467-018-04094-y (2018).

87 Lee, C. D. & Tu, B. P. Glucose-Regulated Phosphorylation of the PUF Protein Puf3 Regulates the Translational Fate of Its Bound mRNAs and Association with RNA Granules. *Cell Rep* **11**, 1638-1650, doi:10.1016/j.celrep.2015.05.014 (2015).

88 Kraut-Cohen, J. *et al.* Translation- and SRP-independent mRNA targeting to the endoplasmic reticulum in the yeast Saccharomyces cerevisiae. *Mol Biol Cell* **24**, 3069-3084, doi:10.1091/mbc.E13-01-0038 (2013).

89 Kornmann, B. & Walter, P. ERMES-mediated ER-mitochondria contacts: molecular hubs for the regulation of mitochondrial biology. *J Cell Sci* **123**, 1389-1393, doi:10.1242/jcs.058636 (2010).

90 Gaspar, I. & Ephrussi, A. Strength in numbers: quantitative single-molecule RNA detection assays. *Wiley Interdiscip Rev Dev Biol* **4**, 135-150, doi:10.1002/wdev.170 (2015).

91 Pichon, X. *et al.* Visualization of single endogenous polysomes reveals the dynamics of translation in live human cells. *The Journal of Cell Biology* **214**, 769, doi:10.1083/jcb.201605024 (2016).

92 Lee, B. H., Bae, S.-W., Shim, J. J., Park, S. Y. & Park, H. Y. Imaging Single-mRNA Localization and Translation in Live Neurons. *Mol Cells* **39**, 841-846, doi:10.14348/molcells.2016.0277 (2016).

93 Rutkowski, D. T. & Kaufman, R. J. A trip to the ER: coping with stress. *Trends Cell Biol* **14**, 20-28 (2004).

94 Skowronek, E., Grzechnik, P., Späth, B., Marchfelder, A. & Kufel, J. tRNA 3' processing in yeast involves tRNase Z, Rex1, and Rrp6. *RNA (New York, N.Y.)* **20**, 115-130, doi:10.1261/rna.041467.113 (2014).

95 Hazbun, T. R. *et al.* Assigning function to yeast proteins by integration of technologies. *Mol Cell* **12**, 1353-1365 (2003).

96 McMahon, A. C. *et al.* TRIBE: Hijacking an RNA-Editing Enzyme to Identify Cell-Specific Targets of RNA-Binding Proteins. *Cell* **165**, 742-753, doi:10.1016/j.cell.2016.03.007 (2016).

97 Rahman, R., Xu, W., Jin, H. & Rosbash, M. Identification of RNA-binding protein targets with HyperTRIBE. *Nat Protoc* **13**, 1829-1849, doi:10.1038/s41596-018-0020-y (2018).

98 Preston, M. A. *et al.* Unbiased screen of RNA tailing activities reveals a poly(UG) polymerase. *Nature Methods* **16**, 437-445, doi:10.1038/s41592-019-0370-6 (2019).

99 Hulsen, T., de Vlieg, J. & Alkema, W. BioVenn - a web application for the comparison and visualization of biological lists using area-proportional Venn diagrams. *BMC Genomics* **9**, 488, doi:10.1186/1471-2164-9-488 (2008).

100 de Hoon, M. J., Imoto, S., Nolan, J. & Miyano, S. Open source clustering software. *Bioinformatics* **20**, 1453-1454, doi:10.1093/bioinformatics/bth078 (2004).

101 Kaiser, C. *Methods in yeast genetics : a Cold Spring Harbor Laboratory course manual*. (1994 edition. Cold Spring Harbor, N.Y. : Cold Spring Harbor Laboratory Press, 1994., 1994).

102 Sheff, M. A. & Thorn, K. S. Optimized cassettes for fluorescent protein tagging in Saccharomyces cerevisiae. *Yeast* **21**, 661-670, doi:10.1002/yea.1130 (2004).

103 Kaplan, C. & Ewers, H. Optimized sample preparation for single-molecule localization-based superresolution microscopy in yeast. *Nat Protoc* **10**, 1007-1021, doi:10.1038/nprot.2015.060 (2015).

104 Schindelin, J. *et al.* Fiji: an open-source platform for biological-image analysis. *Nat Methods* **9**, 676-682, doi:10.1038/nmeth.2019 (2012).

105 Schneider, C. A., Rasband, W. S. & Eliceiri, K. W. NIH Image to ImageJ: 25 years of image analysis. *Nature Methods* **9**, 671, doi:10.1038/nmeth.2089 (2012).

FIGURES

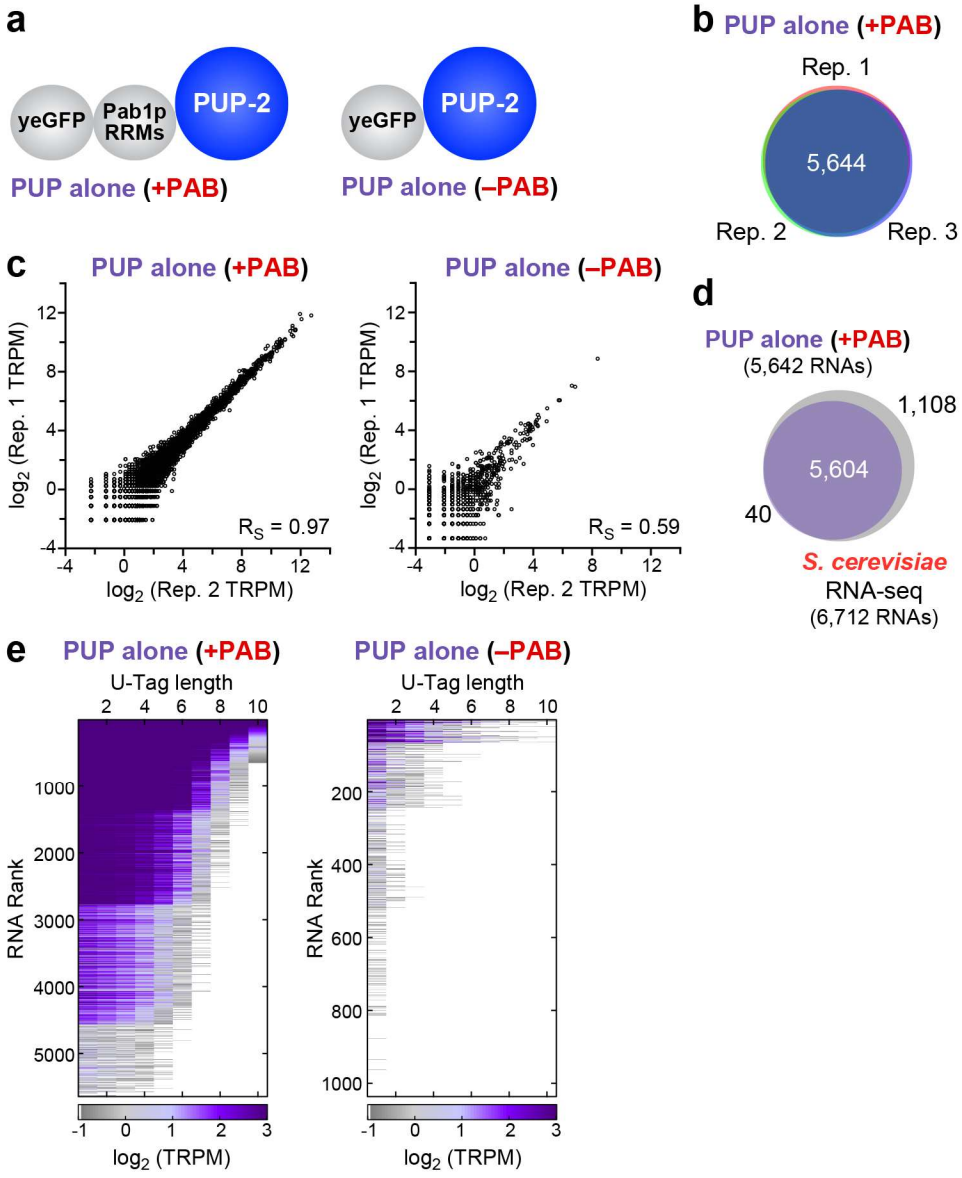
a
yeGFP
Pab1p RRMs
PUP-2
PUP alone (+PAB)
yeGFP
PUP-2
PUP alone (–PAB)
b PUP alone (+PAB)
Rep. 1
5,644
Rep. 2
Rep. 3
c
PUP alone (+PAB)
log2 (Rep. 1 TRPM)
log2 (Rep. 2 TRPM)
RS = 0.97
PUP alone (–PAB)
log2 (Rep. 1 TRPM)
log2 (Rep. 2 TRPM)
RS = 0.59
d
PUP alone (+PAB)
(5,642 RNAs)
1,108
5,604
40
S. cerevisiae
RNA-seq
(6,712 RNAs)
e
PUP alone (+PAB)
U-Tag length
RNA Rank
log2 (TRPM)
PUP alone (–PAB)
U-Tag length
RNA Rank
log2 (TRPM)

Figure 1. Broad specificity cytoplasmic RNA tagging: a baseline.

a) PUP-2 (“PUP alone”) chimeras with or without Pab1p RRMs. **b)** Reproducibility of U-tagged RNA species with the PUP alone (+PAB) construct and of **c)** tagged reads per million (TRPM) for both chimeras. Each dot represents a single RNA species. **d)** RNAs tagged by PUP (+PAB) vs all yeast RNAs. **e)** Ranked U-tagged RNAs (y-axis) with and without RRMs. Each row indicates an individual RNA species; columns represent U-tag length intervals, from 1 to 10 U’s added. Color relates to abundance of reads, as indicated in the key (bottom): purple indicates frequent reads; grey, low reads.

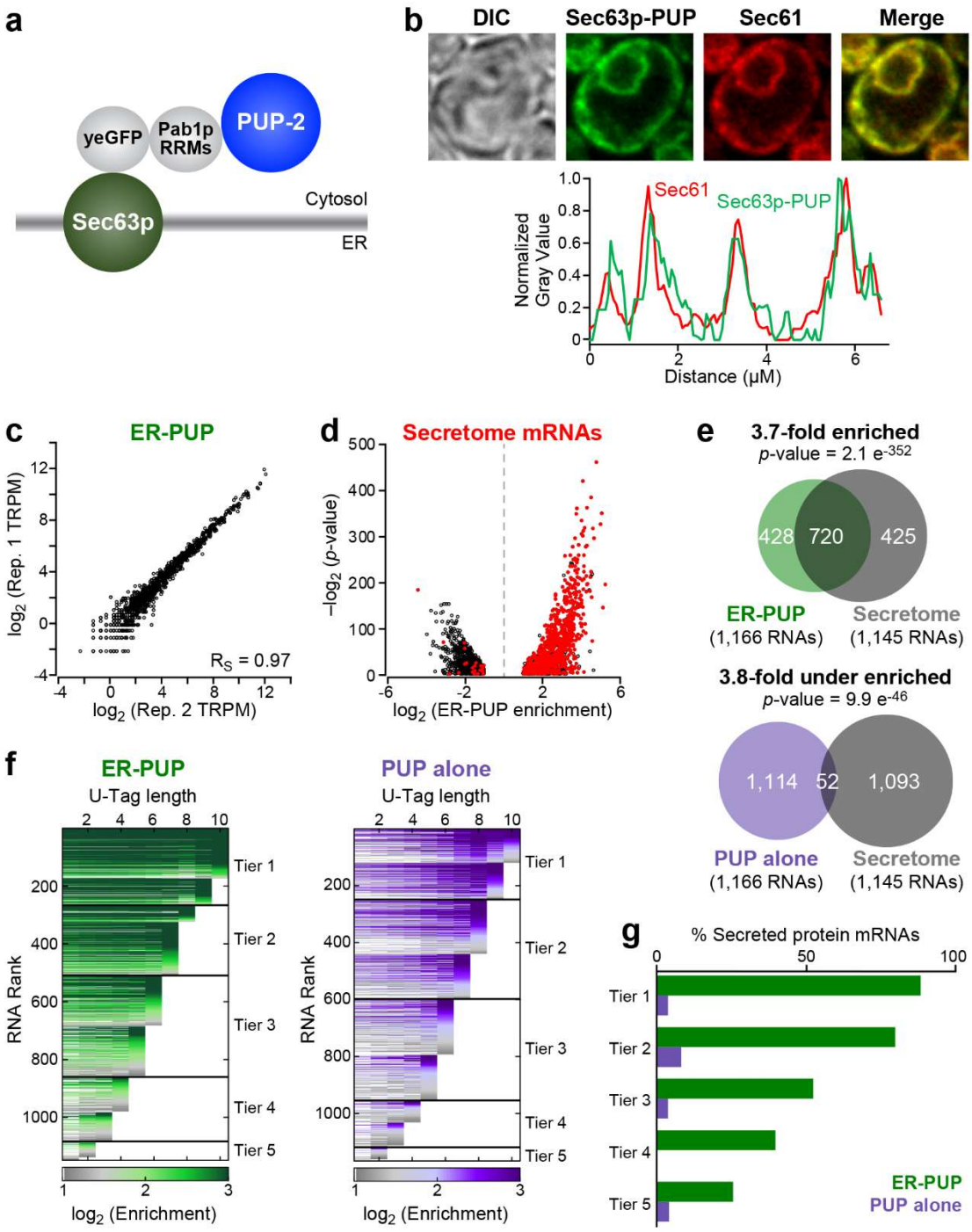
a
yeGFP
Pab1p RRMs
PUP-2
Sec63p
Cytosol
ER
b
DIC
Sec63p-PUP
Sec61
Merge
Sec61
Sec63p-PUP
Normalized Gray Value
Distance (μM)
c
ER-PUP
log2 (Rep. 1 TRPM)
log2 (Rep. 2 TRPM)
RS = 0.97
d
Secretome mRNAs
−log2 (p-value)
log2 (ER-PUP enrichment)
e
3.7-fold enriched
p-value = 2.1 e-352
428
720
425
ER-PUP
(1,166 RNAs)
Secretome
(1,145 RNAs)
3.8-fold under enriched
p-value = 9.9 e-46
1,114
52
1,093
PUP alone
(1,166 RNAs)
Secretome
(1,145 RNAs)
f
ER-PUP
U-Tag length
RNA Rank
Tier 1
Tier 2
Tier 3
Tier 4
Tier 5
log2 (Enrichment)
PUP alone
U-Tag length
RNA Rank
log2 (Enrichment)
g
% Secreted protein mRNAs
Tier 1
Tier 2
Tier 3
Tier 4
Tier 5
ER-PUP
PUP alone

Figure 2. ER-localized tagging provides an *in vivo* record.

a) ER-PUP chimera designed to tag ER-proximal RNAs. PUP(+PAB) was fused to the C-terminus of Sec63p, which tethers the chimera to the cytosolic surface of the ER.[32] **b)** Subcellular distribution: ER-PUP GFP fluorescence (green) vs an ER marker[33,34], Sec61p-mCherry (red); merged (yellow). Fluorescence intensities for ER-PUP (green) and the ER marker (red) across a representative cell. **c)** Reproducibility of ER-PUP tagging across biological replicates. **d)** Distribution of mRNAs that encode secreted proteins ("secretome") among the ER-PUP-tagged mRNAs. **e)** Secretome mRNAs in tagging by ER-PUP and PUP alone. **f)** Distribution of relative enrichment (ER-PUP vs PUP alone) across each U-tag length. RNA species that had significant (adjusted *p*-value < 0.05) difference ($\log_2(\Delta \text{ tagged reads}) \geq 1$)) in tagging efficiency (enrichment) in any of ten U-tag lengths (1U-10Us) were isolated and plotted as horizontal lines. Each row is one mRNA. Lines are segmented, and segments colored in accord with enrichment values: most enriched denoted in green (ER-PUP) or purple (PUP) and the lowest grey (both). RNAs were binned into five groups ("tiers"), and tiers ranked by the highest tag length (e.g., Tier 1 RNAs had a minimum of 9-10 U's; Tier 5 had a minimum of 1-2U's). **g)** Proportion (%) secretome mRNAs in each tier of ER-PUP-tagged (green) or PUP alone-tagged (purple) tier.

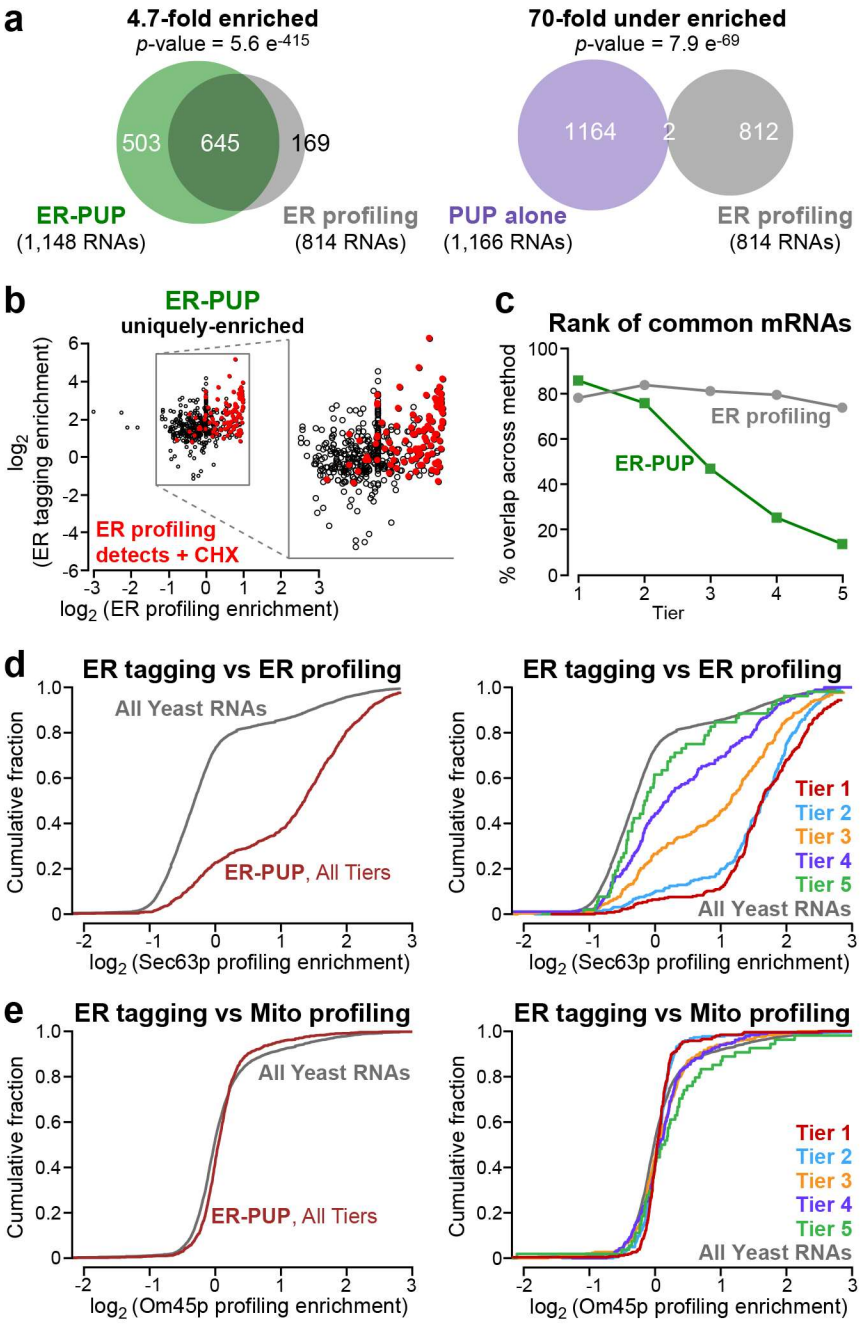
a
4.7-fold enriched
p-value = 5.6 e-415
503
645
169
ER-PUP
(1,148 RNAs)
ER profiling
(814 RNAs)
70-fold under enriched
p-value = 7.9 e-69
1164
2
812
PUP alone
(1,166 RNAs)
ER profiling
(814 RNAs)
b
ER-PUP
uniquely-enriched
log2 (ER tagging enrichment)
ER profiling
detects + CHX
log2 (ER profiling enrichment)
c
Rank of common mRNAs
% overlap across method
ER profiling
ER-PUP
Tier
d
ER tagging vs ER profiling
Cumulative fraction
All Yeast RNAs
ER-PUP, All Tiers
log2 (Sec63p profiling enrichment)
ER tagging vs ER profiling
Tier 1
Tier 2
Tier 3
Tier 4
Tier 5
All Yeast RNAs
log2 (Sec63p profiling enrichment)
e
ER tagging vs Mito profiling
Cumulative fraction
All Yeast RNAs
ER-PUP, All Tiers
log2 (Om45p profiling enrichment)
ER tagging vs Mito profiling
Tier 1
Tier 2
Tier 3
Tier 4
Tier 5
All Yeast RNAs
log2 (Om45p profiling enrichment)

Figure 3. Many but not all ER-enriched RNAs are bound by ER proximal ribosomes.

a) mRNAs enriched by ER-PUP or PUP alone vs positional profiling at the ER.[21] **b)** Enrichment of RNAs uniquely enriched ($\log_2(\Delta$ tagged reads$) \geq 1$)) by ER-PUP, and their enrichment in ER profiling. Red dots mark RNAs whose enrichment increases above the cutoff in profiling after arresting elongation with cycloheximide.[21] **c)** Rank of the commonly enriched RNAs in tagging (green) and profiling (black). **d)** Cumulative fraction distribution of ER-enriched mRNAs vs ER profiling; per tier analysis in right panel. **e)** Cumulative fraction distribution of ER-enriched mRNAs vs mitochondrial profiling[22], with per tier analysis on the right.

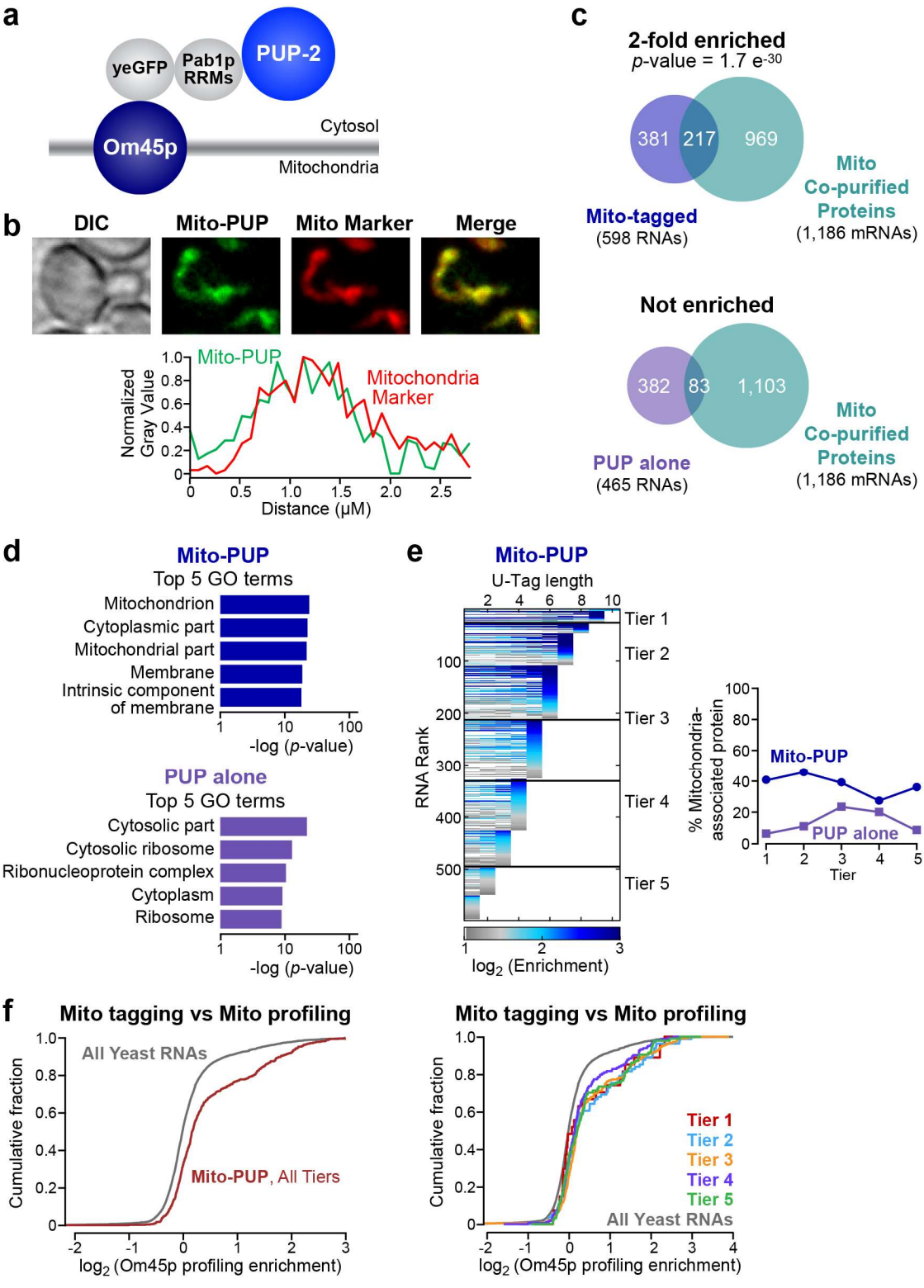
a
yeGFP
Pab1p RRMs
PUP-2
Om45p
Cytosol
Mitochondria
b
DIC
Mito-PUP
Mito Marker
Merge
Mito-PUP
Mitochondria Marker
Normalized Gray Value
Distance (μM)
c
2-fold enriched
p-value = 1.7 e-30
381
217
969
Mito-tagged
(598 RNAs)
Mito Co-purified Proteins
(1,186 mRNAs)
Not enriched
382
83
1,103
PUP alone
(465 RNAs)
Mito Co-purified Proteins
(1,186 mRNAs)
d
Mito-PUP
Top 5 GO terms
Mitochondrion
Cytoplasmic part
Mitochondrial part
Membrane
Intrinsic component of membrane
-log (p-value)
PUP alone
Top 5 GO terms
Cytosolic part
Cytosolic ribosome
Ribonucleoprotein complex
Cytoplasm
Ribosome
-log (p-value)
e
Mito-PUP
U-Tag length
Tier 1
Tier 2
Tier 3
Tier 4
Tier 5
RNA Rank
log2 (Enrichment)
% Mitochondria-associated protein
Mito-PUP
PUP alone
Tier
f
Mito tagging vs Mito profiling
All Yeast RNAs
Mito-PUP, All Tiers
Cumulative fraction
log2 (Om45p profiling enrichment)
Mito tagging vs Mito profiling
Tier 1
Tier 2
Tier 3
Tier 4
Tier 5
All Yeast RNAs
Cumulative fraction
log2 (Om45p profiling enrichment)

Figure 4. RNA contacts with the mitochondrial outer membrane.

a) Architecture of Mito-PUP. PUP alone was fused to the cytosolic C-terminal end of the mitochondrial membrane protein, Om45p.[40-45] **b)** Confocal localization of Mito-PUP fluorescence (green) and the mitochondrial marker, Tom70p-mCherry[34] (red), including fluorescence intensity across a line that bisects the cell (below). **c)** Overlaps of Mito-PUP- and PUP alone-enriched mRNAs, and those that encode proteins that co-purify with biochemically isolated mitochondria.[46,47] **d)** Top five gene ontology (GO) associations for Mito-PUP (top) and PUP alone (bottom). **e)** Rank of Mito-PUP-enriched RNAs plotted across each of ten U-tag lengths (left). The fraction of the RNAs in each Mito-PUP (blue line) and PUP alone tier (purple line) that encode mitochondrial proteins is plotted on the right. **f)** Cumulative fraction of all (left) and per-tier (right) Mito-PUP-enriched mRNAs with a given degree of mitochondrial profiling[22] enrichment.

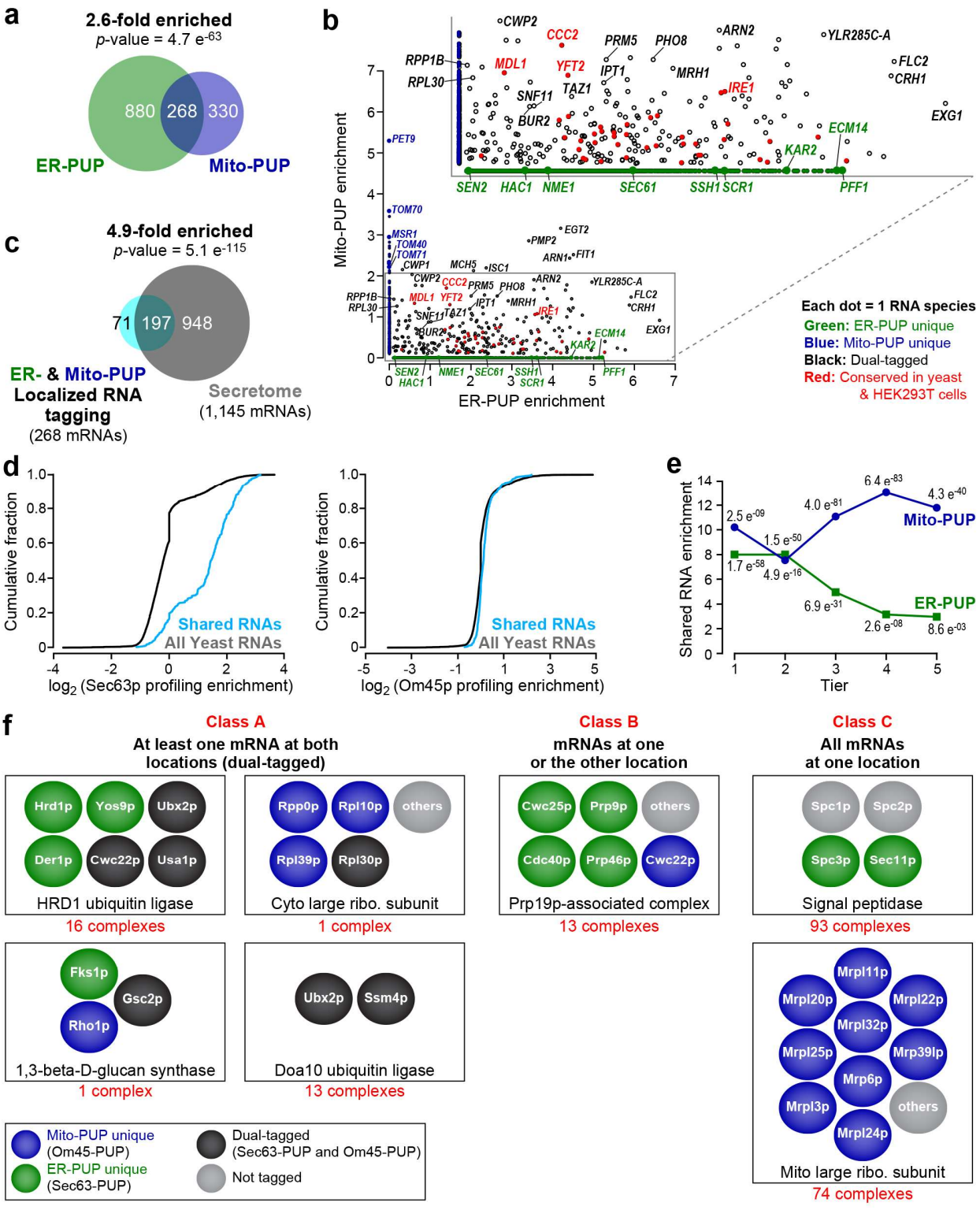
a
2.6-fold enriched
p-value = 4.7 e-63
880
268
330
ER-PUP
Mito-PUP
b
Mito-PUP enrichment
ER-PUP enrichment
Each dot = 1 RNA species
Green: ER-PUP unique
Blue: Mito-PUP unique
Black: Dual-tagged
Red: Conserved in yeast & HEK293T cells
c
4.9-fold enriched
p-value = 5.1 e-115
71
197
948
ER- & Mito-PUP Localized RNA tagging
(268 mRNAs)
Secretome
(1,145 mRNAs)
d
Cumulative fraction
Shared RNAs
All Yeast RNAs
log2 (Sec63p profiling enrichment)
log2 (Om45p profiling enrichment)
e
Shared RNA enrichment
Mito-PUP
ER-PUP
Tier
f
Class A
At least one mRNA at both locations (dual-tagged)
Class B
mRNAs at one or the other location
Class C
All mRNAs at one location
HRD1 ubiquitin ligase
16 complexes
Cyto large ribo. subunit
1 complex
Prp19p-associated complex
13 complexes
Signal peptidase
93 complexes
1,3-beta-D-glucan synthase
1 complex
Doa10 ubiquitin ligase
13 complexes
Mito large ribo. subunit
74 complexes
Mito-PUP unique (Om45-PUP)
ER-PUP unique (Sec63-PUP)
Dual-tagged (Sec63-PUP and Om45-PUP)
Not tagged

Figure 5. Dual tagging at both ER and mitochondria.

a) mRNAs tagged by ER-PUP and Mito-PUP. **b)** Comparison of RNAs uniquely enriched by the ER- (green dots) or Mito-PUP (blue dots), and those that were common to both (black, and red). Larger circles represent mRNAs that encode proteins typical of each organelle, while the red and purple dots denote mRNAs that are detected at the ER (ER-PUP unique) and mitochondria (Mito-PUP unique) by independent, APEX-seq studies in HEK293T cells.[25] **c)** Dual-tagged RNAs vs secretome mRNAs. **d)** Cumulative fraction of common RNAs that have ER-profiling[21] (left) and mitochondrial profiling[22] (right) enrichment. **e)** Distribution of common RNAs among ER- (green line) and Mito-PUP (blue line) rank. **f)** mRNAs that encode subunits of multiprotein complexes exhibit three localization patterns. Representative complexes depicted for each class; physical interactions between proteins not implied. For complete list, see Table 11.

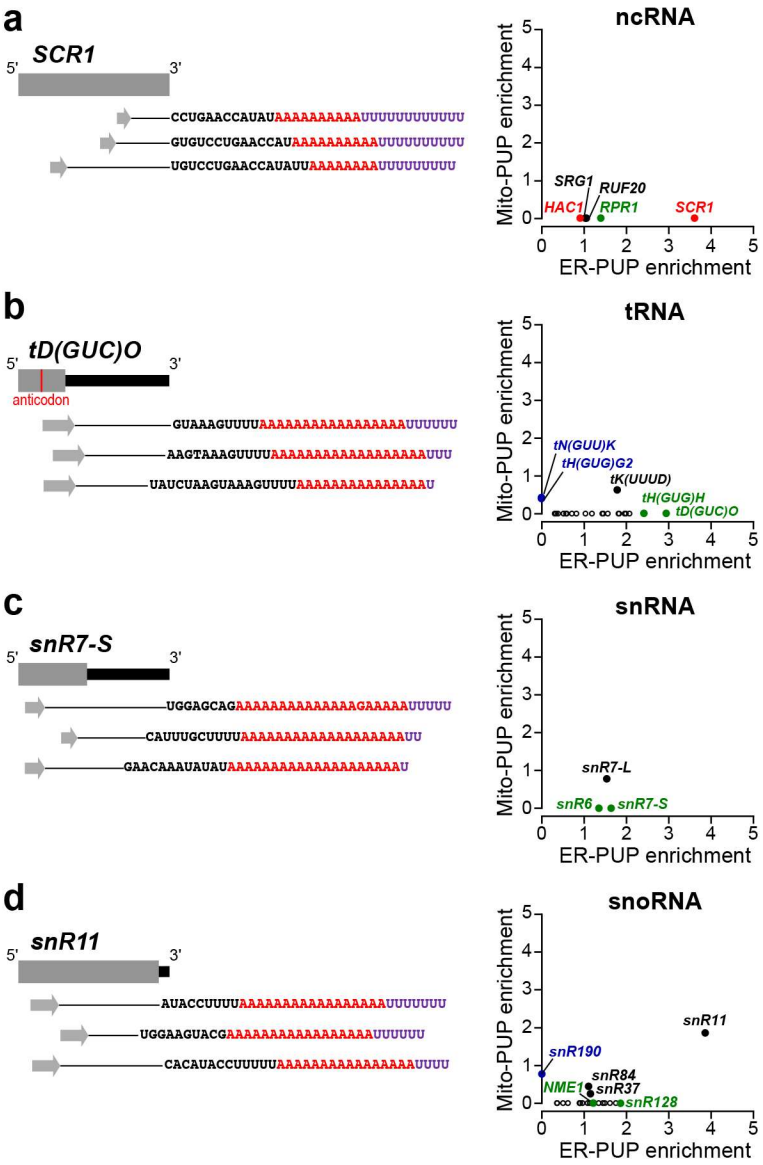
a
SCR1
5'
3'
CCUGAACCAUAUAAAAAAAAAAUUUUUUUUUUUU
GUGUCCUGAACCAUAAAAAAAAAAUUUUUUUUUU
UGUCCUGAACCAUAUUAAAAAAAAUUUUUUUUU
ncRNA
Mito-PUP enrichment
ER-PUP enrichment
SRG1
RUF20
HAC1
RPR1
SCR1
b
tD(GUC)O
anticodon
GUAAAGUUUUAAAAAAAAAAAAAAAAAAUUUUUU
AAGTAAAGUUUUAAAAAAAAAAAAAAAAAAUUU
UAUCUAAGUAAAGUUUUAAAAAAAAAAAAAAU
tRNA
tN(GUU)K
tH(GUG)G2
tK(UUUD)
tH(GUG)H
tD(GUC)O
c
snR7-S
UGGAGCAGAAAAAAAAAAAAAAGAAAAAUUUUU
CAUUUGCUUUUAAAAAAAAAAAAAAAAAAAUU
GAACAAAUAUAUAAAAAAAAAAAAAAAAAAAU
snRNA
snR7-L
snR6
snR7-S
d
snR11
AUACCUUUUAAAAAAAAAAAAAAAAAUUUUUUU
UGGAAGUACGAAAAAAAAAAAAAAAAAUUUUUU
CACAUACCUUUUUAAAAAAAAAAAAAAAAAUUUU
snoRNA
snR11
snR190
snR84
snR37
NME1
snR128

Figure 6. ncRNAs enriched at the ER and mitochondria.

ER- and Mito-PUP scatter analyses on right demonstrate the enrichment distributions for each of the four classes of non-protein coding RNA genes, which includes RNAs derived from **a)** ncRNAs, **b)** tRNAs **c)** snRNAs, and **d)** snoRNAs. Each RNA is represented by a single dot, and the dots are colored to reflect unique enrichment by ER-PUP (green) or Mito-PUP (blue), or both (black). Larger circles highlight notable RNAs such as the top RNAs for each site or, for the ncRNAs, RNAs characteristic of the ER (red dots). The top RNA in each class is diagrammed above each scatter plot. Forward reads are represented by gray arrows, while black sequences represent the DNA-encoded bit, presumably the 3' end of the RNA, detected in the reverse read. This is followed by the sequence of non-templated adenosines (red A's) and uridines (purple U's) that followed the 3' sequence. The line in between these two features represents the section of the gene that is inferred by the mapped paired-end reads.

SUPPLEMENTARY FIGURES

Medina-Muñoz et al. 2019 Figure S1

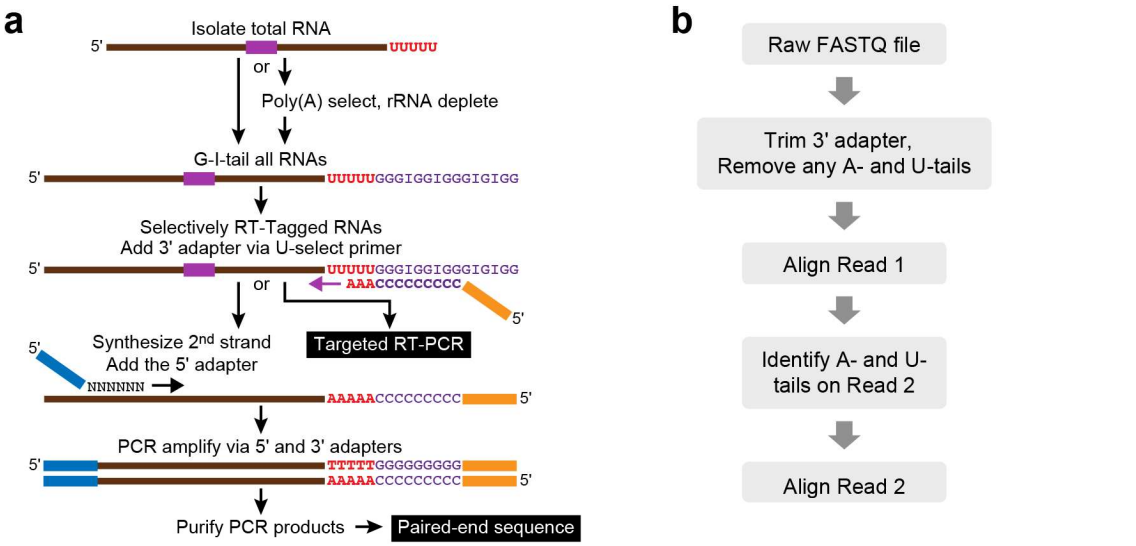

c

PUP alone (+PAB)

Replicate	Total Reads	Uniquely Mapped Reads	Number of Genes Identified
1	26,116,295	4,941,967	5,999
2	25,021,422	3,780,003	5,982
3	21,865,004	4,163,971	5,991

PUP alone (–PAB)

Replicate	Total Reads	Uniquely Mapped Reads	Number of Genes Identified
1	16,143,092	8,368,921	2,090
2	20,430,380	10,462,818	2,208
3	16,713,968	8,274,280	2,080

Figure S1. Detecting U-tagged RNAs.

a) *Experimental protocol.* From a preparation of total yeast RNA, RNAs with 3' terminal uridines were identified using sequential depletion of rRNAs and oligo(dT) selection, G/I-tailing, reverse transcription with a U-selective primer, and amplification.[26] Sequences of the 3' ends and tails were identified by paired-end sequencing (Illumina HiSeq2500) **b)** *Computational analysis.* Flowchart to identify RNAs tagged *in vivo.* **c)** *Representative data.* Sequencing statistics with PUP (+PAB) and PUP (-PAB). Experiments were performed with a minimum of three biological replicates and a minimum of two technical replicates for each one.

Medina-Muñoz et al. 2019 Figure S2

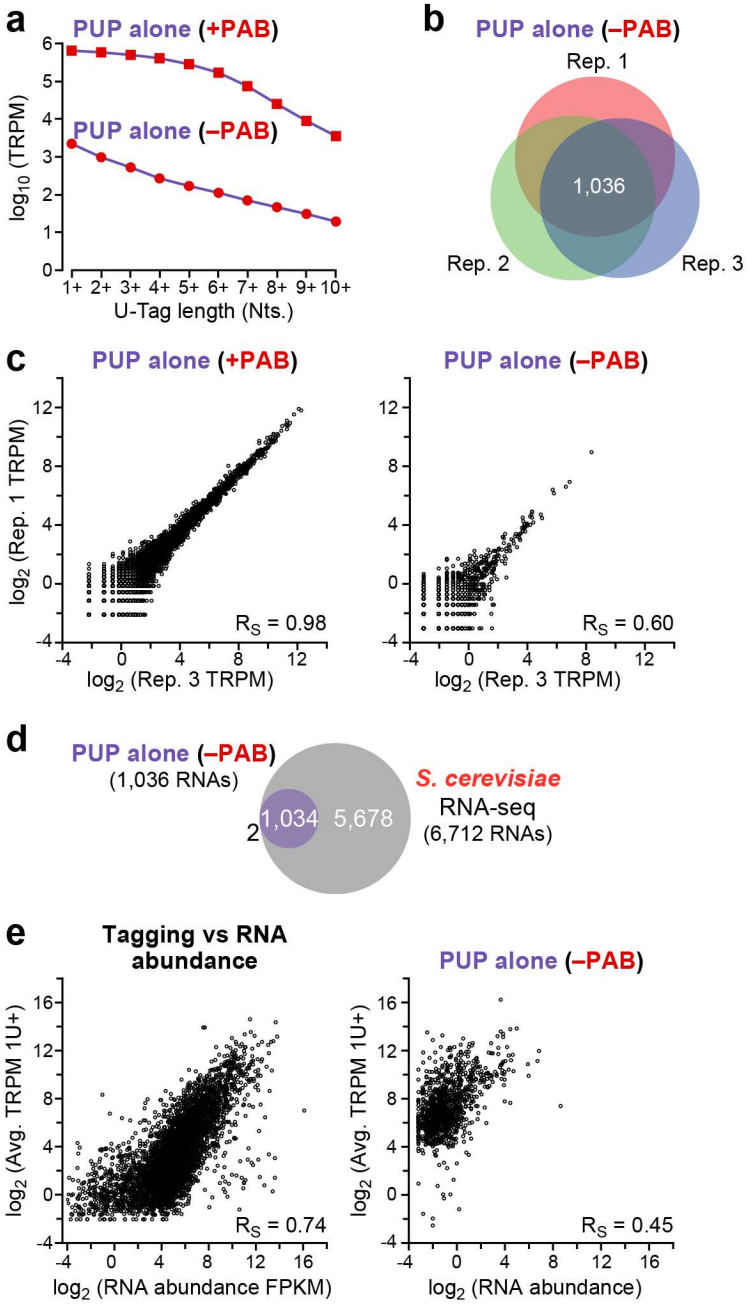

Figure S2. PUP tagging efficiency.

a) U-tag length intervals (1U-10U) and analogous PUP variant U-tag reads (TRPM). **b)** Reproducibility across three PUP alone (-PAB) biological replicates. **c)** Reproducibility and abundances of PUP alone, with (left) or without (right) PAB, for individual tagged mRNAs. Individual RNA species (black dots) reads (TRPM) are compared across two experiments. **d)** Comparison of the number of RNAs identified with PUP (-PAB) vs RNA seq.[26]. **e)** Tagged reads vs RNA abundance[26] for PUP alone with (left) or without (right) PAB.

Medina-Muñoz et al. 2019 Figure S3

a ER-PUP

Replicate	Total Reads	Uniquely Mapped Reads	Number of Genes Identified
1	15,779,019	4,455,578	5,285
2	20,712,699	4,716,985	5,684
3	15,357,796	4,345,423	5,506

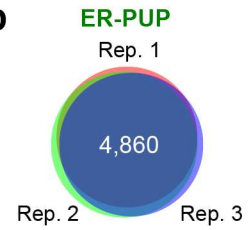

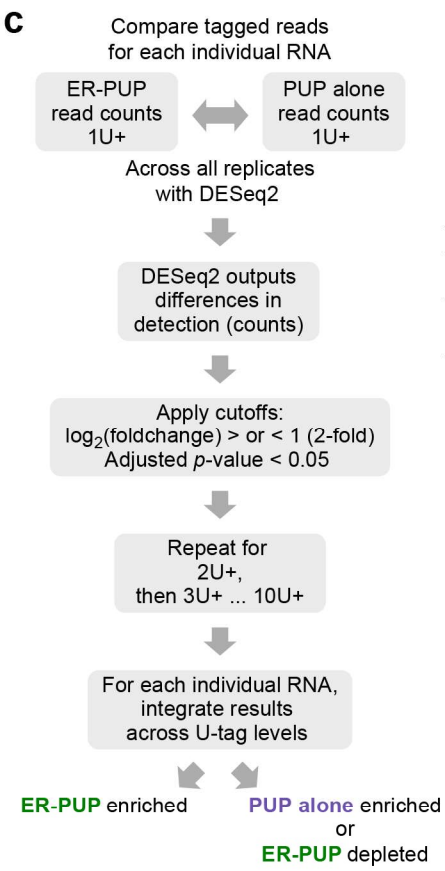

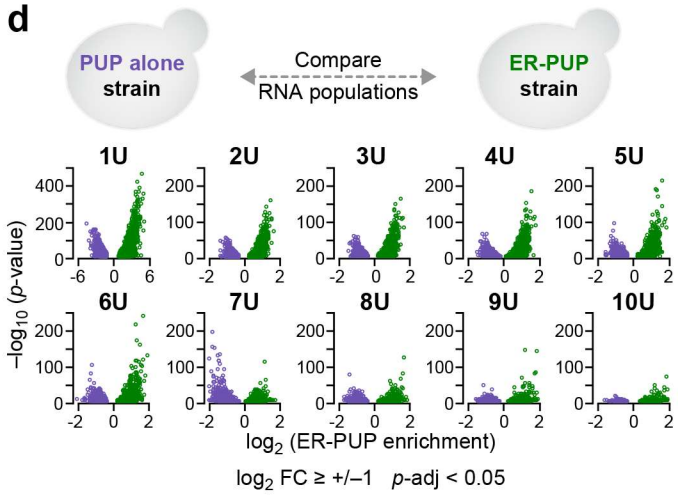

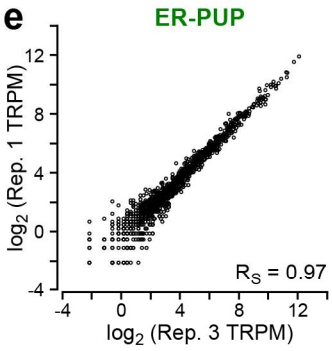

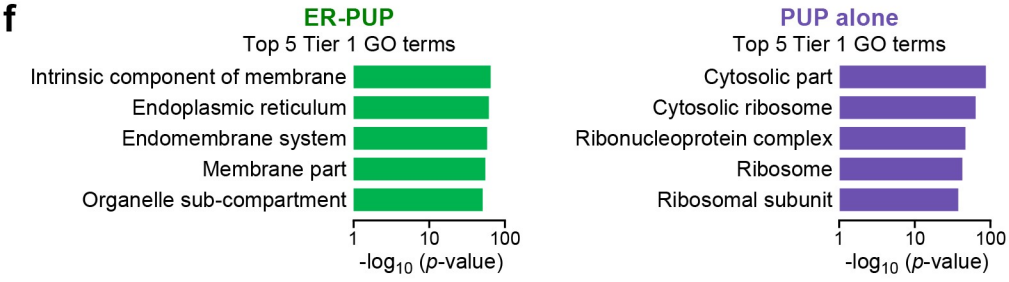

Figure S3. ER-enriched tagging events.

a) *Statistics.* ER-PUP sequencing statistics across three biological replicates. **b)** *Reproducibility.* Data as in (a). **c)** *Flowchart of computational analysis.* The steps used to identify RNAs whose tagging was enriched with ER-PUP or PUP alone are depicted. DESeq2[35] was used to identify statistically significant differences (adjusted *p*-value < 0.05), ($\log_2(\Delta$ tagged reads$) \geq 1$)). **d)** Enrichment of individual RNAs vs number of U's added. Differences (x-axis) and significance (y-axis) values distinguish individual RNA species (dots). Each U-tag length (1U-10U) was analyzed separately. RNAs to the right of zero on the x-axis are enriched by ER-PUP (green dots), while the ones on the left are depleted from ER PUP (aka enriched by PUP alone, purple dots). **e)** *Reproducibility.* Comparison of data from two biological ER-PUP replicates. **f)** *Functional enrichments.* Top five ER-PUP (top) and PUP alone (bottom) gene ontology (GO) terms are depicted.

Medina-Muñoz et al. 2019 Figure S4

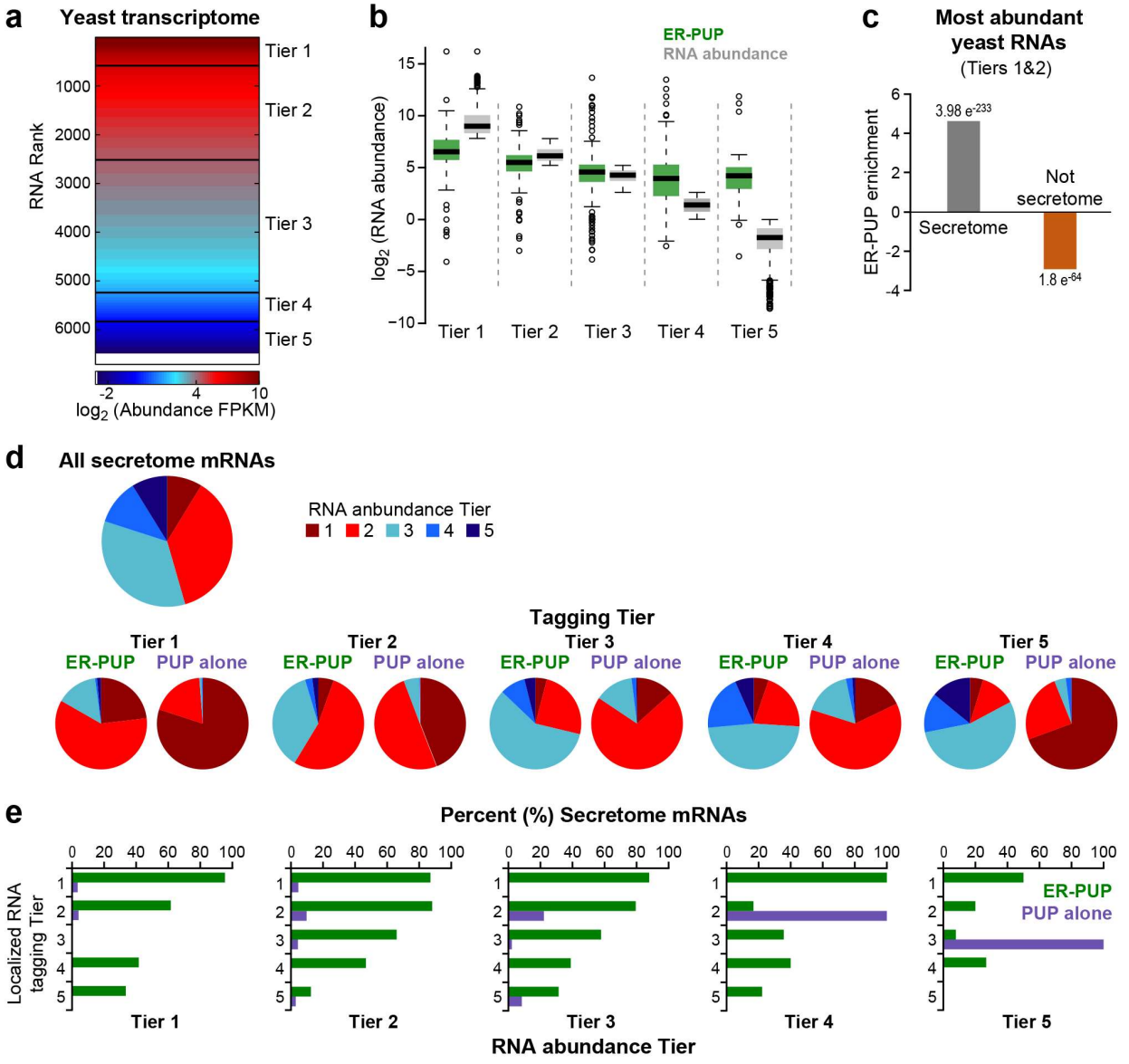

Figure S4. DESeq2 analysis of tagging and abundance.

a) The yeast transcriptome comprises five RNA abundance[26] (FPKM) tiers (clusters, K-means), ranked from most (Tier 1) to least abundant (Tier 5). **b)** Per tier RNA abundance of ER-enriched RNAs (green) and of all yeast transcripts (grey). **c)** Relationship of ER-PUP enrichment and secretome mRNAs in abundance Tiers 1 & 2. Hypergeometric distribution significance (*p*-values) are reported **d)** Per Tier ER-PUP and PUP alone abundance composition. **e)** Tagged RNAs populate five distinct RNA abundance bins (bar graphs). For each, the ER-PUP (green) and PUP alone Tiers (purple) (y-axes) project the proportion (%, x-axes) of secretome mRNAs.

Medina-Muñoz et al. 2019 Figure S5

a

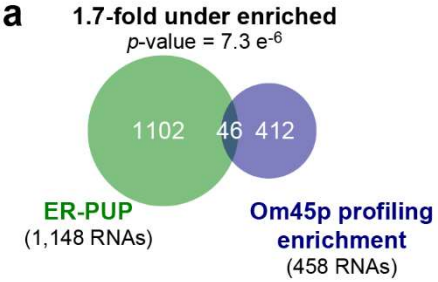

b

ER-PUP unique (503)		ER profiling unique (169)	
RNA type	Number	RNA type	Number
mRNA	453	mRNA	169
ncRNA	50		

c

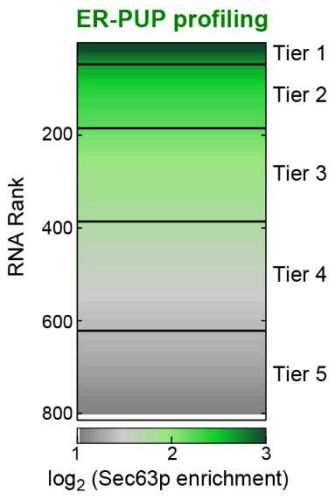

Figure S5. ER tagging and ribosome association.

a) Comparison of ER-tagged RNAs with mRNAs identified by mitochondrial (Om45) profiling.[22] **b)** RNAs identified uniquely by either tagging or profiling. **c)** ER (Sec63p) profiling data[21] comprises five enrichment clusters (tiers from K-means), from most (Tier 1) to least ribosome association (Tier 5).

Medina-Muñoz et al. 2019 Figure S6

a

Mito-PUP

Replicate	Total Reads	Uniquely Mapped Reads	Number of Genes Identified
1	10,474,965	3,145,944	4,545
2	8,972,024	2,547,077	4,816
3	8,833,263	2,196,090	4,016

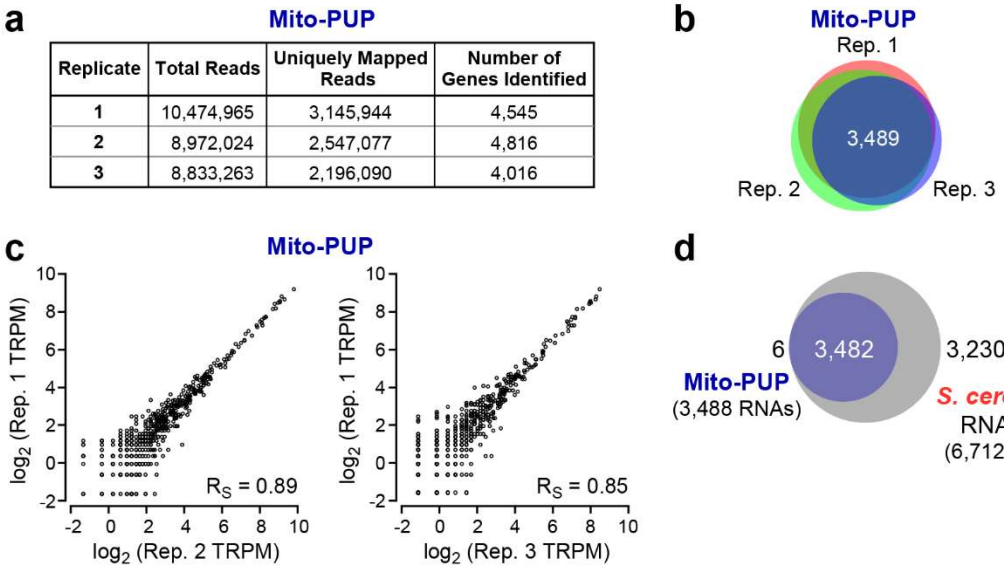

Figure S6. Mito-PUP tagging statistics and reproducibility.

a) *Statistics*. Data from three biological replicates. **b)** RNA species detected reproducibly across three replicates. **c)** Reproducibility of Mito-PUP tagging data. Relative abundance of Mito-PUP tagged RNAs (expressed as TRPM) (black dots) in pairs of biological replicates. **d)** Mito-PUP tagged RNAs vs the yeast transcriptome.[26]

Medina-Muñoz et al. 2019 Figure S7

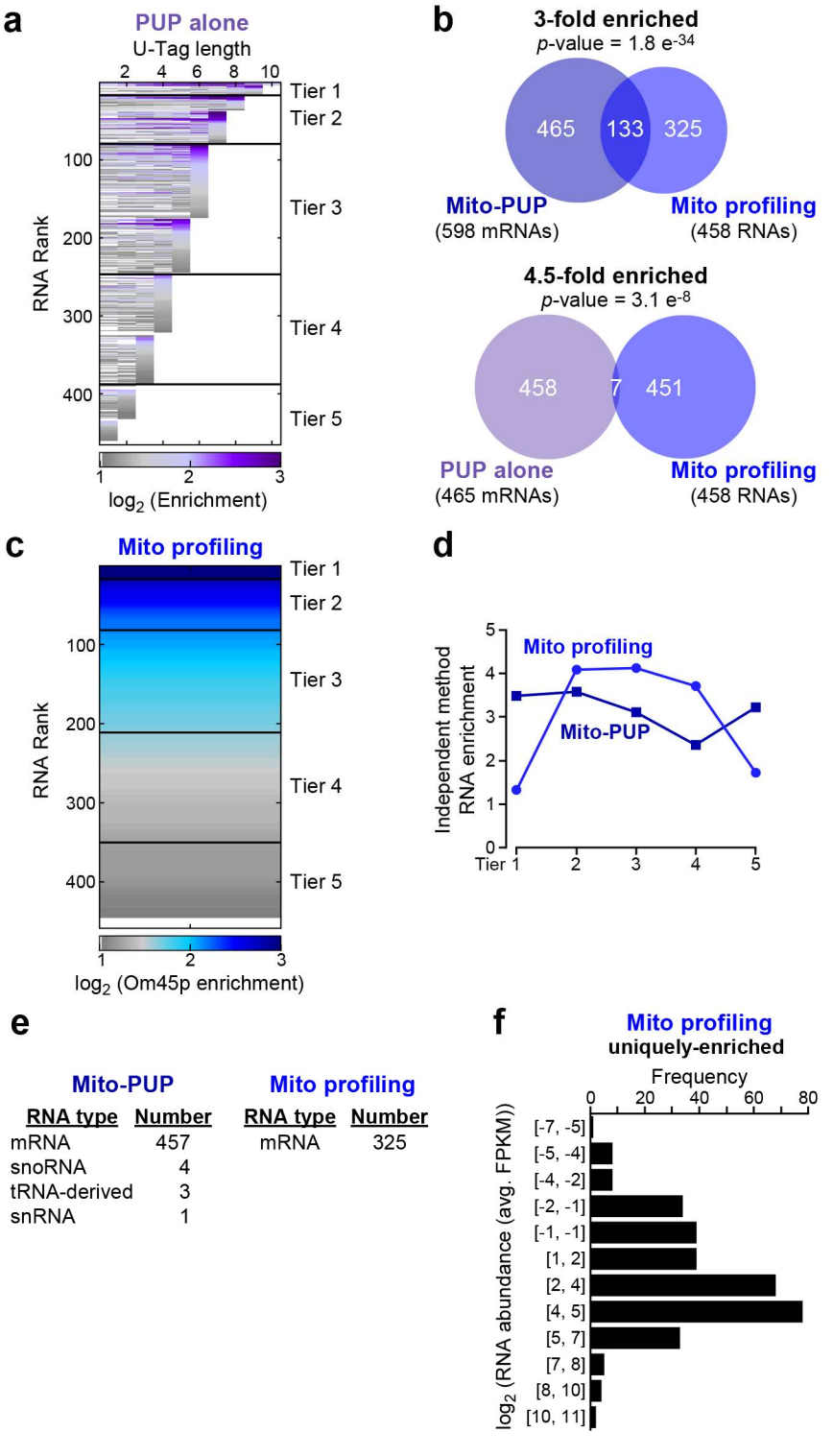

Figure S7. Mito-PUP tagging.

a) PUP alone-enriched RNAs (relative to Mito-PUP) clustered and ranked. Higher U-tag length yields a higher rank, from Tier 1 (longest) to Tier 5 (shortest). **b)** RNAs tagged by Mito-PUP (top) or PUP alone (bottom) vs mitochondria-proximal ribosome associated mRNAs (obtained using Om45 as an anchor[22]). **c)** Mitochondrial ribosome profiling data[22] used to define five (K-means) RNA clusters (Tiers) from the highest (Tier 1) to lowest (Tier 5) association with ribosomes. **d)** RNAs detected by both mitochondrial tagging and profiling. For RNAs detected by both tagging and profiling, the rank in each tier of the two individual methods is depicted. **e)** RNAs unique to tagging and profiling. **f)** Distribution of mRNAs unique to mitochondrial profiling across a series of RNA abundance[26] bins. Each bin (y-axis) represents a range of RNA abundance limits ($\log_2$(FPKM)). The number of RNAs that fall within those limits is projected by a black bar along the x-axis.

Medina-Muñoz et al. 2019 Figure S8

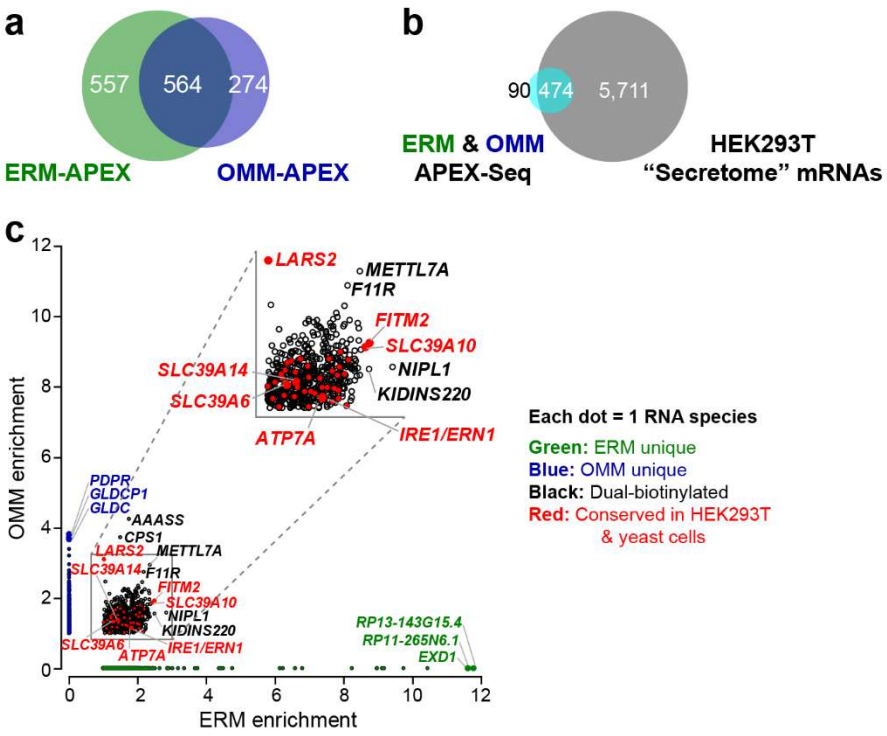

Figure S8. Conservation of dual-tagged RNA species in yeast and human cultured cells.

a) RNAs detected by APEX-seq in human (HEK293T) cells at ER membrane (ERM) vs outer mitochondrial membrane (OMM) (data reprocessed from *ref 25*). **b)** Dual-labeled secretome mRNAs from APEX-Seq. **c)** RNAs identified in tagging vs APEX-seq: conservation of RNAs at both ER and mitochondria. Each mRNA is represented by a dot, and plotted vs enrichment in ERM (x-axis) and OMM (y-axis). Organelle-specific mRNAs are green (ER) or blue (OMM), and lie on the x- or y-axes, respectively. Dual localized mRNAs in HEK293T cells are black. Red indicates RNAs that are identified at both the ER and mitochondria in both yeast and HEK293T cells. Blow-up insert highlights dual-tagged RNAs.

Medina-Muñoz et al. 2019 Figure S9

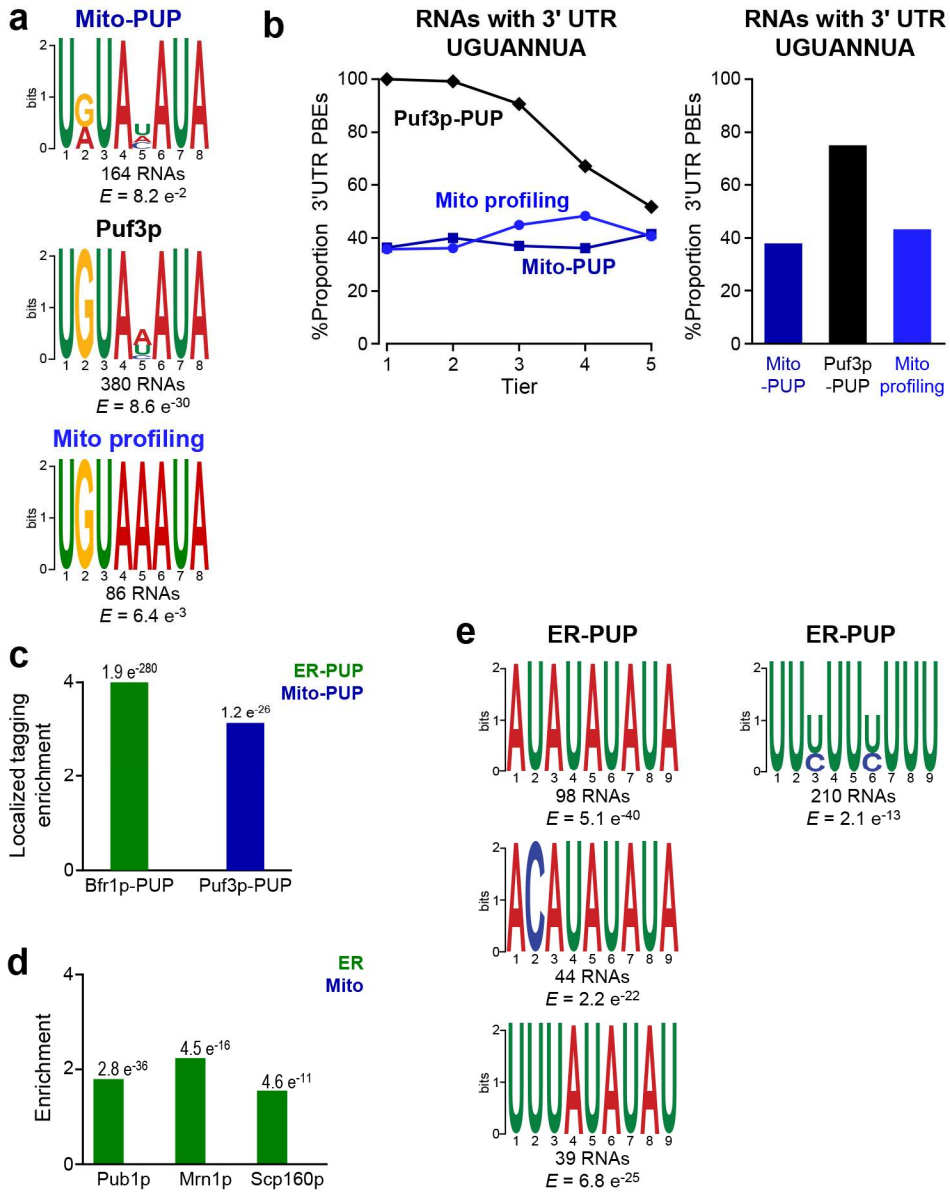

Figure S9. Sequence elements correlated with ER or mitochondrial localization.

a) Enrichment of motifs associated with mRNAs tagged by Mito-PUP (top), physically associated with Puf3p[26] (center), or bound by mitochondria-proximal ribosomes inferred from profiling[22] (bottom). **b)** fraction of mRNAs that with one or more Puf3p-binding element (PBE) in their 3' UTR, as a function of their tier in Mito-PUP tagging (dark blue), Puf3p-tagging[26] (black) or mitochondrial profiling[22] (light blue) tier Bar graph shows percent (%) of all RNAs detected that contain at least one PBE in the 3' UTR. **c)** RNAs that physically interact with Bfr1p and Puf3p targets[26] from among ER-PUP- (green) and Mito-PUP-tagged (blue) RNAs. Hypergeometric distribution significance (p-values) are shown. **d)** ER-PUP enriches additional RNA-binding protein targets (identified in RIP-chip[62]). **e)** Enrichment of motifs associated with mRNAs tagged by ER-PUP.

SUPPLEMENTARY TABLES

Supplementary Table I. ER-enriched RNAs: GO Terms.

Biological Process GO Terms	p-Value	Matches
transmembrane transport [GO:0055085]	1.1E-44	205
ion transport [GO:0006811]	1.7E-40	177
glycosylation [GO:0070085]	2.0E-32	67
ion transmembrane transport [GO:0034220]	4.2E-32	130
glycoprotein metabolic process [GO:0009100]	3.5E-31	66
transport [GO:0006810]	5.5E-30	376
glycoprotein biosynthetic process [GO:0009101]	1.5E-29	62
protein glycosylation [GO:0006486]	2.5E-29	60
macromolecule glycosylation [GO:0043413]	2.5E-29	60
establishment of localization [GO:0051234]	6.3E-28	380
localization [GO:0051179]	4.0E-27	416
mannosylation [GO:0097502]	1.1E-26	43
lipid metabolic process [GO:0006629]	9.8E-25	142
cation transport [GO:0006812]	1.4E-23	106
membrane lipid metabolic process [GO:0006643]	2.1E-23	58
anion transport [GO:0006820]	1.9E-22	96
membrane lipid biosynthetic process [GO:0046467]	1.9E-21	50
cellular lipid metabolic process [GO:0044255]	2.5E-21	130
metal ion transport [GO:0030001]	1.7E-20	56
protein N-linked glycosylation [GO:0006487]	6.0E-19	39
lipid biosynthetic process [GO:0008610]	7.2E-19	96
cation transmembrane transport [GO:0098655]	1.4E-18	88
metal ion homeostasis [GO:0055065]	1.1E-17	65
cation homeostasis [GO:0055080]	1.7E-16	76
anion transmembrane transport [GO:0098656]	2.3E-16	59
cellular metal ion homeostasis [GO:0006875]	8.1E-16	59

inorganic ion homeostasis [GO:0098771]	2.1E-15	72
carbohydrate derivative biosynthetic process [GO:1901137]	5.9E-15	104
organic anion transport [GO:0015711]	6.0E-15	74
glycolipid metabolic process [GO:0006664]	1.3E-14	31
liposaccharide metabolic process [GO:1903509]	1.3E-14	31
glycolipid biosynthetic process [GO:0009247]	1.5E-14	29
transition metal ion transport [GO:0000041]	3.3E-14	36
cellular cation homeostasis [GO:0030003]	3.5E-14	69
ion homeostasis [GO:0050801]	8.1E-14	76
chemical homeostasis [GO:0048878]	1.3E-13	87
protein lipidation [GO:0006497]	1.5E-13	35
lipoprotein biosynthetic process [GO:0042158]	1.5E-13	35
cell wall organization or biogenesis [GO:0071554]	2.4E-13	108
GPI anchor metabolic process [GO:0006505]	3.7E-13	28
lipoprotein metabolic process [GO:0042157]	4.1E-13	35
inorganic ion transmembrane transport [GO:0098660]	1.1E-12	73
GPI anchor biosynthetic process [GO:0006506]	2.1E-12	26
transition metal ion homeostasis [GO:0055076]	2.4E-12	49
protein O-linked glycosylation [GO:0006493]	4.4E-12	21
cellular homeostasis [GO:0019725]	5.3E-12	88
cellular chemical homeostasis [GO:0055082]	5.4E-12	76
cellular ion homeostasis [GO:0006873]	5.8E-12	69
cellular transition metal ion homeostasis [GO:0046916]	1.5E-11	45
inorganic cation transmembrane transport [GO:0098662]	4.5E-11	65
divalent inorganic cation transport [GO:0072511]	6.5E-11	28
divalent metal ion transport [GO:0070838]	9.4E-11	27
organic acid transport [GO:0015849]	1.5E-10	46
phospholipid metabolic process [GO:0006644]	1.9E-10	67
carboxylic acid transport [GO:0046942]	4.7E-10	45
sphingolipid metabolic process [GO:0006665]	1.0E-09	32
cell wall macromolecule metabolic process [GO:0044036]	1.0E-09	32
glycerolipid metabolic process [GO:0046486]	1.1E-09	59
organic substance transport [GO:0071702]	1.8E-09	237

amino acid transmembrane transport [GO:0003333]	2.2E-09	29
carbohydrate derivative metabolic process [GO:1901135]	4.5E-09	120
amino acid transport [GO:0006865]	5.4E-09	33
glycerophospholipid metabolic process [GO:0006650]	7.1E-09	54
glycerolipid biosynthetic process [GO:0045017]	8.6E-09	42
phospholipid biosynthetic process [GO:0008654]	8.6E-09	51
divalent inorganic cation homeostasis [GO:0072507]	8.7E-09	24
organic acid transmembrane transport [GO:1903825]	2.2E-08	35
cellular divalent inorganic cation homeostasis [GO:0072503]	3.9E-08	23
glycerophospholipid biosynthetic process [GO:0046474]	4.9E-08	40
carboxylic acid transmembrane transport [GO:1905039]	7.5E-08	34
phosphatidylinositol biosynthetic process [GO:0006661]	9.8E-08	28
sphingolipid biosynthetic process [GO:0030148]	1.0E-07	25
phosphatidylinositol metabolic process [GO:0046488]	1.0E-07	38
external encapsulating structure organization [GO:0045229]	3.5E-07	83
cell wall organization [GO:0071555]	3.5E-07	83
cell wall macromolecule biosynthetic process [GO:0044038]	3.6E-07	27
cellular component macromolecule biosynthetic process [GO:0070589]	3.6E-07	27
homeostatic process [GO:0042592]	6.2E-07	103
cell wall biogenesis [GO:0042546]	6.9E-07	47
nitrogen compound transport [GO:0071705]	1.0E-06	206
fungal-type cell wall organization or biogenesis [GO:0071852]	3.1E-06	76
response to endoplasmic reticulum stress [GO:0034976]	1.5E-05	38
maintenance of protein localization in endoplasmic reticulum [GO:0035437]	1.5E-05	11
drug transport [GO:0015893]	1.8E-05	37
cell wall mannoprotein biosynthetic process [GO:0000032]	2.3E-05	15
mannoprotein metabolic process [GO:0006056]	2.3E-05	15
mannoprotein biosynthetic process [GO:0006057]	2.3E-05	15
cell wall glycoprotein biosynthetic process [GO:0031506]	2.3E-05	15
iron ion transport [GO:0006826]	3.3E-05	17
protein retention in ER lumen [GO:0006621]	9.1E-05	10
polysaccharide metabolic process [GO:0005976]	1.1E-04	39
aromatic amino acid transport [GO:0015801]	1.5E-04	11

protein mannosylation [GO:0035268]	1.5E-04	11
drug transmembrane transport [GO:0006855]	1.6E-04	26
oligosaccharide-lipid intermediate biosynthetic process [GO:0006490]	1.6E-04	12
regulation of biological quality [GO:0065008]	2.0E-04	145
protein localization to endoplasmic reticulum [GO:0070972]	3.8E-04	27
ERAD pathway [GO:0036503]	4.4E-04	26
N-glycan processing [GO:0006491]	5.5E-04	9
calcium ion transport [GO:0006816]	8.5E-04	10
beta-glucan metabolic process [GO:0051273]	8.5E-04	16
beta-glucan biosynthetic process [GO:0051274]	8.5E-04	16
calcium ion transmembrane transport [GO:0070588]	3.3E-03	8
cofactor transport [GO:0051181]	4.3E-03	18
zinc ion transport [GO:0006829]	4.3E-03	10
nucleobase transport [GO:0015851]	4.6E-03	9
cellular manganese ion homeostasis [GO:0030026]	4.6E-03	9
protein O-linked mannosylation [GO:0035269]	4.6E-03	9
manganese ion homeostasis [GO:0055071]	4.6E-03	9
fungal-type cell wall organization [GO:0031505]	4.9E-03	61
regulation of membrane lipid distribution [GO:0097035]	5.8E-03	14
basic amino acid transport [GO:0015802]	6.8E-03	12
lipid translocation [GO:0034204]	1.0E-02	13
cellular potassium ion transport [GO:0071804]	1.1E-02	11
potassium ion transmembrane transport [GO:0071805]	1.1E-02	11
inorganic anion transport [GO:0015698]	1.3E-02	18
cellular zinc ion homeostasis [GO:0006882]	1.6E-02	10
zinc ion homeostasis [GO:0055069]	1.6E-02	10
basic amino acid transmembrane transport [GO:1990822]	1.6E-02	10
polysaccharide biosynthetic process [GO:0000271]	1.8E-02	26
tyrosine transport [GO:0015828]	2.0E-02	7
ceramide metabolic process [GO:0006672]	2.2E-02	9
copper ion import [GO:0015677]	2.2E-02	9
zinc ion transmembrane transport [GO:0071577]	2.2E-02	9
iron ion homeostasis [GO:0055072]	2.2E-02	25

manganese ion transport [GO:0006828]	2.5E-02	8
fungal-type cell wall beta-glucan metabolic process [GO:0070879]	2.5E-02	8
fungal-type cell wall beta-glucan biosynthetic process [GO:0070880]	2.5E-02	8
response to unfolded protein [GO:0006986]	2.9E-02	22
calcium ion homeostasis [GO:0055074]	2.9E-02	11
maintenance of protein localization in organelle [GO:0072595]	2.9E-02	11
phospholipid translocation [GO:0045332]	4.0E-02	12
cellular polysaccharide biosynthetic process [GO:0033692]	4.5E-02	25
response to organonitrogen compound [GO:0010243]	4.6E-02	31
coenzyme transport [GO:0051182]	4.7E-02	10

Molecular Function GO Terms	p-Value	Matches
transmembrane transporter activity [GO:0022857]	5.1E-54	185
transporter activity [GO:0005215]	7.5E-53	192
ion transmembrane transporter activity [GO:0015075]	5.7E-39	136
inorganic molecular entity transmembrane transporter activity [GO:0015318]	5.1E-31	119
transferase activity, transferring hexosyl groups [GO:0016758]	2.7E-30	63
mannosyltransferase activity [GO:0000030]	9.4E-27	41
transferase activity, transferring glycosyl groups [GO:0016757]	2.5E-26	68
cation transmembrane transporter activity [GO:0008324]	1.0E-24	94
metal ion transmembrane transporter activity [GO:0046873]	1.4E-20	44
anion transmembrane transporter activity [GO:0008509]	2.8E-18	60
active transmembrane transporter activity [GO:0022804]	4.7E-17	77
organic anion transmembrane transporter activity [GO:0008514]	4.6E-15	50
inorganic cation transmembrane transporter activity [GO:0022890]	7.3E-15	69
secondary active transmembrane transporter activity [GO:0015291]	3.0E-14	50
transition metal ion transmembrane transporter activity [GO:0046915]	6.0E-13	27
organic acid transmembrane transporter activity [GO:0005342]	2.6E-11	39
carboxylic acid transmembrane transporter activity [GO:0046943]	9.6E-11	38
drug transmembrane transporter activity [GO:0015238]	1.9E-10	35
amino acid transmembrane transporter activity [GO:0015171]	1.6E-08	27
alpha-1,2-mannosyltransferase activity [GO:0000026]	8.2E-08	13
signaling receptor activity [GO:0038023]	1.6E-07	14
hydrolase activity, hydrolyzing O-glycosyl compounds [GO:0004553]	3.4E-06	26
hydrolase activity, acting on glycosyl bonds [GO:0016798]	1.7E-05	29
symporter activity [GO:0015293]	2.3E-05	24
antiporter activity [GO:0015297]	1.0E-04	19
alpha-1,6-mannosyltransferase activity [GO:0000009]	1.4E-04	9
aromatic amino acid transmembrane transporter activity [GO:0015173]	1.4E-04	9
transmembrane signaling receptor activity [GO:0004888]	2.1E-04	10

nucleobase-containing compound transmembrane transporter activity [GO:0015932]	3.4E-04	16
basic amino acid transmembrane transporter activity [GO:0015174]	7.8E-04	11
cofactor transmembrane transporter activity [GO:0051184]	8.8E-04	13
calcium ion transmembrane transporter activity [GO:0015085]	9.1E-04	8
nucleobase transmembrane transporter activity [GO:0015205]	1.2E-03	9
ATPase activity, coupled to movement of substances [GO:0043492]	2.6E-03	28
oxidoreductase activity, oxidizing metal ions [GO:0016722]	4.0E-03	10
xenobiotic transmembrane transporter activity [GO:0042910]	4.0E-03	10
solute:cation symporter activity [GO:0015294]	5.3E-03	19
zinc ion transmembrane transporter activity [GO:0005385]	5.7E-03	9
dolichyl-phosphate-mannose-protein mannosyltransferase activity [GO:0004169]	5.8E-03	7
monovalent inorganic cation transmembrane transporter activity [GO:0015077]	9.0E-03	36
carbohydrate derivative transmembrane transporter activity [GO:1901505]	1.0E-02	14
potassium ion transmembrane transporter activity [GO:0015079]	1.2E-02	10
ammonium transmembrane transporter activity [GO:0008519]	1.7E-02	11
ATPase activity, coupled to transmembrane movement of substances [GO:0042626]	1.7E-02	26
divalent inorganic cation transmembrane transporter activity [GO:0072509]	2.0E-02	9
alpha-1,3-mannosyltransferase activity [GO:0000033]	3.7E-02	6
L-tyrosine transmembrane transporter activity [GO:0005302]	3.7E-02	6
manganese ion transmembrane transporter activity [GO:0005384]	4.0E-02	7
protein-cysteine S-palmitoyltransferase activity [GO:0019706]	4.0E-02	7
protein-cysteine S-acyltransferase activity [GO:0019707]	4.0E-02	7
vitamin transmembrane transporter activity [GO:0090482]	4.0E-02	7
exopeptidase activity [GO:0008238]	4.8E-02	15

Pathways	p-Value	Matches
sphingolipid metabolism	1.3E-08	15
lipid-linked oligosaccharide biosynthesis	2.9E-07	11
triglyceride biosynthesis	3.6E-02	5

Supplementary Table II. Mitochondria-enriched RNAs: GO Terms.

Biological Process GO Terms	p-Value	Matches
transmembrane transport [GO:0055085]	7.8E-17	108
metal ion homeostasis [GO:0055065]	5.6E-16	48
metal ion transport [GO:0030001]	8.5E-16	40
ion transport [GO:0006811]	5.9E-14	91
cation homeostasis [GO:0055080]	7.4E-13	52
transition metal ion homeostasis [GO:0055076]	1.1E-12	38
inorganic ion homeostasis [GO:0098771]	1.7E-12	50
chemical homeostasis [GO:0048878]	2.5E-12	61
ion homeostasis [GO:0050801]	8.7E-12	53
cellular metal ion homeostasis [GO:0006875]	2.4E-11	40
transition metal ion transport [GO:0000041]	1.1E-09	25
ion transmembrane transport [GO:0034220]	2.6E-09	64
cellular chemical homeostasis [GO:0055082]	2.6E-09	51
iron ion homeostasis [GO:0055072]	3.1E-09	27
inorganic ion transmembrane transport [GO:0098660]	4.9E-09	48
cellular cation homeostasis [GO:0030003]	6.2E-09	44
cellular transition metal ion homeostasis [GO:0046916]	1.7E-08	31
cellular ion homeostasis [GO:0006873]	3.0E-08	45
inorganic cation transmembrane transport [GO:0098662]	5.7E-08	43
cellular homeostasis [GO:0019725]	1.6E-07	55
cation transport [GO:0006812]	2.6E-07	54
iron ion transport [GO:0006826]	1.2E-06	15
homeostatic process [GO:0042592]	1.4E-06	69
cation transmembrane transport [GO:0098655]	4.7E-06	46
cellular iron ion homeostasis [GO:0006879]	9.3E-05	20
mitochondrion organization [GO:0007005]	1.4E-04	56
transport [GO:0006810]	1.7E-04	180
divalent inorganic cation transport [GO:0072511]	5.7E-04	16
regulation of biological quality [GO:0065008]	6.2E-04	92
establishment of localization [GO:0051234]	8.3E-04	182

divalent metal ion transport [GO:0070838]	1.7E-03	15
mitochondrial transport [GO:0006839]	2.2E-03	26
cofactor transport [GO:0051181]	3.3E-03	14
divalent inorganic cation homeostasis [GO:0072507]	3.3E-03	14
phosphate ion transport [GO:0006817]	4.1E-03	9
protein localization to mitochondrion [GO:0070585]	9.2E-03	21
establishment of protein localization to mitochondrion [GO:0072655]	9.2E-03	21
anion transport [GO:0006820]	1.1E-02	40
iron ion transmembrane transport [GO:0034755]	1.2E-02	8
mitochondrial genome maintenance [GO:0000002]	1.2E-02	16
mitochondrial transmembrane transport [GO:1990542]	1.4E-02	20
cellular divalent inorganic cation homeostasis [GO:0072503]	1.5E-02	13
iron coordination entity transport [GO:1901678]	2.0E-02	9
localization [GO:0051179]	3.0E-02	195

Cellular Component GO Terms	p-Value	Matches
mitochondrion [GO:0005739]	1.1E-23	220
mitochondrial part [GO:0044429]	2.8E-21	141
cytoplasmic part [GO:0044444]	6.2E-21	446
intrinsic component of membrane [GO:0031224]	3.1E-20	253
membrane [GO:0016020]	2.8E-18	326
membrane part [GO:0044425]	1.5E-17	279
integral component of membrane [GO:0016021]	7.8E-15	231
mitochondrial membrane [GO:0031966]	1.2E-14	94
organelle membrane [GO:0031090]	1.2E-14	170
mitochondrial envelope [GO:0005740]	1.4E-14	100
organelle inner membrane [GO:0019866]	3.0E-12	69
mitochondrial inner membrane [GO:0005743]	3.5E-12	67
cell periphery [GO:0071944]	1.5E-11	142
organelle envelope [GO:0031967]	1.1E-10	111
envelope [GO:0031975]	1.1E-10	111
cytoplasm [GO:0005737]	2.5E-10	509
intracellular membrane-bounded organelle [GO:0043231]	3.2E-09	486
extracellular region [GO:0005576]	3.9E-09	38
membrane-bounded organelle [GO:0043227]	5.2E-09	490
endoplasmic reticulum [GO:0005783]	6.5E-09	117
intracellular organelle [GO:0043229]	2.0E-08	511
organelle [GO:0043226]	2.3E-08	511
storage vacuole [GO:0000322]	3.6E-08	87
fungal-type vacuole [GO:0000324]	3.6E-08	87
lytic vacuole [GO:0000323]	4.0E-08	87
plasma membrane [GO:0005886]	8.0E-08	100
vacuole [GO:0005773]	1.1E-06	92
cell part [GO:0044464]	3.2E-06	573

mitochondrial matrix [GO:0005759]	4.4E-06	52
cell wall [GO:0005618]	6.0E-06	36
external encapsulating structure [GO:0030312]	6.0E-06	36
fungal-type cell wall [GO:0009277]	6.1E-06	35
cell [GO:0005623]	6.6E-06	573
endomembrane system [GO:0012505]	1.6E-05	153
endoplasmic reticulum part [GO:0044432]	2.4E-05	73
endoplasmic reticulum subcompartment [GO:0098827]	4.3E-05	70
mitochondrial membrane part [GO:0044455]	1.0E-04	42
endoplasmic reticulum membrane [GO:0005789]	1.9E-04	67
anchored component of membrane [GO:0031225]	2.6E-04	21
intrinsic component of mitochondrial membrane [GO:0098573]	3.0E-04	22
intracellular organelle part [GO:0044446]	3.2E-04	351
organelle subcompartment [GO:0031984]	3.8E-04	84
organelle part [GO:0044422]	4.7E-04	351
nuclear outer membrane-endoplasmic reticulum membrane network [GO:0042175]	6.9E-04	67
integral component of mitochondrial membrane [GO:0032592]	2.0E-03	20
intrinsic component of organelle membrane [GO:0031300]	2.1E-03	31
bounding membrane of organelle [GO:0098588]	2.5E-03	92
mitochondrial protein complex [GO:0098798]	3.1E-03	42
integral component of organelle membrane [GO:0031301]	7.0E-03	29
intrinsic component of mitochondrial inner membrane [GO:0031304]	7.7E-03	14
plasma membrane part [GO:0044459]	9.1E-03	35
intrinsic component of plasma membrane [GO:0031226]	1.3E-02	28
whole membrane [GO:0098805]	1.4E-02	82
vacuolar membrane [GO:0005774]	2.4E-02	48
integral component of plasma membrane [GO:0005887]	3.6E-02	26

Molecular Function GO Terms	p-Value	Matches
transmembrane transporter activity [GO:0022857]	7.3E-15	92
transporter activity [GO:0005215]	1.5E-13	94
metal ion transmembrane transporter activity [GO:0046873]	2.1E-11	29
inorganic molecular entity transmembrane transporter activity [GO:0015318]	2.5E-07	58
ion transmembrane transporter activity [GO:0015075]	4.1E-07	61
transition metal ion transmembrane transporter activity [GO:0046915]	6.0E-07	18
inorganic cation transmembrane transporter activity [GO:0022890]	2.8E-05	39
active transmembrane transporter activity [GO:0022804]	2.0E-04	40
cation transmembrane transporter activity [GO:0008324]	2.8E-04	43
secondary active transmembrane transporter activity [GO:0015291]	4.0E-03	25
peptide transmembrane transporter activity [GO:1904680]	5.0E-03	14
inorganic phosphate transmembrane transporter activity [GO:0005315]	1.4E-02	6
amide transmembrane transporter activity [GO:0042887]	4.1E-02	15
iron ion transmembrane transporter activity [GO:0005381]	4.8E-02	7

Supplementary Table III. 133 mRNAs common to Mitochondria tagging and Mitochondrial Profiling: GO Terms.

Biological Process GO Terms	p-Value	Matches
mitochondrion organization [GO:0007005]	2.3E-20	41
mitochondrial transport [GO:0006839]	3.1E-11	20
protein localization to mitochondrion [GO:0070585]	5.3E-10	17
establishment of protein localization to mitochondrion [GO:0072655]	5.3E-10	17
mitochondrial transmembrane transport [GO:1990542]	3.2E-09	16
mitochondrial gene expression [GO:0140053]	3.9E-08	24
mitochondrial membrane organization [GO:0007006]	3.9E-07	13
protein targeting to mitochondrion [GO:0006626]	3.8E-06	13
mitochondrial RNA metabolic process [GO:0000959]	1.0E-05	11
mitochondrial genome maintenance [GO:0000002]	1.3E-05	11
protein transmembrane transport [GO:0071806]	1.8E-05	14
transmembrane transport [GO:0055085]	4.7E-05	31
iron ion homeostasis [GO:0055072]	2.6E-04	11
protein transmembrane import into intracellular organelle [GO:0044743]	5.3E-04	11
inner mitochondrial membrane organization [GO:0007007]	6.6E-04	8
transition metal ion homeostasis [GO:0055076]	2.8E-03	12
mitochondrial RNA processing [GO:0000963]	5.1E-03	7
mitochondrial translation [GO:0032543]	5.9E-03	16
intracellular protein transmembrane transport [GO:0065002]	6.3E-03	11
cellular iron ion homeostasis [GO:0006879]	7.7E-03	9
protein import into mitochondrial matrix [GO:0030150]	3.9E-02	6
metal ion homeostasis [GO:0055065]	5.0E-02	12

Cellular Component GO Terms	p-Value	Matches
mitochondrion [GO:0005739]	8.4E-71	120
mitochondrial part [GO:0044429]	3.4E-55	89
mitochondrial envelope [GO:0005740]	1.5E-43	70
mitochondrial membrane [GO:0031966]	7.7E-43	67
organelle envelope [GO:0031967]	4.1E-35	70
envelope [GO:0031975]	4.1E-35	70
mitochondrial inner membrane [GO:0005743]	1.5E-34	51
organelle inner membrane [GO:0019866]	1.5E-33	51
cytoplasmic part [GO:0044444]	1.1E-22	126
organelle membrane [GO:0031090]	3.1E-19	68
mitochondrial membrane part [GO:0044455]	1.0E-15	30
intrinsic component of mitochondrial membrane [GO:0098573]	2.8E-12	18
intracellular membrane-bounded organelle [GO:0043231]	3.8E-11	126
cytoplasm [GO:0005737]	1.8E-10	128
membrane-bounded organelle [GO:0043227]	1.8E-10	126
integral component of mitochondrial membrane [GO:0032592]	3.0E-10	16
intracellular organelle [GO:0043229]	2.1E-09	128
organelle [GO:0043226]	2.2E-09	128
intrinsic component of mitochondrial inner membrane [GO:0031304]	1.4E-08	12
mitochondrial matrix [GO:0005759]	1.0E-07	24
intrinsic component of organelle membrane [GO:0031300]	3.0E-07	18
integral component of mitochondrial inner membrane [GO:0031305]	1.8E-06	10
integral component of organelle membrane [GO:0031301]	9.4E-06	16
mitochondrial protein complex [GO:0098798]	1.8E-05	20
mitochondrial outer membrane [GO:0005741]	3.5E-05	14
organelle outer membrane [GO:0031968]	7.1E-05	14
outer membrane [GO:0019867]	7.9E-05	14
intracellular organelle part [GO:0044446]	9.2E-05	95
organelle part [GO:0044422]	1.1E-04	95
membrane [GO:0016020]	9.8E-04	76

intracellular part [GO:0044424]	3.5E-03	130
intracellular [GO:0005622]	3.8E-03	130
intrinsic component of membrane [GO:0031224]	2.0E-02	55
membrane part [GO:0044425]	2.6E-02	62
i-AAA complex [GO:0031942]	3.7E-02	3

Molecular Function GO Terms	p-Value	Matches
peptide transmembrane transporter activity [GO:1904680]	6.6E-06	10
amide transmembrane transporter activity [GO:0042887]	1.2E-04	10
protein transmembrane transporter activity [GO:0008320]	2.0E-04	8
macromolecule transmembrane transporter activity [GO:0022884]	2.0E-04	8
protein transporter activity [GO:0008565]	3.8E-04	8
small molecule binding [GO:0036094]	8.2E-03	42
anion binding [GO:0043168]	3.6E-02	41

Supplementary Table IV. Mitochondria tagging Unique vs Mitochondrial Profiling: GO Terms.

Biological Process GO Terms	p-Value	Matches
metal ion transport [GO:0030001]	5.0E-12	32
ion transport [GO:0006811]	7.3E-11	72
metal ion homeostasis [GO:0055065]	2.1E-10	36
transmembrane transport [GO:0055085]	5.2E-09	77
cation homeostasis [GO:0055080]	6.4E-09	40
ion transmembrane transport [GO:0034220]	6.6E-09	54
inorganic ion homeostasis [GO:0098771]	2.4E-08	38
chemical homeostasis [GO:0048878]	5.1E-08	46
ion homeostasis [GO:0050801]	1.2E-07	40
cellular metal ion homeostasis [GO:0006875]	3.4E-07	30
transition metal ion transport [GO:0000041]	3.9E-07	20
inorganic ion transmembrane transport [GO:0098660]	9.2E-07	38
inorganic cation transmembrane transport [GO:0098662]	1.7E-06	35
cellular chemical homeostasis [GO:0055082]	3.4E-06	39
transition metal ion homeostasis [GO:0055076]	3.4E-06	26
cation transport [GO:0006812]	3.9E-06	44
cellular cation homeostasis [GO:0030003]	4.0E-06	34
cellular homeostasis [GO:0019725]	2.3E-05	43
cation transmembrane transport [GO:0098655]	2.7E-05	38
cellular ion homeostasis [GO:0006873]	3.6E-05	34
homeostatic process [GO:0042592]	2.7E-04	53
transport [GO:0006810]	6.3E-04	143
cell wall organization or biogenesis [GO:0071554]	1.1E-03	47
cellular transition metal ion homeostasis [GO:0046916]	1.3E-03	21
iron ion transport [GO:0006826]	1.6E-03	11
external encapsulating structure organization [GO:0045229]	2.7E-03	41
cell wall organization [GO:0071555]	2.7E-03	41
establishment of localization [GO:0051234]	5.5E-03	143
divalent inorganic cation transport [GO:0072511]	7.5E-03	13
anion transport [GO:0006820]	8.3E-03	34

divalent inorganic cation homeostasis [GO:0072507]	9.1E-03	12
glycerophospholipid metabolic process [GO:0006650]	1.2E-02	25
regulation of biological quality [GO:0065008]	1.9E-02	71
iron ion homeostasis [GO:0055072]	2.0E-02	16
glycerolipid metabolic process [GO:0046486]	2.5E-02	26
divalent metal ion transport [GO:0070838]	2.6E-02	12
anion transmembrane transport [GO:0098656]	3.0E-02	22
localization [GO:0051179]	4.0E-02	155
fungal-type cell wall organization or biogenesis [GO:0071852]	4.3E-02	36
cellular divalent inorganic cation homeostasis [GO:0072503]	4.7E-02	11

Cellular Component GO Terms	p-Value	Matches
cell periphery [GO:0071944]	1.3E-16	130
endoplasmic reticulum [GO:0005783]	3.5E-16	114
intrinsic component of membrane [GO:0031224]	1.4E-15	198
endomembrane system [GO:0012505]	8.4E-14	149
membrane part [GO:0044425]	4.4E-13	217
membrane [GO:0016020]	2.0E-12	250
plasma membrane [GO:0005886]	2.6E-12	94
storage vacuole [GO:0000322]	2.9E-12	82
fungal-type vacuole [GO:0000324]	2.9E-12	82
lytic vacuole [GO:0000323]	3.3E-12	82
integral component of membrane [GO:0016021]	4.2E-11	180
vacuole [GO:0005773]	4.4E-10	85
endoplasmic reticulum part [GO:0044432]	1.2E-09	71
extracellular region [GO:0005576]	1.4E-09	34
endoplasmic reticulum subcompartment [GO:0098827]	3.6E-09	68
organelle subcompartment [GO:0031984]	7.4E-09	82
endoplasmic reticulum membrane [GO:0005789]	3.2E-08	65
nuclear outer membrane-endoplasmic reticulum membrane network [GO:0042175]	1.4E-07	65
cytoplasmic part [GO:0044444]	1.4E-06	320
cell wall [GO:0005618]	8.0E-06	31
external encapsulating structure [GO:0030312]	8.0E-06	31
fungal-type cell wall [GO:0009277]	1.1E-05	30
plasma membrane part [GO:0044459]	2.4E-04	33
vacuolar membrane [GO:0005774]	2.9E-04	45
anchored component of membrane [GO:0031225]	5.8E-04	18
vacuolar part [GO:0044437]	9.7E-04	45
intrinsic component of plasma membrane [GO:0031226]	1.1E-03	26
cell part [GO:0044464]	4.0E-03	443
bounding membrane of organelle [GO:0098588]	4.0E-03	75
integral component of plasma membrane [GO:0005887]	4.4E-03	24

cytoplasm [GO:0005737]	4.4E-03	381
cell [GO:0005623]	6.7E-03	443
fungal-type vacuole membrane [GO:0000329]	1.3E-02	35
lytic vacuole membrane [GO:0098852]	1.3E-02	35
membrane-bounded organelle [GO:0043227]	4.3E-02	364
intracellular organelle [GO:0043229]	4.3E-02	383
intracellular membrane-bounded organelle [GO:0043231]	4.6E-02	360
organelle [GO:0043226]	4.6E-02	383

Molecular Function GO Terms	p-Value	Matches
metal ion transmembrane transporter activity [GO:0046873]	2.5E-11	26
transmembrane transporter activity [GO:0022857]	3.4E-10	70
transporter activity [GO:0005215]	5.6E-09	71
inorganic molecular entity transmembrane transporter activity [GO:0015318]	8.5E-09	52
ion transmembrane transporter activity [GO:0015075]	2.6E-08	54
inorganic cation transmembrane transporter activity [GO:0022890]	3.3E-06	35
transition metal ion transmembrane transporter activity [GO:0046915]	1.3E-05	15
cation transmembrane transporter activity [GO:0008324]	1.3E-05	39

Supplementary Table V. Mitochondrial Profiling Unique vs Mitochondria tagging: GO Terms.

Biological Process GO Terms	p-Value	Matches
mitochondrial gene expression [GO:0140053]	6.7E-09	35
mitochondrial RNA metabolic process [GO:0000959]	8.5E-09	17
mitochondrial translation [GO:0032543]	3.6E-05	27
small molecule metabolic process [GO:0044281]	4.7E-05	70
respiratory electron transport chain [GO:0022904]	9.2E-05	13
cellular respiration [GO:0045333]	1.2E-04	20
tRNA aminoacylation for mitochondrial protein translation [GO:0070127]	1.5E-04	8
amino acid activation [GO:0043038]	5.0E-04	12
tRNA aminoacylation [GO:0043039]	5.0E-04	12
tRNA aminoacylation for protein translation [GO:0006418]	1.5E-03	11
energy derivation by oxidation of organic compounds [GO:0015980]	1.7E-03	23
ornithine biosynthetic process [GO:0006592]	1.9E-02	4
electron transport chain [GO:0022900]	2.1E-02	13
mitochondrion organization [GO:0007005]	4.8E-02	29

Cellular Component GO Terms	p-Value	Matches
mitochondrion [GO:0005739]	9.4E-45	163
mitochondrial part [GO:0044429]	8.9E-43	118
mitochondrial envelope [GO:0005740]	2.9E-27	82
mitochondrial membrane [GO:0031966]	1.4E-25	76
mitochondrial inner membrane [GO:0005743]	1.8E-24	60
organelle inner membrane [GO:0019866]	2.4E-23	60
organelle envelope [GO:0031967]	1.2E-20	85
envelope [GO:0031975]	1.2E-20	85
mitochondrial matrix [GO:0005759]	2.8E-10	40
mitochondrial membrane part [GO:0044455]	7.8E-08	32
organelle membrane [GO:0031090]	2.3E-07	86
cytoplasmic part [GO:0044444]	3.7E-05	205
mitochondrial protein complex [GO:0098798]	4.3E-03	26

chloroplast [GO:0009507]	4.3E-03	4
chloroplast thylakoid [GO:0009534]	4.3E-03	4
chloroplast thylakoid membrane [GO:0009535]	4.3E-03	4
plastid [GO:0009536]	4.3E-03	4
thylakoid [GO:0009579]	4.3E-03	4
plastid thylakoid [GO:0031976]	4.3E-03	4
photosynthetic membrane [GO:0034357]	4.3E-03	4
thylakoid membrane [GO:0042651]	4.3E-03	4
chloroplast part [GO:0044434]	4.3E-03	4
plastid part [GO:0044435]	4.3E-03	4
thylakoid part [GO:0044436]	4.3E-03	4
plastid thylakoid membrane [GO:0055035]	4.3E-03	4
respiratory chain [GO:0070469]	9.9E-03	10
membrane [GO:0016020]	1.5E-02	140
respiratory chain complex [GO:0098803]	1.8E-02	9
membrane part [GO:0044425]	2.1E-02	118
mitochondrial respiratory chain [GO:0005746]	2.9E-02	9
extrinsic component of mitochondrial inner membrane [GO:0031314]	3.0E-02	8
integral component of mitochondrial membrane [GO:0032592]	4.3E-02	12

Molecular Function GO Terms	p-Value	Matches
aminoacyl-tRNA ligase activity [GO:0004812]	6.5E-04	11
ligase activity, forming carbon-oxygen bonds [GO:0016875]	6.5E-04	11
catalytic activity, acting on a tRNA [GO:0140101]	6.8E-04	18
electron transfer activity [GO:0009055]	1.1E-02	12

Supplementary Table VI. ER tagging Unique vs Mitochondria Tagging: GO Terms.

Biological Process GO Terms	p-Value	Matches
glycoprotein metabolic process [GO:0009100]	1.4E-25	55
glycosylation [GO:0070085]	1.4E-25	55
glycoprotein biosynthetic process [GO:0009101]	1.5E-24	52
protein glycosylation [GO:0006486]	7.4E-24	50
macromolecule glycosylation [GO:0043413]	7.4E-24	50
mannosylation [GO:0097502]	1.2E-20	36
transmembrane transport [GO:0055085]	8.8E-20	135
transport [GO:0006810]	2.0E-18	276
establishment of localization [GO:0051234]	4.5E-17	279
localization [GO:0051179]	6.0E-17	307
protein O-linked glycosylation [GO:0006493]	1.0E-14	21
ion transport [GO:0006811]	1.3E-14	110
lipid metabolic process [GO:0006629]	3.0E-13	100
protein N-linked glycosylation [GO:0006487]	2.5E-12	30
membrane lipid metabolic process [GO:0006643]	7.9E-12	40
cellular lipid metabolic process [GO:0044255]	1.7E-11	92
ion transmembrane transport [GO:0034220]	3.3E-11	80
anion transport [GO:0006820]	1.3E-10	65
organic substance transport [GO:0071702]	1.4E-10	193
membrane lipid biosynthetic process [GO:0046467]	2.8E-10	34
lipid biosynthetic process [GO:0008610]	1.2E-09	67
carbohydrate derivative biosynthetic process [GO:1901137]	2.5E-09	77
nitrogen compound transport [GO:0071705]	2.0E-08	170
organic anion transport [GO:0015711]	1.1E-07	52
cation transport [GO:0006812]	1.2E-07	65
anion transmembrane transport [GO:0098656]	2.6E-06	38
protein lipidation [GO:0006497]	2.7E-06	24
lipoprotein biosynthetic process [GO:0042158]	2.7E-06	24
lipoprotein metabolic process [GO:0042157]	4.6E-06	24
protein mannosylation [GO:0035268]	6.8E-06	11

GPI anchor metabolic process [GO:0006505]	1.0E-05	19
glycolipid biosynthetic process [GO:0009247]	1.0E-05	19
GPI anchor biosynthetic process [GO:0006506]	1.2E-05	18
organic acid transport [GO:0015849]	1.4E-05	33
glycolipid metabolic process [GO:0006664]	1.5E-05	20
liposaccharide metabolic process [GO:1903509]	1.5E-05	20
cation transmembrane transport [GO:0098655]	3.1E-05	53
carboxylic acid transport [GO:0046942]	4.2E-05	32
carbohydrate derivative metabolic process [GO:1901135]	4.7E-05	88
cell wall macromolecule metabolic process [GO:0044036]	4.8E-05	23
maintenance of protein localization in endoplasmic reticulum [GO:0035437]	5.0E-05	10
protein localization to endoplasmic reticulum [GO:0070972]	1.2E-04	24
cell wall mannoprotein biosynthetic process [GO:0000032]	1.3E-04	13
mannoprotein metabolic process [GO:0006056]	1.3E-04	13
mannoprotein biosynthetic process [GO:0006057]	1.3E-04	13
cell wall glycoprotein biosynthetic process [GO:0031506]	1.3E-04	13
sphingolipid metabolic process [GO:0006665]	2.7E-04	22
protein retention in ER lumen [GO:0006621]	3.6E-04	9
protein O-linked mannosylation [GO:0035269]	3.6E-04	9
response to endoplasmic reticulum stress [GO:0034976]	5.0E-04	30
phosphatidylinositol biosynthetic process [GO:0006661]	9.5E-04	20
response to unfolded protein [GO:0006986]	9.6E-04	21
organic acid transmembrane transport [GO:1903825]	1.7E-03	24
cell wall macromolecule biosynthetic process [GO:0044038]	3.4E-03	19
cellular component macromolecule biosynthetic process [GO:0070589]	3.4E-03	19
phospholipid biosynthetic process [GO:0008654]	3.7E-03	34
response to topologically incorrect protein [GO:0035966]	3.8E-03	25
phospholipid metabolic process [GO:0006644]	3.9E-03	43
sphingolipid biosynthetic process [GO:0030148]	4.9E-03	17
carboxylic acid transmembrane transport [GO:1905039]	5.1E-03	23
cell wall biogenesis [GO:0042546]	5.9E-03	33
ammonium transport [GO:0015696]	6.4E-03	13
ammonium transmembrane transport [GO:0072488]	8.7E-03	11

amino acid transport [GO:0006865]	9.1E-03	21
drug transmembrane transport [GO:0006855]	1.0E-02	20
drug transport [GO:0015893]	1.1E-02	27
glycerolipid biosynthetic process [GO:0045017]	1.1E-02	27
amino acid transmembrane transport [GO:0003333]	1.2E-02	18
nucleobase transport [GO:0015851]	1.2E-02	8
regulation of membrane lipid distribution [GO:0097035]	1.5E-02	12
cell wall organization or biogenesis [GO:0071554]	1.6E-02	65
glycerophospholipid biosynthetic process [GO:0046474]	1.7E-02	26
glycerolipid metabolic process [GO:0046486]	1.8E-02	37
maintenance of protein localization in organelle [GO:0072595]	2.0E-02	10
ERAD pathway [GO:0036503]	2.0E-02	20
cellular response to unfolded protein [GO:0034620]	2.7E-02	17
lipid translocation [GO:0034204]	3.6E-02	11
endoplasmic reticulum unfolded protein response [GO:0030968]	4.0E-02	14
oligosaccharide-lipid intermediate biosynthetic process [GO:0006490]	4.5E-02	9

Cellular Component GO Terms	p-Value	Matches
intrinsic component of membrane [GO:0031224]	9.1E-135	516
integral component of membrane [GO:0016021]	5.9E-131	500
membrane part [GO:0044425]	8.8E-104	526
endoplasmic reticulum [GO:0005783]	1.4E-100	298
endomembrane system [GO:0012505]	1.9E-87	367
membrane [GO:0016020]	2.6E-79	554
organelle subcompartment [GO:0031984]	1.7E-64	219
endoplasmic reticulum part [GO:0044432]	6.5E-62	187
endoplasmic reticulum subcompartment [GO:0098827]	3.7E-58	178
endoplasmic reticulum membrane [GO:0005789]	1.0E-56	174
nuclear outer membrane-endoplasmic reticulum membrane network [GO:0042175]	1.1E-55	176
lytic vacuole [GO:0000323]	8.7E-36	164
storage vacuole [GO:0000322]	2.8E-35	163
fungal-type vacuole [GO:0000324]	2.8E-35	163
vacuole [GO:0005773]	7.7E-35	177
bounding membrane of organelle [GO:0098588]	3.5E-30	187
Golgi apparatus [GO:0005794]	4.5E-22	107
vacuolar part [GO:0044437]	8.6E-22	105
vacuolar membrane [GO:0005774]	4.0E-19	98
organelle membrane [GO:0031090]	3.2E-18	226
cytoplasmic part [GO:0044444]	7.1E-18	584
fungal-type vacuole membrane [GO:0000329]	2.7E-16	81
lytic vacuole membrane [GO:0098852]	2.7E-16	81
whole membrane [GO:0098805]	2.9E-16	147
intrinsic component of endoplasmic reticulum membrane [GO:0031227]	3.6E-16	44
cell periphery [GO:0071944]	5.0E-16	193
integral component of endoplasmic reticulum membrane [GO:0030176]	1.6E-15	43
Golgi membrane [GO:0000139]	1.4E-14	60
Golgi subcompartment [GO:0098791]	5.7E-14	68
plasma membrane [GO:0005886]	8.0E-14	143

Golgi apparatus part [GO:0044431]	6.5E-13	72
intrinsic component of plasma membrane [GO:0031226]	3.8E-09	47
integral component of plasma membrane [GO:0005887]	2.8E-08	44
integral component of Golgi membrane [GO:0030173]	6.7E-08	20
intrinsic component of Golgi membrane [GO:0031228]	6.7E-08	20
plasma membrane part [GO:0044459]	2.2E-07	54
intracellular membrane-bounded organelle [GO:0043231]	3.9E-07	650
membrane-bounded organelle [GO:0043227]	1.1E-06	655
organelle part [GO:0044422]	2.6E-05	480
endoplasmic reticulum lumen [GO:0005788]	6.8E-05	12
intracellular organelle part [GO:0044446]	8.7E-05	476
mannosyltransferase complex [GO:0031501]	1.8E-04	12
dolichyl-phosphate-mannose-protein mannosyltransferase complex [GO:0031502]	6.1E-04	7
endoplasmic reticulum-Golgi intermediate compartment [GO:0005793]	2.3E-03	14
nuclear membrane [GO:0031965]	3.3E-03	27
dolichyl-phosphate-mannose-protein mannosyltransferase Pmt1p-Pmt2p dimer complex [GO:0097582]	4.7E-03	6
COPII-coated ER to Golgi transport vesicle [GO:0030134]	1.0E-02	17
intracellular organelle [GO:0043229]	4.7E-02	667

Molecular Function GO Terms	p-Value	Matches
transporter activity [GO:0005215]	1.6E-25	126
transmembrane transporter activity [GO:0022857]	1.0E-24	119
transferase activity, transferring hexosyl groups [GO:0016758]	8.2E-22	49
mannosyltransferase activity [GO:0000030]	9.4E-21	34
transferase activity, transferring glycosyl groups [GO:0016757]	1.4E-19	53
ion transmembrane transporter activity [GO:0015075]	1.0E-16	86
inorganic molecular entity transmembrane transporter activity [GO:0015318]	1.2E-10	71
anion transmembrane transporter activity [GO:0008509]	3.5E-10	42
cation transmembrane transporter activity [GO:0008324]	2.2E-09	58
active transmembrane transporter activity [GO:0022804]	6.0E-09	53
alpha-1,2-mannosyltransferase activity [GO:0000026]	1.4E-07	12
organic anion transmembrane transporter activity [GO:0008514]	1.6E-07	34
drug transmembrane transporter activity [GO:0015238]	1.3E-06	26
organic acid transmembrane transporter activity [GO:0005342]	1.7E-06	28
secondary active transmembrane transporter activity [GO:0015291]	2.0E-06	33
carboxylic acid transmembrane transporter activity [GO:0046943]	6.2E-06	27
dolichyl-phosphate-mannose-protein mannosyltransferase activity [GO:0004169]	6.5E-04	7
ammonium transmembrane transporter activity [GO:0008519]	6.9E-04	11
antiporter activity [GO:0015297]	2.4E-03	15
nucleobase transmembrane transporter activity [GO:0015205]	2.7E-03	8
nucleobase-containing compound transmembrane transporter activity [GO:0015932]	3.4E-03	13
alpha-1,3-mannosyltransferase activity [GO:0000033]	5.7E-03	6
L-tyrosine transmembrane transporter activity [GO:0005302]	5.7E-03	6
exopeptidase activity [GO:0008238]	6.2E-03	14
amino acid transmembrane transporter activity [GO:0015171]	7.3E-03	17
carbohydrate derivative transmembrane transporter activity [GO:1901505]	1.5E-02	12
inorganic cation transmembrane transporter activity [GO:0022890]	1.7E-02	37
aromatic amino acid transmembrane transporter activity [GO:0015173]	1.9E-02	7
signaling receptor activity [GO:0038023]	2.2E-02	9
nucleotide-sugar transmembrane transporter activity [GO:0005338]	5.0E-02	5

Supplementary Table VII. Mitochondria Tagging Unique vs ER tagging: GO Terms.

Biological Process GO Terms	p-Value	Matches
mitochondrion organization [GO:0007005]	1.1E-10	49
mitochondrial gene expression [GO:0140053]	2.3E-08	38
protein localization to mitochondrion [GO:0070585]	1.6E-05	19
establishment of protein localization to mitochondrion [GO:0072655]	1.6E-05	19
mitochondrial translation [GO:0032543]	3.9E-05	30
mitochondrial transport [GO:0006839]	7.3E-05	21
mitochondrial genome maintenance [GO:0000002]	2.8E-04	14
protein targeting to mitochondrion [GO:0006626]	4.1E-03	15
mitochondrial transmembrane transport [GO:1990542]	9.4E-03	15
protein transmembrane transport [GO:0071806]	9.8E-03	17
protein targeting [GO:0006605]	1.8E-02	28
positive regulation of mitochondrial translation [GO:0070131]	2.6E-02	7
carboxylic acid metabolic process [GO:0019752]	4.1E-02	45

Cellular Component GO Terms	p-Value	Matches
mitochondrion [GO:0005739]	2.4E-43	175
mitochondrial part [GO:0044429]	4.7E-39	122
mitochondrial envelope [GO:0005740]	6.2E-23	82
mitochondrial membrane [GO:0031966]	1.3E-21	76
organelle envelope [GO:0031967]	1.1E-17	87
envelope [GO:0031975]	1.1E-17	87
mitochondrial inner membrane [GO:0005743]	1.4E-16	54
organelle inner membrane [GO:0019866]	2.3E-16	55
mitochondrial matrix [GO:0005759]	5.1E-16	51
cytoplasm [GO:0005737]	3.6E-10	292
mitochondrial protein complex [GO:0098798]	2.8E-09	39
cytoplasmic part [GO:0044444]	9.8E-09	241
intracellular [GO:0005622]	1.5E-08	318
mitochondrial membrane part [GO:0044455]	1.2E-07	34
intracellular part [GO:0044424]	1.5E-07	317
cell part [GO:0044464]	2.7E-07	320
cell [GO:0005623]	4.5E-07	320
intracellular organelle [GO:0043229]	1.9E-06	288
organelle membrane [GO:0031090]	2.0E-06	92
organelle [GO:0043226]	2.0E-06	288
membrane-bounded organelle [GO:0043227]	2.9E-05	273
intrinsic component of mitochondrial membrane [GO:0098573]	8.2E-05	17
intracellular membrane-bounded organelle [GO:0043231]	9.8E-05	269
organellar ribosome [GO:0000313]	1.4E-04	19
mitochondrial ribosome [GO:0005761]	1.4E-04	19
integral component of mitochondrial membrane [GO:0032592]	1.2E-03	15

nucleoid [GO:0009295]	2.3E-03	9
mitochondrial nucleoid [GO:0042645]	2.3E-03	9
intrinsic component of mitochondrial inner membrane [GO:0031304]	3.4E-03	11
intracellular organelle part [GO:0044446]	4.4E-02	196

Molecular Function GO Terms	p-Value	Matches
protein transmembrane transporter activity [GO:0008320]	2.1E-02	9
macromolecule transmembrane transporter activity [GO:0022884]	2.1E-02	9
peptide transmembrane transporter activity [GO:1904680]	3.1E-02	10
protein transporter activity [GO:0008565]	4.1E-02	9

Supplementary Table VIII. Yeast Dual-tagged RNAs: GO Terms.

Biological Process GO Terms	p-Value	Matches
ion transport [GO:0006811]	7.1E-22	67
transmembrane transport [GO:0055085]	2.8E-19	70
metal ion transport [GO:0030001]	3.3E-18	31
ion transmembrane transport [GO:0034220]	8.6E-17	50
metal ion homeostasis [GO:0055065]	2.4E-16	34
cation homeostasis [GO:0055080]	1.0E-14	37
inorganic ion homeostasis [GO:0098771]	1.1E-13	35
ion homeostasis [GO:0050801]	2.0E-13	37
cellular metal ion homeostasis [GO:0006875]	1.1E-12	29
cation transport [GO:0006812]	1.5E-12	41
inorganic ion transmembrane transport [GO:0098660]	4.6E-12	35
transition metal ion homeostasis [GO:0055076]	8.1E-12	26
chemical homeostasis [GO:0048878]	8.5E-12	39
transition metal ion transport [GO:0000041]	1.1E-11	20
cellular cation homeostasis [GO:0030003]	2.0E-11	32
inorganic cation transmembrane transport [GO:0098662]	3.7E-11	32
cation transmembrane transport [GO:0098655]	1.7E-10	35
cellular ion homeostasis [GO:0006873]	2.1E-10	32
cellular chemical homeostasis [GO:0055082]	4.4E-10	34
cellular homeostasis [GO:0019725]	4.8E-10	38
cell wall organization or biogenesis [GO:0071554]	1.3E-09	43
cellular transition metal ion homeostasis [GO:0046916]	5.7E-09	22
homeostatic process [GO:0042592]	3.3E-08	44
external encapsulating structure organization [GO:0045229]	4.0E-08	37
cell wall organization [GO:0071555]	4.0E-08	37
iron ion transport [GO:0006826]	2.1E-07	12
anion transport [GO:0006820]	4.9E-07	31

transport [GO:0006810]	5.7E-07	100
lipid metabolic process [GO:0006629]	1.1E-06	42
fungal-type cell wall organization or biogenesis [GO:0071852]	1.4E-06	33
establishment of localization [GO:0051234]	1.8E-06	101
localization [GO:0051179]	7.1E-06	109
iron ion homeostasis [GO:0055072]	8.7E-06	16
anion transmembrane transport [GO:0098656]	9.0E-06	21
divalent inorganic cation transport [GO:0072511]	1.0E-05	13
cellular lipid metabolic process [GO:0044255]	2.2E-05	38
membrane lipid metabolic process [GO:0006643]	3.0E-05	18
divalent metal ion transport [GO:0070838]	6.3E-05	12
membrane lipid biosynthetic process [GO:0046467]	6.3E-05	16
fungal-type cell wall organization [GO:0031505]	7.2E-05	28
lipid biosynthetic process [GO:0008610]	8.2E-05	29
glycerophospholipid metabolic process [GO:0006650]	1.7E-04	21
glycerolipid metabolic process [GO:0046486]	2.2E-04	22
regulation of biological quality [GO:0065008]	2.2E-04	52
phospholipid metabolic process [GO:0006644]	2.2E-04	24
divalent inorganic cation homeostasis [GO:0072507]	2.6E-04	11
glycolipid metabolic process [GO:0006664]	1.3E-03	11
liposaccharide metabolic process [GO:1903509]	1.3E-03	11
manganese ion transport [GO:0006828]	2.1E-03	6
cellular divalent inorganic cation homeostasis [GO:0072503]	2.2E-03	10
organic anion transport [GO:0015711]	3.6E-03	22
glycolipid biosynthetic process [GO:0009247]	4.1E-03	10
cellular iron ion homeostasis [GO:0006879]	5.6E-03	12
amino acid transmembrane transport [GO:0003333]	6.8E-03	11
glycerolipid biosynthetic process [GO:0045017]	8.5E-03	15
phosphatidylinositol metabolic process [GO:0046488]	1.3E-02	14
amino acid transport [GO:0006865]	1.3E-02	12

protein lipidation [GO:0006497]	2.2E-02	11
lipoprotein biosynthetic process [GO:0042158]	2.2E-02	11
phospholipid biosynthetic process [GO:0008654]	2.3E-02	17
lipoprotein metabolic process [GO:0042157]	2.7E-02	11
glycerophospholipid biosynthetic process [GO:0046474]	2.9E-02	14
cofactor transport [GO:0051181]	3.0E-02	9
sodium ion transmembrane transport [GO:0035725]	3.4E-02	5
manganese ion transmembrane transport [GO:0071421]	3.4E-02	5
GPI anchor metabolic process [GO:0006505]	3.9E-02	9

Cellular Component GO Terms	p-Value	Matches
intrinsic component of membrane [GO:0031224]	1.2E-58	192
membrane part [GO:0044425]	1.3E-47	195
integral component of membrane [GO:0016021]	1.0E-46	175
membrane [GO:0016020]	1.1E-39	205
endoplasmic reticulum [GO:0005783]	1.0E-31	103
cell periphery [GO:0071944]	6.8E-30	111
endomembrane system [GO:0012505]	3.7E-25	121
storage vacuole [GO:0000322]	1.8E-20	71
fungal-type vacuole [GO:0000324]	1.8E-20	71
lytic vacuole [GO:0000323]	2.0E-20	71
plasma membrane [GO:0005886]	3.0E-20	79
endoplasmic reticulum part [GO:0044432]	7.9E-20	66
endoplasmic reticulum subcompartment [GO:0098827]	1.0E-18	63
organelle subcompartment [GO:0031984]	3.2E-18	73
vacuole [GO:0005773]	4.0E-18	73
endoplasmic reticulum membrane [GO:0005789]	4.6E-17	60
nuclear outer membrane-endoplasmic reticulum membrane network [GO:0042175]	2.6E-16	60
extracellular region [GO:0005576]	6.5E-14	31
intrinsic component of plasma membrane [GO:0031226]	2.2E-10	28
cytoplasmic part [GO:0044444]	6.4E-10	205
plasma membrane part [GO:0044459]	7.4E-10	32
cell wall [GO:0005618]	1.6E-09	28
external encapsulating structure [GO:0030312]	1.6E-09	28
integral component of plasma membrane [GO:0005887]	2.6E-09	26
fungal-type cell wall [GO:0009277]	3.3E-09	27
bounding membrane of organelle [GO:0098588]	9.8E-08	61
vacuolar membrane [GO:0005774]	3.5E-07	37

anchored component of membrane [GO:0031225]	9.5E-07	17
vacuolar part [GO:0044437]	1.2E-06	37
whole membrane [GO:0098805]	2.9E-06	54
organelle membrane [GO:0031090]	6.6E-06	78
integral component of endoplasmic reticulum membrane [GO:0030176]	1.5E-04	16
intrinsic component of endoplasmic reticulum membrane [GO:0031227]	1.7E-04	16
fungal-type vacuole membrane [GO:0000329]	2.5E-03	26
lytic vacuole membrane [GO:0098852]	2.5E-03	26
intracellular membrane-bounded organelle [GO:0043231]	1.6E-02	217
Golgi apparatus [GO:0005794]	2.1E-02	29

Molecular Function GO Terms	p-Value	Matches
transmembrane transporter activity [GO:0022857]	3.1E-22	66
transporter activity [GO:0005215]	3.1E-20	66
metal ion transmembrane transporter activity [GO:0046873]	1.2E-17	26
inorganic molecular entity transmembrane transporter activity [GO:0015318]	9.8E-17	48
ion transmembrane transporter activity [GO:0015075]	1.2E-16	50
cation transmembrane transporter activity [GO:0008324]	2.4E-11	36
inorganic cation transmembrane transporter activity [GO:0022890]	3.7E-11	32
transition metal ion transmembrane transporter activity [GO:0046915]	3.4E-09	15
active transmembrane transporter activity [GO:0022804]	3.5E-04	24
secondary active transmembrane transporter activity [GO:0015291]	5.8E-04	17
anion transmembrane transporter activity [GO:0008509]	1.2E-03	18
organic anion transmembrane transporter activity [GO:0008514]	2.0E-03	16
manganese ion transmembrane transporter activity [GO:0005384]	1.6E-02	5
sodium ion transmembrane transporter activity [GO:0015081]	1.6E-02	5
cofactor transmembrane transporter activity [GO:0051184]	1.8E-02	7
transferase activity, transferring hexosyl groups [GO:0016758]	2.5E-02	14
amino acid transmembrane transporter activity [GO:0015171]	2.6E-02	10
potassium ion transmembrane transporter activity [GO:0015079]	3.0E-02	6

Pathways	p-Value	Matches
sphingolipid metabolism	9.9E-03	6

Supplementary Table IX. 45 RNAs tagged about equally by both ER- and Mito-PUP.

Systematic Name	Feature Type	ER-PUP Tier	Mito-PUP Tier
YER019W	ORF	1	1
YHR071W	ORF	1	1
YLR056W	ORF	1	1
YEL017C-A	ORF	1	1
YHL040C	ORF	1	2
YNL327W	ORF	1	2
YCR024C-B	ORF	1	2
YHL047C	ORF	1	3
YDR534C	ORF	1	3
YKR072C	ORF	1	4
YDR481C	ORF	2	3
YDR072C	ORF	2	3
YIL117C	ORF	2	3
YLR188W	ORF	2	3
YCR015C	ORF	3	2
YOR306C	ORF	3	2
YDR422C	ORF	3	3
YPR140W	ORF	3	3
YDR319C	ORF	3	3
YDR270W	ORF	3	3
YLR138W	ORF	3	3
YDR073W	ORF	3	3
YNL186W	ORF	3	3
YDR320C-A	ORF	4	2
snR7-L	snRNA gene	3	4
YGR146C-A	ORF	3	4
YLR226W	ORF	3	4

YLR404W	ORF	3	4
YIL090W	ORF	3	4
YBR262C	ORF	3	4
YDR124W	ORF	4	3
YKR052C	ORF	4	3
YDR374W-A	ORF	4	3
YGR171C	ORF	3	5
YNR045W	ORF	4	4
YHL028W	ORF	4	4
YPL216W	ORF	4	4
YMR195W	ORF	4	4
YHR143W-A	ORF	4	4
YDL232W	ORF	4	4
YJR082C	ORF	5	3
YNL211C	ORF	4	5
YBL051C	ORF	4	5
YOR384W	ORF	5	5
YEL061C	ORF	5	5

Supplementary Table X. Dual-localization conservation in yeast and HEK293T cells.

Yeast (BY4742):

Systematic Name	ER-PUP Tier	Mito-PUP Tier
YKL008C	1	2
YGL054C	1	2
YDR107C	2	2
YHR079C	1	3
YPR124W	1	3
YIL005W	1	3
YEL042W	1	3
YJR116W	1	3
YKL140W	2	3
YCR026C	2	3
YBR086C	2	3
YOR316C	2	3
YML072C	2	3
YHR050W	2	3
YOR288C	2	3
YDR270W	3	3
YOR344C	3	3
YDR319C	3	3
YKR044W	3	3
YIL023C	3	3
YGR055W	1	4
YBR068C	1	4
YBR229C	1	4
YLR207W	1	4
YMR296C	1	4
YBR219C	1	4

YIL030C	2	4
YBR029C	2	4
YOL003C	2	4
YDR456W	2	4
YML019W	2	4
YML013W	3	4
YOR154W	3	4
YOR175C	1	5
YBR296C	1	5
YJL019W	3	5
YGR036C	3	5
YGR171C	3	5
YDR038C	3	5
YPR079W	3	5
YPL176C	3	5

HEK293T Cells (from ref 25):

ENSEMBL ID	OMM Tier	ERM Tier
ENSG00000171714	3	2
ENSG00000172292	3	2
ENSG00000197296	3	2
ENSG00000102158	3	2
ENSG00000196950	3	2
ENSG00000136868	4	2
ENSG00000065308	4	2
ENSG00000180776	4	2
ENSG00000139641	5	2
ENSG00000113194	5	2
ENSG00000152078	5	2
ENSG00000071537	3	3
ENSG00000125827	3	3
ENSG00000117868	4	3
ENSG00000065923	4	3
ENSG00000094975	4	3
ENSG00000072274	4	3
ENSG00000166479	4	3
ENSG00000165240	5	3
ENSG00000100528	5	3
ENSG00000178607	5	3
ENSG00000170385	5	3
ENSG00000139514	5	3
ENSG00000092068	5	3
ENSG00000167130	3	4
ENSG00000089597	3	4
ENSG00000197081	3	4

ENSG00000197594	4	4
ENSG00000104635	4	4
ENSG00000141424	4	4
ENSG00000197818	4	4
ENSG00000143797	5	4
ENSG00000100926	5	4
ENSG00000011376	1	5
ENSG00000182372	4	5
ENSG00000107798	4	5
ENSG00000114988	4	5
ENSG00000198689	4	5
ENSG00000101337	4	5
ENSG00000001561	5	5
ENSG00000144136	5	5
ENSG00000164828	5	5

Supplementary Table XI. Dual-, and ER- or Mito-PUP-tagged complex components.

Class A: Individual components dual-tagged (31 Complexes)

acyl-CoA ceramide synthase complex

Both	ER-PUP
Lac1p	Lag1p

alpha-1,6-mannosyltransferase complex

Both	ER-PUP
Anp1p	Mnn11p
Van1p	Hoc1p
	Mnn10p
	Mnn9p

DASH complex

Both	ER-PUP
Dad4p	Dad1p
	Dad3p

DNF1-LEM3 P4-ATPase complex

Both	ER-PUP
Dnf1p	Lem3p

FET3-FTR1 high affinity iron permease complex

Both	ER-PUP
Ftr1p	Fet3p

Glucosidase II complex

Both	ER-PUP

Rot2p	Gtb1p

Glycosylphosphatidylinositol-N-acetylglucosaminyltransferase complex

Both	ER-PUP
Gpi1p	Gpi15p
Eri1p	
Gpi2p	

GPI-anchor transamidase complex

Both	ER-PUP
Gpi16p	Gaa1p
	Gab1p
	Gpi17p
	Gpi8p

HRD1 ubiquitin ligase complex

Both	ER-PUP
Hrd3p	Hrd1p
Ubx2p	Der1p
Usa1p	Yos9p

Luminal surveillance complex

Both	ER-PUP
Hrd3p	Kar2p
	Yos9p

Mannosyl phosphorylinositol ceramide synthase CSH1-CSG2

Both	ER-PUP
Csg2p	Csh1p

Oligosaccharyl transferase complex variant 1

Both	ER-PUP
Ost6p	Wbp1p
Ost4p	Stt3p
	Ost1p
	Swp1p

Oligosaccharyl transferase complex variant 2

Both	ER-PUP
Ost4p	Wbp1p
	Stt3p
	Ost1p
	Swp1p
	Ost3p

OPY2-MSB2 osmosensory complex

Both	ER-PUP
Msb2p	Opy2p

SPOTS complex

Both	ER-PUP
Lcb1p	Lcb2p
	Orm1p
	Orm2p
	Sac1p

SWI/SNF chromatin remodelling complex

Both	ER-PUP
Snf11p	Snf6p

60S cytosolic large ribosomal subunit

Both	Mito-PUP
Rpl30p	Rpp0p
	Rpl39p
	Rpl10p

1,3-beta-D-glucan synthase complex

Both	ER-PUP	Mito-PUP
Gsc2p	Fks1p	Rho1p

BUR1-BUR2 kinase complex

Both
Bur2p

Doa10 ubiquitin ligase complex

Both
Ssm4p
Ubx2p

Exomer complex

Both
Bch2p

FET5-FTH1 high affinity iron exporter complex

Both
Fth1p
Fet5p

Glycosylphosphatidylinositol-mannosyltransferase II complex

Both

Gpi18p

Ire1 complex

Both

Ire1p

Mannosyl phosphorylinositol ceramide synthase SUR1-CSG2

Both

Csg2p
Sur1p

MICOS complex

Both

Mic12p

NuA3 histone acetyltransferase complex

Both

Eaf6p

NuA4 histone acetyltransferase complex

Both

Eaf6p

PCL5-PHO85 kinase complex

Both

Pcl5p

Seipin complex

Both

Sei1p

UBP3-BRE5 ubiquitin hydrolase complex

Both

Bre5p

Class B: Components tagged at either ER or Mitochondria (13 complexes).

37S mitochondrial small ribosomal subunit

ER-PUP	Mito-PUP
Sws2p	Mrp17p
	Rsm26p
	Mrps5p
	Rsm23p
	Mrps18p

40S cytosolic small ribosomal subunit

ER-PUP	Mito-PUP
Rps12p	Rps20p

ESCRT-II complex

ER-PUP	Mito-PUP
Snf8p	Vps36p

Golgi transport complex

ER-PUP	Mito-PUP
Cog8p	Cog6p

MEX67-MTR2 nuclear RNA export factor complex

ER-PUP	Mito-PUP
Mtr2p	Mex67p

Nuclear pore complex

ER-PUP	Mito-PUP

Pom34p	Nup60p
Ndc1p	Gle2p
Pom152p	
Nup2p	

PAS complex

ER-PUP	Mito-PUP
Vac7p	Fab1p

PRP19-associated complex

ER-PUP	Mito-PUP
Cdc40p	Cwc22p
Prp46p	
Prp9p	
Cwc25p	

RNA polymerase I upstream activating factor complex

ER-PUP	Mito-PUP
Rrn10p	Hhf2p
Uaf30p	
Rrn5p	

SEC62-SEC63 complex

ER-PUP	Mito-PUP
Sec66p	Sec63p
Sec62p	

SMC5-SMC6 SUMO ligase complex

ER-PUP	Mito-PUP
Nse5p	Kre29p

Translocon complex

ER-PUP	Mito-PUP
Sec61p	Sec63p
Sec66p	
Sec62p	

TRAPPII protein complex

ER-PUP	Mito-PUP
Trs31p	Trs65p

Class C: Components ER- or Mito-tagged

RED	Component in more than one complex
YELLOW	Same complex

ER-tagged components:

Standard Name	Complex	ER-PUP Tier
Aga1p	a-agglutinin	1
Apc5p	Anaphase-Promoting Complex variant 1	4
Apc5p	Anaphase-Promoting Complex variant 2	4
Apc5p	Anaphase-Promoting Complex variant 3	4
Apc5p	Anaphase-Promoting Complex variant 4	4
Asi1p	Asi complex	4
Asi2p	Asi complex	3
Asi3p	Asi complex	3
Atg31p	ATG1 kinase complex	4
Atg31p	Atg17-Atg31-Atg29 complex	4
Cnl1p	BLOC-1 complex	5
Ssn8p	CKM complex	4
Cks1p	CLN1-CDC28 kinase complex	2
Cln1p	CLN1-CDC28 kinase complex	3
Cks1p	CLN2-CDC28 kinase complex	2
Cln2p	CLN2-CDC28 kinase complex	3
Cks1p	CLN3-CDC28 kinase complex	2
Ctf19p	COMA complex	3
Cox14p	COX1 pre-assembly complex	1
Cue1p	CUE1-UBC7 ubiquitin-conjugating enzyme complex	2
Ela1p	CUL3-HRT1/ELC1/ELA1 ubiquitin ligase complex	4

Nus1p	Dehydrodolichyl diphosphate synthase complex variant RER2	2
Nus1p	Dehydrodolichyl diphosphate synthase complex variant SRT1	2
Lif1p	DNA ligase IV complex	4
Rev7p	DNA polymerase zeta complex	4
Lem3p	DNF2-LEM3 P4-ATPase complex	4
Dnf3p	DNF3-CRF1 P4-ATPase complex	3
Ynr048Wp	DNF3-CRF1 P4-ATPase complex	4
Sld3p	DPB11-SLD3-SLD2 DNA replication complex	4
Cdc50p	DRS2-CDC50 P4-ATPase complex	1
Drs2p	DRS2-CDC50 P4-ATPase complex	3
Ldb18p	Dynactin	4
Slm4p	EGO complex	5
Emp24p	EMP24 complex	1
Erp1p	EMP24 complex	1
Erp2p	EMP24 complex	1
Erv25p	EMP24 complex	1
Emc1p	Endoplasmic Reticulum Membrane Complex	1
Emc3p	Endoplasmic Reticulum Membrane Complex	1
Mmm1p	ERMES complex	2
Erv41p	ERV41-ERV46 retrograde receptor complex	2
Erv46p	ERV41-ERV46 retrograde receptor complex	2
Far11p	FAR complex	3
Rad3p	General transcription factor complex TFIIH	4
Get1p	GET complex	1
Rad7p	Global genome repair CUL3/RAD7/RAD16/ELC1 ubiquitin ligase complex	5
Dug3p	Glutathione hydrolase complex	3
Gpi14p	Glycosylphosphatidylinositol-mannosyltransferase I complex	1
Hda1p	HDA1 complex	3
Hda2p	HDA1 complex	3
Sho1p	HICS complex	2
Hpa2p	Hpa2 acetyltransferase	2

Mnl1p	HTM1-PDI1 exomannosidase complex	1
Pdi1p	HTM1-PDI1 exomannosidase complex	1
Ies3p	INO80 chromatin remodeling complex	4
Aur1p	Inositol phosphorylceramide synthase complex	1
Kei1p	Inositol phosphorylceramide synthase complex	2
Cyt1p	Mitochondrial electron transport complex III	5
Mot1p	MOT1-TBP transcription regulation complex	2
Mst28p	MST27-MST28 vesicle formation complex	4
Ncb2p	Negative cofactor 2 complex	3
Spo7p	Nem1-Spo7 phosphatase complex	4
Neo1p	NEO1-MON2-ARL1-DOP1 membrane remodeling complex	2
Pop8p	Nucleolar ribonuclease MRP complex	4
Pop8p	Nucleolar ribonuclease P complex	4
Rad4p	Nucleotide excision repair factor 2 complex	4
Rad7p	Nucleotide excision repair factor 4 complex	5
Erf2p	Palmitoyltransferase ERF2/SHR5 complex	3
Pcl10p	PCL10-PHO85 kinase complex	4
Pcl7p	PCL7-PHO85 kinase complex	3
Pex13p	Peroxisomal docking Pex13/Pex14/Pex 15 complex	2
Pex17p	Peroxisomal docking Pex13/Pex14/Pex 15 complex	3
Pex2p	Pex2/Pex10/Pex12 ubiquitin ligase complex	2
Pex21p	Pex7-Pex21 receptor complex	3
Pdr16p	Phosphatidylinositol transporter complex	4
Pmt1p	PMT1-PMT2 dolichyl-phosphate-mannose-protein mannosyltransferase complex	1
Pmt2p	PMT1-PMT2 dolichyl-phosphate-mannose-protein mannosyltransferase complex	1
Pmt1p	PMT1-PMT3 dolichyl-phosphate-mannose-protein mannosyltransferase complex	1
Pmt3p	PMT1-PMT3 dolichyl-phosphate-mannose-protein mannosyltransferase complex	2
Pmt4p	PMT4 dolichyl-phosphate-mannose-protein mannosyltransferase complex	1
Pmt2p	PMT5-PMT2 dolichyl-phosphate-mannose-protein mannosyltransferase complex	1
Pmt5p	PMT5-PMT2 dolichyl-phosphate-mannose-protein mannosyltransferase complex	1
Pmt3p	PMT5-PMT3 dolichyl-phosphate-mannose-protein mannosyltransferase complex	2

Pmt5p	PMT5-PMT3 dolichyl-phosphate-mannose-protein mannosyltransferase complex	1
Msb4p	Polarisome	2
Rad55p	RAD55-RAD57 complex	4
Sas5p	SAS acetyltransferase complex	5
Scc4p	SCC2-SCC4 cohesin loader complex	4
Sec61p	SEC61 translocon complex	1
Prp9p	SF3A complex	4
Hsh49p	SF3B complex	2
Shu1p	Shu complex	3
Sec11p	Signal peptidase complex	1
Spc3p	Signal peptidase complex	1
Srp102p	Signal recognition particle receptor	1
Srp102p	Signal recognition particle receptor complex	1
Ssh1p	SSH1 translocon complex	1
Red1p	Synaptonemal complex	5
Tel2p	TEL2-TTI1-TTI2 complex	5
Est3p	Telomerase holoenzyme complex	3
Trs31p	TRAPPI protein complex	4
Trs31p	TRAPPIII protein complex	4
Sen2p	tRNA-intron endonuclease complex	5
Dsc2p	TUL1 E3 ubiquitin ligase complex	2
Tul1p	TUL1 E3 ubiquitin ligase complex	2
Ubx3p	TUL1 E3 ubiquitin ligase complex	3
Prp42p	U1 snRNP	4
Hsh49p	U2 snRNP	2
Prp9p	U2 snRNP	4
Alg14p	UDP-N-acetylglucosamine transferase complex	4
Utp5p	UTP-A complex	1
Stv1p	Vacuolar proton translocating ATPase complex, Golgi variant	2
Vma16p	Vacuolar proton translocating ATPase complex, Golgi variant	1
Vma3p	Vacuolar proton translocating ATPase complex, Golgi variant	1

Vma16p	Vacuolar proton translocating ATPase complex, vacuole variant	1
Vma3p	Vacuolar proton translocating ATPase complex, vacuole variant	1
Vph1p	Vacuolar proton translocating ATPase complex, vacuole variant	2
Vps55p	VPS55-VPS68 sorting complex	3
Vps68p	VPS55-VPS68 sorting complex	4
Whi2p	WHI2-PSR1 phosphatase complex	3
Whi2p	WHI2-PSR2 phosphatase complex	3

RED	Same mRNA in more than one complex
YELLOW	Multiple mRNAs tagged for same complex

Mitochondria-tagged components:

Standard Name	Complex	Mito-PUP Tier
Mrp20p	54S mitochondrial large ribosomal subunit	5
Mrpl11p	54S mitochondrial large ribosomal subunit	5
Mrpl22p	54S mitochondrial large ribosomal subunit	3
Mrpl24p	54S mitochondrial large ribosomal subunit	3
Mrpl25p	54S mitochondrial large ribosomal subunit	3
Mrpl32p	54S mitochondrial large ribosomal subunit	2
Mrpl39p	54S mitochondrial large ribosomal subunit	2
Mrpl3p	54S mitochondrial large ribosomal subunit	3
Mrpl6p	54S mitochondrial large ribosomal subunit	4
Rtc6p	54S mitochondrial large ribosomal subunit	5
Mrs1p	bI3 intron splicing factor complex	3
Rad6p	BRE1-RAD6 ubiquitin ligase complex	3
Tpk1p	cAMP-dependent protein kinase complex variant 1	4
Tpk1p	cAMP-dependent protein kinase complex variant 4	4
Tpk1p	cAMP-dependent protein kinase complex variant 5	4
Cbp3p	CBP3-CBP6 complex	4
Cbp6p	CBP3-CBP6 complex	3
Hap3p	CCAAT-binding factor complex	4
Bem1p	CLA4-BEM1-CDC24 polarity complex	3
Cat5p	CoQ biosynthetic complex	3
Cka2p	CURI complex variant 1	4
Rrp7p	CURI complex variant 1	4
Rrp7p	CURI complex variant 2	4

Cka2p	CURI complex variant 3	4
Rrp7p	CURI complex variant 3	4
Pri1p	DNA polymerase alpha:primase complex	3
Dpb4p	DNA polymerase epsilon complex	1
Hse1p	ESCRT-0 complex	4
Sec6p	Exocyst	5
Cap1p	F-actin capping protein complex	1
Mgm1p	FZO1-MGM1-UGO1 complex	3
Vps54p	GARP complex	3
Tfa1p	General transcription factor complex TFIIE	4
Vid24p	GID ubiquitin ligase complex	4
Gcv1p	Glycine decarboxylase multienzyme complex	3
Ssa1p	HAP1 transcriptional repressor complex - variant 1	2
Hsc82p	HMC complex	2
Ssa1p	HMC complex	2
Dpb4p	ISW2 chromatin remodeling complex	1
Pbi2p	LMA1 complex, TRX1 variant	3
Pbi2p	LMA1 complex, TRX2 variant	3
Mcm5p	MCM complex	3
Mcm7p	MCM complex	4
Iqg1p	MIH complex	2
Imp2'p	Mitochondrial inner membrane peptidase complex	4
Tim44p	Mitochondrial inner membrane pre-sequence translocase complex	2
Tim50p	Mitochondrial inner membrane pre-sequence translocase complex	4
Idh1p	Mitochondrial isocitrate dehydrogenase complex (NAD+)	3
Idh2p	Mitochondrial isocitrate dehydrogenase complex (NAD+)	3
Tom40p	Mitochondrial outer membrane translocase core complex	1
Tom40p	Mitochondrial outer membrane translocase holocomplex	1
Tom70p	Mitochondrial outer membrane translocase holocomplex	1
Mas2p	Mitochondrial processing peptidase complex	3
Atp15p	Mitochondrial proton-transporting ATP synthase complex	2

Atp2p	Mitochondrial proton-transporting ATP synthase complex	2
Atp4p	Mitochondrial proton-transporting ATP synthase complex	1
Sam50p	Mitochondrial sorting and assembly machinery complex	3
Rad50p	MRE11-RAD50-XRS2 meiotic recombination initiation complex	5
Rad6p	MUB1-RAD6-UBR2 ubiquitin ligase complex	3
Vac17p	MYO2-VAC17-VAC8 transport complex	3
Btt1p	Nascent polypeptide-associated complex, BTT1-EGD2 variant	4
Nfs1p	NFS1-ISD11 cysteine desulphurase complex	3
Hhf2p	Nucleosome, variant HTA1-HTB1	5
Hta1p	Nucleosome, variant HTA1-HTB1	2
Htb1p	Nucleosome, variant HTA1-HTB1	2
Hhf2p	Nucleosome, variant HTA1-HTB2	5
Hta1p	Nucleosome, variant HTA1-HTB2	2
Hhf2p	Nucleosome, variant HTA2-HTB1	5
Htb1p	Nucleosome, variant HTA2-HTB1	2
Hhf2p	Nucleosome, variant HTA2-HTB2	5
Hhf2p	Nucleosome, variant HTZ1-HTB1	5
Htb1p	Nucleosome, variant HTZ1-HTB1	2
Hhf2p	Nucleosome, variant HTZ1-HTB2	5
Ctr9p	PAF1 complex	5
Pcl1p	PCL1-PHO85 kinase complex	2
Vps15p	Phosphatidylinositol 3-kinase complex I	5
Vps15p	Phosphatidylinositol 3-kinase complex II	5
Rad6p	RAD6-RAD18 ubiquitin ligase complex	3
Sth1p	RSC complex variant RSC1	2
Sth1p	RSC complex variant RSC2	2
Rsp5p	RSP5-BUL1 ubiquitin ligase complex	5
Bul2p	RSP5-BUL2 ubiquitin ligase complex	3
Rsp5p	RSP5-BUL2 ubiquitin ligase complex	5
Cpr1p	SET3C histone deacetylase complex	2
Sit4p	SIT4-SAP155 phosphatase complex	5

Sap185p	SIT4-SAP185 phosphatase complex	3
Sit4p	SIT4-SAP185 phosphatase complex	5
Sit4p	SIT4-SAP190 phosphatase complex	5
Dig1p	Ste12/Dig1/Dig2 transcription regulation complex	3
Bdf1p	Swr1 chromatin remodelling complex	3
Sit4p	TAP42-RRD1-SIT4 phosphatase complex	5
Dig1p	Tec1/Ste12/Dig1 transcription regulation complex	3
Toa2p	Transcription factor TFIIA complex	3
Snu66p	U4/U6.U5 tri-snRNP complex	5
Rad6p	UBR1-RAD6 ubiquitin ligase complex	3
Cka2p	UTP-C complex variant 1	4
Rrp7p	UTP-C complex variant 1	4
Rrp7p	UTP-C complex variant 2	4
Cka2p	UTP-C complex variant 3	4
Rrp7p	UTP-C complex variant 3	4
Sec9p	Vesicular t-SNARE complex, SSO1 variant	3
Sec9p	Vesicular t-SNARE complex, SSO2 variant	3

Supplementary Table XII. Tagged non-mRNAs.

Dual-tagged:

Systematic Name	ER-PUP Tier	Mito-PU Tier
snR11	1	3
tK(UUU)D	2	4
snR7-L	3	4
snR84	3	5
snR37	4	5

ER-tagged Unique:

SGD ID	Feature Type	ER-PUP Tier
SCR1	ncRNA gene	1
tD(GUC)O	tRNA gene	2
snR35	snoRNA gene	2
tQ(UUG)H	tRNA gene	2
snR47	snoRNA gene	2
snR33	snoRNA gene	2
snR31	snoRNA gene	2
tK(UUU)L	tRNA gene	2
tH(GUG)E1	tRNA gene	3
tV(AAC)K2	tRNA gene	3
tH(GUG)H	tRNA gene	3
snR7-S	snRNA gene	3
snR128	snoRNA gene	3
RPR1	ncRNA gene	3
snR45	snoRNA gene	3
RUF20	ncRNA gene	3
snR6	snRNA gene	3
NME1	snoRNA gene	3
tT(AGU)B	tRNA gene	3
snR67	snoRNA gene	3
tD(GUC)G1	tRNA gene	3
tM(CAU)J2	tRNA gene	3
tD(GUC)M	tRNA gene	3
tK(UUU)O	tRNA gene	3
snR32	snoRNA gene	3
snR30	snoRNA gene	3

snR48	snoRNA gene	3
SRG1	ncRNA gene	3
snR4	snoRNA gene	3
snR63	snoRNA gene	3
tR(UCU)G3	tRNA gene	4
snR66	snoRNA gene	4
tR(UCU)G1	tRNA gene	4
tG(GCC)G1	tRNA gene	4
snR55	snoRNA gene	4
snR3	snoRNA gene	4
snR64	snoRNA gene	4
tK(UUU)G1	tRNA gene	4
snR42	snoRNA gene	4
tS(AGA)H	tRNA gene	4
tY(GUA)F1	tRNA gene	4
tN(GUU)O2	tRNA gene	4
tX(XXX)L	tRNA gene	4
tG(GCC)O2	tRNA gene	4
snR69	snoRNA gene	4

Mitochondria-tagged Unique:

Systematic Name	Mito-PU Tier
snR190	3
tH(GUG)G2	4
tN(GUU)K	5

Chapter 3

Perspectives

Contributions to the field

Localized RNA tagging fills gaps in the available methods. Several techniques now give insight into the regulation of hundreds of mRNAs with “snapshots” that capture localized mRNAs (APEX-Seq), their translation efficiencies (proximity specific ribosome profiling), and their associated proteins (APEX-Rip) (1-4). However, labeling in those methods is induced by chemical treatments, and RNAs that localize outside of the labeling window (~1-5 mins) are not detected (1-4). By contrast, localized RNA tagging is constitutive, and RNAs that interact with a site at different times (e.g., different stages of the cell cycle) can be identified. The approach is advantageous in that addition of the 3’ uridine tag is cumulative, and therefore RNAs that briefly sample a location are more likely to be detected than in the “snap-shot” approaches. Further, the length of the tag can function as a proxy for the degree of RNA-site associations. Localized RNA tagging thus offers unprecedented genome-wide insight into RNA localization, and the method will likely help identify new localized RNA species and new functions and mechanism for localization.

New roles for localization?

Localized RNA tagging potentially increases the functional repertoire of RNAs being localized. As predicted by results in flies and humans, localized tagging found extensive mRNA localization to the yeast ER and mitochondria (1, 5). Additionally, tens of non-mRNAs were labeled at those sites. The reads that corresponded to the non-mRNAs whose reads had properties that are characteristic of misprocessed precursors (see below). This suggests that maturation and/or turnover of some non-mRNAs may involve relocation from the nucleus to the ER or the mitochondria, and/or that the non-

mRNAs function at those sites. These results challenge the conventional view that localization functions exclusively as a protein targeting mechanism and suggest new roles for localization.

Localized non-mRNAs: a closer look.

Derivatives of several ncRNA, tRNA, snoRNA, and snRNA genes were tagged at the ER and mitochondria. Several features indicate that the tagged non-mRNAs are misprocessed precursors. For example, inspection of the 3' reads revealed untemplated poly(A) tails upstream of the 3' uridine tags. Indeed, poly(A) tails on some non-mRNAs mark them for destruction in the nucleus by the TRAMP and exosome surveillance pathways (6-9). While the reasons that misprocessed non-mRNA precursors are tagged in the cytoplasm are unclear, recent work in yeast suggests that these represent molecules that are relocated from the nucleus to the cytoplasm to avoid their incorporation into mature RNP complexes (10, 11). Alternatively, the anchored PUP chimeras may have moved from the cytoplasm to the nucleus along the contiguous ER-nuclear membranes. This possibility is predicted by imaging experiments that detected specific ER components (e.g., Sec61p) inside the nucleus of yeast and human cells (12, 13). Examination with targeted methods (e.g., MTRIP) will distinguish between these possibilities.

RNA-binding proteins

Tagging of RBP targets at specific locations can help refine our knowledge of RBP-mediated regulation of localized RNAs. The Puf3p protein is an archetype of this model—Puf3p is implicated in localization of specific mRNAs to the mitochondria, and many of its

targets are enriched by mitochondria-localized RNA tagging (14, 15). Yet, not all mitochondria-tagged RNAs were associated with Puf3p, and we did not observe a strong correlation between more localization to the mitochondria (longer U-tags) and the strength of Puf3p association (14, 15). This may indicate that Puf3p does not drive localization *per se*, but that its effects (e.g., translational repression) may be required for the proper localization of a subset of mRNAs to the mitochondria (16).

ER-tagged mRNAs included species that physically associate with Bfr1p. Many mRNAs that physically associate with Bfr1p are highly enriched by ER-localized RNA tagging, and they were among the best ER-tagged RNAs (judged by the length of uridine tags, not shown). The role of Bfr1p in mRNA localization is likely redundant or indirect, however, as interruptions to Bfr1p's ability to associate with an ER-localized mRNA do block mRNA localization to the ER (17). It was also found that Bfr1p regulates translation elongation at the ER (17). If true, our analysis adds hundreds of candidate mRNAs to the network of Bfr1p-regulated mRNAs at the ER (17). Together, these observations demonstrate that localized RNA tagging can inform studies of RBP-mediated regulation of localized mRNAs. This analytical strategy can also be extended to other sites (e.g., plasma membrane), and other types of interactions (e.g., genetic interactions).

Motifs

Additional experiments are needed to determine whether the motifs enriched in ER- and mitochondria-tagged mRNA 3' UTRs are involved in localization. The involvement of these sequences in localization can be tested with a reporter system that has the candidate motif inserted into the 3' UTR of a synthetic mRNA reporter. The synthetic reporter will help reduce gene-specific effects, and its localization can be

observed with imaging (e.g., smFISH) (18). Mutations to the start codon in these experiments will also help distinguish the contributions of the motifs from translation-dependent localization systems (e.g., the signal recognition particle) (19). Indeed, localization to the ER independent of translation and the SRP occurs in yeast, and our data likely contain RNAs that localize in a manner that is independent of these systems (20). Thus, our experiments can identify new motifs involved in localization. As an added bonus, the large amount of data produced by our experiments can also help refine motif prediction software (e.g., MEME) (21).

Opportunities for improvement

The current version of Localized RNA tagging can be improved to reduce bias, increase the number of RNAs that are detected, and improve the sequencing efficiency. I discuss some options below.

Protein design

Changes to the PUP tagging chimera can reduce bias for specific types of RNAs. For example, the poly(A) binding protein RRMs can be replaced with basic amino acids, or with a poly(U) polymerase that has inherent RNA-binding activity (i.e., TUT7) (22). These changes will yield a more accurate view of the distribution of localized RNAs and reduce the influence of polyadenylation and processing status. Flexible (e.g., RGS) linkers in conjunction with a size reduction of the PUP tagging chimera, can also help detect RNAs that are missed due to steric hindrance (23). Size reduction can be partially achieved with the use of epitope tags and immunohistochemistry in place of GFP; minimal anchors and smaller PUPs (i.e., a truncated PUP) will also help make the tagging chimera

smaller. Size reduction also presents an opportunity for experiments that probe tight spaces and may permit experiments that probe for RNAs at specified distances away from the anchor site (23).

Localized RNA tagging has potential applications in live animals. This is because RNAs are tagged independently of chemical treatments. However, several challenges must be overcome. For example, many organisms have endogenous uridylation systems (e.g., *S. pombe*), and U-tags in some organisms mark specific RNAs for enzymatic destruction (22, 24-26). Further, the activity of endogenous U-adding enzymes can be mistaken for true signal, and controls should be added to ensure that the model organism does not alter the activity of the chimera. This can be a problem if the enzyme used is normally present in the experimental model (e.g., using PUP-2 in *C. elegans*). Lastly, tagging chimeras that use different tags (see below) can also help overcome these challenges.

Dual- or "Multi-tagging"

Multiple tagging devices will help distinguish whether the ER and mitochondrial dual-localization reflects RNA molecules that are divided between sites, molecules that move from one location to another, or molecules that are localized to organelle-organelle junctions. For dual-tagging, a PUP will be anchored to one location (e.g., the ER), and an enzyme that adds a different tag ((e.g., hypothetical poly(X) polymerase or PXP)) will be anchored to the other site (e.g., the mitochondria). The order of tags added to the 3' end can be used to deduce the mode of localization. The candidates can then be confirmed with independent, targeted methods (e.g., the MS2-MCP system).

Dual-tagging will help define the order of molecular events in localization mechanisms. For example, the point at which an RBP associates with an RNA for localization can be narrowed down. To do so, a PUP will be anchored to the location of interest (e.g., the mitochondria), while the hypothetical PXP enzyme is fused to the RBP of interest (e.g., Puf3p). The order of nucleotides in the tag will reveal whether the RBP bound first, or whether the RNA was first localized.

Snapshots of localization

Several systems offer an opportunity to get snapshots of localized RNAs with localized tagging. A simple solution is to turn on PUP expression with an inducible promoter (e.g., galactose induction) (27). However, induction can be more immediate if the PUP chimera is already synthesized. This is possible in part because detection of tagging is similarly low in wild-type yeast that do not express PUP-2, and in cells that express the PUP-2 without RNA-association domains (i.e., PUP alone -PAB in this work). These results also hint that distance between the RNA-association domain and the PUP-2 moieties can function as an on/off switch for tagging. Fusion of each domain to inducible dimerization moieties (e.g., rapid blue-light inducible system) or rigging a non-inducible system to dimerize on demand (e.g., biotin and streptavidin) offers an entry point to this end (28, 29).

Library preparation

The library preparation can be improved to make sequencing more efficient and to increase sensitivity. For example, a significant portion of our reads are now lost to viral DNA (PhiX) that is added to the sequencing reaction. While the exogenous DNA is a

required internal control for Illumina sequencing, we now add it at a concentration of 30% of the total library. A lot of PhiX is required to sequence U-tagging libraries to prevent the reduction of base calling accuracy that is caused by high densities of uridine tags on the sequencing chip. An enzyme that adds a more complex tag ((e.g., a poly (UG) polymerase or PUG)) will reduce problems caused by cluster homogeneity and will allow reduction in the concentration of PhiX used. Consequently, more reads will also go to tagged RNAs, and less abundant RNA molecules will have improved detection and reproducibility (30).

The poly(A) selection in the library prep leads to a bias for mature mRNAs. While desirable for some experiments, other studies may want to examine the localization of pre-mRNAs and ncRNAs. However, poly(A) selection is required to ensure ribosomal RNA (rRNA) removal, as rRNAs are abundant and reduce the detection of mRNAs. To reduce ribosomal RNAs, the poly(A) selection can be replaced with targeted enzymatic removal of rRNAs. This procedure, in tandem with the current magnetic bead-mediated removal of rRNAs, will adequately deplete rRNAs and retain others in the sample. Finally, an RT enzyme that is active at higher temperatures can help reduce 3’ bias to capture sequences that are closer to the 5’ end (e.g., some introns).

Localization in response to environmental changes

Localized RNA tagging can be used to identify RNAs that are in specific sites under different cellular growth conditions. The conditions can be different carbon sources (e.g., glucose vs glycerol), or treatment with stressors (e.g., DTT or tunicamycin) (31, 32). Indeed, the abundance of specific mitochondrial proteins changes in yeast shifted from fermentable to non-fermentable media, which predicts that localized RNAs may also change (33). Similarly, ER-localized RNAs changes when the unfolded protein response

is chemically induced (34-37). Further, the roles of dual-localized RNAs in the UPR can be studied by localized tagging, and the experiments may identify mRNAs involved in ER-stress mediated increase of mitochondrial respiration (38). Indeed, the role of an ER-localized RNA in UPR signaling predicts that other localized RNAs may be involved in mediating response to stimuli. Thus, Localized RNA tagging will give local insight into RNA dynamics and help study multi-organelle cooperation via RNA in response to environmental changes.

Where the field is going

A global perspective to RNA biology is now accessible. Aside from the global insight into localization offered by localized RNA tagging, domains can be customized and changed to select for RNA features at specific sites. For example, the domains can select for RNA modifications (e.g., RNA methylation), RNA structures, or specific RNA regions (e.g., introns). The adaptations are ideal for the rapid identification of candidates that can then be confirmed with more targeted methods. Consequently, the localized tagging approach holds promise to identify new functions (e.g., processing) and new mechanisms for localization. My thesis work provides a method to study RNA localization and offers a platform to advance our understanding of RNA biology.

REFERENCES

1. Fazal FM, Han S, Kaewsapsak P, Parker KR, Xu J, Boettiger AN, et al. Atlas of Subcellular RNA Localization Revealed by APEX-seq. bioRxiv. 2018:454470.

2. Kaewsapsak P, Shechner DM, Mallard W, Rinn JL, Ting AY. Live-cell mapping of organelle-associated RNAs via proximity biotinylation combined with protein-RNA crosslinking. eLife. 2017;6:e29224.

3. Williams CC, Jan CH, Weissman JS. Targeting and plasticity of mitochondrial proteins revealed by proximity-specific ribosome profiling. Science. 2014;346(6210):748-51.

4. Jan CH, Williams CC, Weissman JS. Principles of ER cotranslational translocation revealed by proximity-specific ribosome profiling. Science. 2014;346(6210):1257521.

5. Lecuyer E, Yoshida H, Parthasarathy N, Alm C, Babak T, Cerovina T, et al. Global analysis of mRNA localization reveals a prominent role in organizing cellular architecture and function. Cell. 2007;131(1):174-87.

6. LaCava J, Houseley J, Saveanu C, Petfalski E, Thompson E, Jacquier A, et al. RNA degradation by the exosome is promoted by a nuclear polyadenylation complex. Cell. 2005;121(5):713-24.

7. Wyers F, Rougemaille M, Badis G, Rousselle JC, Dufour ME, Boulay J, et al. Cryptic pol II transcripts are degraded by a nuclear quality control pathway involving a new poly(A) polymerase. Cell. 2005;121(5):725-37.

8. Vanacova S, Wolf J, Martin G, Blank D, Dettwiler S, Friedlein A, et al. A new yeast poly(A) polymerase complex involved in RNA quality control. PLoS Biol. 2005;3(6):e189.

9. Houseley J, LaCava J, Tollervey D. RNA-quality control by the exosome. Nat Rev Mol Cell Biol. 2006;7(7):529-39.

10. Becker D, Hirsch AG, Bender L, Lingner T, Salinas G, Krebber H. Nuclear Pre-snRNA Export Is an Essential Quality Assurance Mechanism for Functional Spliceosomes. Cell Rep. 2019;27(11):3199-214 e3.

11. Grzechnik P, Szczepaniak SA, Dhir S, Pastucha A, Parslow H, Matuszek Z, et al. Nuclear fate of yeast snoRNA is determined by co-transcriptional Rnt1 cleavage. Nat Commun. 2018;9(1):1783.

12. Smoyer CJ, Katta SS, Gardner JM, Stoltz L, McCroskey S, Bradford WD, et al. Analysis of membrane proteins localizing to the inner nuclear envelope in living cells. J Cell Biol. 2016;215(4):575-90.

13. Isaac C, Pollard JW, Meier UT. Intranuclear endoplasmic reticulum induced by Nopp140 mimics the nucleolar channel system of human endometrium. Journal of Cell Science. 2001;114(23):4253.

14. Saint-Georges Y, Garcia M, Delaveau T, Jourdren L, Le Crom S, Lemoine S, et al. Yeast mitochondrial biogenesis: a role for the PUF RNA-binding protein Puf3p in mRNA localization. PLoS One. 2008;3(6):e2293.

15. Lapointe CP, Wilinski D, Saunders HA, Wickens M. Protein-RNA networks revealed through covalent RNA marks. Nat Methods. 2015;12(12):1163-70.

16. Walters R, Parker R. Quality control: Is there quality control of localized mRNAs? J Cell Biol. 2014;204(6):863-8.

17. Manchalu S, Mittal N, Spang A, Jansen R-P. Local translation of yeast ERG4 mRNA at the endoplasmic reticulum requires the brefeldin A resistance protein Bfr1. bioRxiv. 2019:656405.

18. Raj A, van den Bogaard P, Rifkin SA, van Oudenaarden A, Tyagi S. Imaging individual mRNA molecules using multiple singly labeled probes. Nature Methods. 2008;5:877.

19. Akopian D, Shen K, Zhang X, Shan S-o. Signal recognition particle: an essential protein-targeting machine. Annual review of biochemistry. 2013;82:693-721.

20. Kraut-Cohen J, Afanasieva E, Haim-Vilmovsky L, Slobodin B, Yosef I, Bibi E, et al. Translation- and SRP-independent mRNA targeting to the endoplasmic reticulum in the yeast Saccharomyces cerevisiae. Mol Biol Cell. 2013;24(19):3069-84.

21. Bailey TL, Elkan C. Fitting a mixture model by expectation maximization to discover motifs in biopolymers. Proc Int Conf Intell Syst Mol Biol. 1994;2:28-36.

22. Lapointe CP, Wickens M. The nucleic acid-binding domain and translational repression activity of a Xenopus terminal uridylyl transferase. J Biol Chem. 2013;288(28):20723-33.

23. Chen X, Zaro JL, Shen WC. Fusion protein linkers: property, design and functionality. Adv Drug Deliv Rev. 2013;65(10):1357-69.

24. Kwak JE, Wickens M. A family of poly(U) polymerases. RNA. 2007;13(6):860-7.

25. Warkocki Z, Liudkovska V, Gewartowska O, Mroczek S, Dziembowski A. Terminal nucleotidyl transferases (TENTs) in mammalian RNA metabolism. Philosophical transactions of the Royal Society of London Series B, Biological sciences. 2018;373(1762):20180162.

26. Chung CZ, Jaramillo JE, Ellis MJ, Bour DYN, Seidl LE, Jo DHS, et al. RNA surveillance by uridylation-dependent RNA decay in Schizosaccharomyces pombe. Nucleic Acids Res. 2019;47(6):3045-57.

27. Weinhandl K, Winkler M, Glieder A, Camattari A. Carbon source dependent promoters in yeasts. Microb Cell Fact. 2014;13:5-.

28. Kennedy MJ, Hughes RM, Peteya LA, Schwartz JW, Ehlers MD, Tucker CL. Rapid blue-light-mediated induction of protein interactions in living cells. Nat Methods. 2010;7(12):973-5.

29. Dundas CM, Demonte D, Park S. Streptavidin–biotin technology: improvements and innovations in chemical and biological applications. Applied Microbiology and Biotechnology. 2013;97(21):9343-53.

30. Preston MA, Porter DF, Chen F, Buter N, Lapointe CP, Keles S, et al. Unbiased screen of RNA tailing activities reveals a poly(UG) polymerase. Nature Methods. 2019;16(5):437-45.

31. Shamu CE, Cox JS, Walter P. The unfolded-protein-response pathway in yeast. Trends Cell Biol. 1994;4(2):56-60.

32. Shamu CE, Walter P. Oligomerization and phosphorylation of the Ire1p kinase during intracellular signaling from the endoplasmic reticulum to the nucleus. Embo j. 1996;15(12):3028-39.

33. Morgenstern M, Stiller SB, Lubbert P, Peikert CD, Dannenmaier S, Drepper F, et al. Definition of a High-Confidence Mitochondrial Proteome at Quantitative Scale. Cell Rep. 2017;19(13):2836-52.

34. Cox JS, Walter P. A novel mechanism for regulating activity of a transcription factor that controls the unfolded protein response. Cell. 1996;87(3):391-404.

35. Hollien J, Lin JH, Li H, Stevens N, Walter P, Weissman JS. Regulated Ire1-dependent decay of messenger RNAs in mammalian cells. The Journal of cell biology. 2009;186(3):323-31.

36. Kimmig P, Diaz M, Zheng J, Williams CC, Lang A, Aragon T, et al. The unfolded protein response in fission yeast modulates stability of select mRNAs to maintain protein homeostasis. Elife. 2012;1:e00048.

37. Reid DW, Chen Q, Tay ASL, Shenolikar S, Nicchitta CV. The unfolded protein response triggers selective mRNA release from the endoplasmic reticulum. Cell. 2014;158(6):1362-74.

38. Knupp J, Arvan P, Chang A. Increased mitochondrial respiration promotes survival from endoplasmic reticulum stress. Cell Death & Differentiation. 2019;26(3):487-501.